



**Assessing flood-prone area in an ungauged basin by calibrating a hydrological model using various hydrological components (ET, Surface runoff, Soil moisture) driven from remote sensing**

File Number : PDF/2023/000079

Submitted By : Dr. Ankit Singh

[SERB Qualified Unique Identification Document: SQUID-1991-AS-2733]

Submission Date : 26-Jul-2023

PROPOSAL DETAILS

( PDF/2023/000079 )

Principal Investigator	Mentor & Host Institution
<b>Dr. Ankit Singh</b> asankitsingh2010@gmail.com (Department of Civil Engineering) <b>Contact No</b> : +919977734807 <b>Date of Birth</b> : 02-Sep-1991 <b>Name of Father/Spouse :</b> Suraj Pal Singh	<b>D. Nagesh D</b> nagesh@iisc.ac.in Professor(Civil Engineering) <b>Indian Institute of Science</b> Cv raman rd, bengaluru, Bangalore urban district, Karnataka-560012 <b>Contact No.</b> : +919739050057 <b>Registrar Email</b> : registrar@iisc.ac.in <b>No. of PHD Scholars</b> : 8 <b>No. Post-Doctoral Fellow</b> : 3

Details of Post Doctorate
<b>Ph.D. (Earth and Environmental Sciences (Hydrology))</b> [ Degree Awarded on : 08-Jul-2023 ] <i>On the utility of precipitation forecast products, hydrological models, and multi-model approaches for streamflow forecasting</i> <b>Research Supervisor/Guide &amp; Institution :</b> Dr. Sanjeev Kumar Jha Indian Institute of Science Education and Research Bhopal (IISERB), Madhya Pradesh, India <b>Brief details of Thesis work :</b> The success of streamflow forecasting primarily depends on the quality of the precipitation forecast and the hydrological model. A reliable forecast of summer monsoon rainfall is crucial in India. In my Ph.D. work, medium-range precipitation forecasts available from various global and national forecasting agencies are used. Since the focus here is streamflow forecasting in Indian River basins, both deterministic and ensembles of <b>quantitative precipitation forecasts (QPFs)</b> available from various numerical weather prediction (NWP) models had to be assessed at the river basin scale against the observed precipitation data. <b>In the absence of a dense network of in-situ measurements for the observation data, options included rain gauge interpolated data, satellite products, satellite-gauge merged data, and reanalysis datasets.</b> The utility of available QPFs from the THORPEX Interactive Grand Global Ensemble (TIGGE) archives and observation data were studied at the basin scale and at the grid level in different river basins of India. <b>Due to the availability of long-term observed discharge data of good quality in the Narmada River basin, the development of hydrological models was focused on this basin.</b> The hydrological models are the main tools for streamflow forecasting, but in the last few decades, development in the hydrological models has increased the complexity of the hydrological models due to an increase in the parameters and development in the algorithms and structure of the hydrological models. Thus, <b>selecting a set of sensitive parameters is essential before using them for calibration purposes of the hydrological models.</b> The different global sensitivity analysis methods are adopted to find the set of sensitive parameters that cover the entire hydrological process. Also, due to different algorithms and structures in hydrological models, <b>the level of uncertainty in the hydrological models is different in different hydrological models.</b> Different multi-model methods are evolving with time to overcome the uncertainty in the different hydrological models. Some of the established multi-model methods are compared with two proposed multi-model methods. <b>After evaluating the rainfall forecasts from different QPFs and the accuracy of hydrological models, the next step in developing a streamflow forecasting system is to select a combination of a hydrological model and a rainfall forecast product that gives a reliable and more accurate streamflow forecast.</b> For this, two selected global agencies' rainfall forecasts were compared with a global agency's rainfall forecasts using two hydrological models. The results of my Ph.D. study will have tremendous value for organizations like the Central Water Commission in producing streamflow forecasts,Agro-Advisory Services of IMD in farming operations, and the National Disaster Management Authority in estimating risks involved during low or high flow events

Technical Details :

**Research Area :** Earth & Atmospheric Sciences (Earth & Atmospheric Sciences)

Project Summary :

Flood events in river basins are significant natural disasters causing loss of livelihoods and resources. Hydrological models are essential tools for simulating hydrological processes in these basins. However, **calibration issues arise when the basin is ungauged or data-poor.** Remote sensing data can be used to calibrate a hydrologic model in an ungauged basin, allowing researchers to evaluate various hydrologic components. **The research aims to evaluate the accuracy of available RS data sets, choose the best RS data, and consider the multi-criteria calibration approach.** Water balance analysis is also considered in identifying flood-prone areas. The methodology involves collecting long-term hydrologic component data from remote sensing data (MODIS and Landsat), pre-processing and accuracy assessment, and calibrating the hydrologic model using multiple criteria. The selected flood-prone area is validated based on past events and projections of future flood-prone areas under different climate scenarios. Novelty:

- A comprehensive analysis is carried out to identify the more reliable remote sensing data for calibrating a hydrological model for an ungauged basin.**
- Analyzing the pre-existing multi-criteria calibration approaches using more than one remote sensing hydrological component to overcome the equifinality issues in hydrological modeling.
- A complete study of water cycle components of an ungauged basin to identify the flood-prone area.**
- Generate a future landuse map by considering the ongoing and proposed projects** (infrastructure and biodiversity).

Objectives :

- Evaluating the accuracy of various available RS data sets using observational data.**
- Calibration of a hydrologic model using multiple criteria rather than single runoff data.**
- Evaluation of hydrologic variables (such as groundwater infiltration, surface runoff, subsurface runoff, etc.) in different sub-basins**
- Identification of the flood-prone sub-basin or area in the basin based on the water balance.**
- Validation of the selected flood-prone area based on past events and projection of the future flood-prone area under different climate scenarios.**

Keywords :

Flood events, Remote Sensing, Machine Learning, Ungauged River Basin, Multi-Criteria Calibration, Hydrological modeling

Expected Output and Outcome of the proposal :

The outcomes of this proposed project are helpful to identify a reliable remote sensing data set to calibrate a hydrological model for an ungauged basin. The generated present and future flood-prone area map helps various agencies to plan accordingly such as urban planners, natural disaster agencies, and ecologists. There is the possibility of four publications out of this proposed project. A tool is developed during this tenure to generate the future landuse map.

Reference Details :

S.No	Reference Details
1	<b>Dr. Somil Swarnkar</b> <b>Room No: 209, Plasma Building, EES Department, IISER Bhopal</b>  [+7552691473] somilswarnkar@iiserb.ac.in
2	<b>Dr. Sanjeev Kumar Jha (Ph.D. Supervisor)</b> <b>Room No: 304, Elements Block, EES Department, IISER Bhopal</b>  [+7552691391] sanjeevj@iiserb.ac.in

# **Assessing flood-prone area in an ungauged basin by calibrating a hydrological model using various hydrological components (ET, Surface runoff, Soil moisture) driven from remote sensing**

**Submitted by: Ankit Singh**

## **Motivation:**

Flood events in a river basin are one of the most important natural disasters causing the loss of livelihoods and resources. Flood events in recent decades, such as the Maharashtra flood of 2005, the Leh flood of 2010, the Himalayan flash flood of 2012, the Kedarnath flood of 2013, the Gujarat floods of 2015 and 2017, the South Indian flood of 2015, the Kerala flood of 2019, and the Chamoli flood of 2021 are examples of some major floods in India. The hydrological models are powerful tools to simulate the hydrological processes for each river basin after calibration. River basins that have observed runoff data are easy to calibrate, but problems arise when the basin is ungauged or data-poor. However, several methods exist for calibrating a hydrologic model in an ungauged or data-poor basin. In the absence of observed discharge data, researchers have used other hydrologic components, such as evapotranspiration (ET), surface runoff, soil moisture, etc. to calibrate the hydrologic model. In an evolving society, these data sets are available with reasonable accuracy through remote sensing. Remote sensing data allows us to calibrate a hydrologic model in an ungauged basin to evaluate the various hydrologic components in the desired sub-basin.

## **Research Questions:**

- 1) Are remote sensing (RS) data helpful in calibrating a hydrologic model?
- 2) Which RS data are best for calibrating a hydrologic model?
- 3) Is the multi-criteria calibration approach more appropriate for calibrating a hydrologic model?
- 4) Is water balance analysis helpful in identifying flood-prone areas or not?

## **Objective:**

- Evaluating the accuracy of various available RS data sets using observational data.
- Calibration of a hydrologic model using multiple criteria rather than single runoff data.
- Evaluation of hydrologic variables (such as groundwater infiltration, surface runoff, subsurface runoff, etc.) in different sub-basins

- Identification of the flood-prone sub-basin or area in the basin based on the water balance.
- Validation of the selected flood-prone area based on past events and projection of the future flood-prone area under different climate scenarios.

### **Methodology:**

#### *Step 1: Data collection*

Long-term hydrologic component data (ET, surface runoff, soil moisture, etc.) are collected from remote sensing data (MODIS and Landsat) for the study area.

#### *Step 2: Data pre-processing and accuracy assessment*

Pre-processing of the data includes removing noise and errors by filtering, atmospheric correction, and scaling of the data. After pre-processing the data, the accuracy of the different data sets is evaluated with respect to the observed data (if available).

#### *Step 3: Calibration of a hydrological model using a multi-criteria approach*

If the ungauged basin is a sub-basin of a gauged basin or is within a gauged basin, then use the multisite calibration approach first to reduce parameter optimization and the first round of remote sensing data verification. If the ungauged basin is independent, then the hydrologic model is calibrated directly with a multi-criteria approach using RS data.

#### *Step 4: Evaluation of water balance in different subbasins*

After the hydrological models are calibrated, the water balance for each sub-basin is calculated. Based on the water balance, the amount of runoff, infiltration, and the amount of runoff contributing to the main stream are calculated.

#### *Step 5: Identify the flood-prone area based on step 4.*

After evaluating the water balance of each sub-basin, the amount of water remaining in the sub-basin is calculated. The flood hazard areas or sub-basins are identified based on the amount of water remaining in the sub-basin. The flood-prone area is validated based on past flood records or flood frequency analysis.

#### *Step 6: Identify the flood-prone area for the future*

Machine learning is used to generate various scenarios for future land use. After generating land use data, various future meteorological data are used to calculate the hydrological components in the basin and identify the flood-prone areas in the basin.

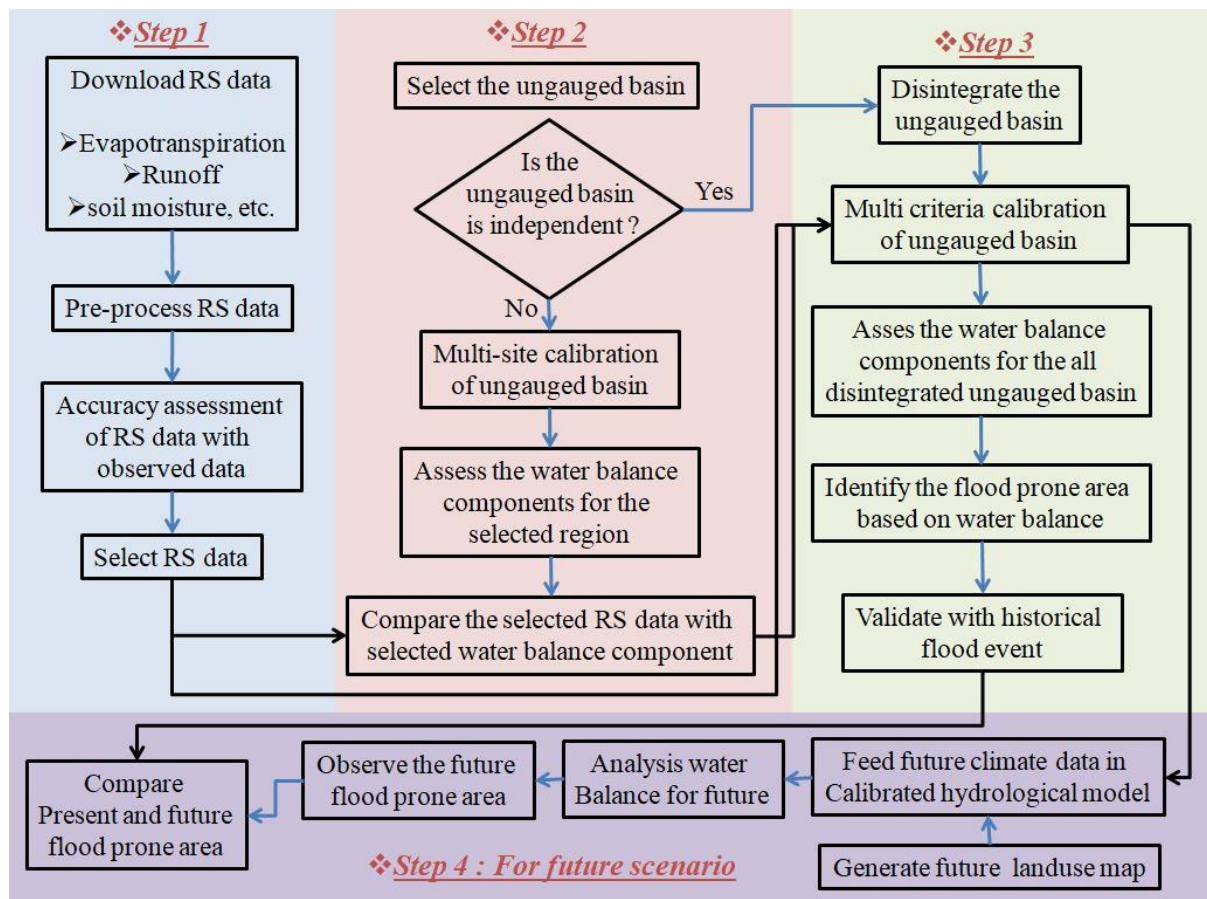


Figure 1. Step-by-step flowchart of the proposed methodology to implement the proposed project

### **Conclusion:**

This project aims to identify the flood-prone areas in an ungauged basin for the present and the future. This project also proves the applicability of remote sensing data for calibrating a hydrological model in an ungauged basin using a multi-criteria approach.

### **Skills I have:**

- Programming language: MATLAB and Python.
- Gis platform: Arc-GIS, QGIS and GrrenKennue
- Hydrological models: SWAT, VIC, WATFLOOD, and HEC-HMS
- Hydraulic models: HEC-RAS 1-D and 2-D

**Timeline:**

	Months							
Work	1 to 3	4 to 6	7 to 9	10 to 12	13 to 15	16 to 18	19 to 20	21 to 24
Literature Review (Identify Study Area)								
Data collection and shorting								
Data Comparison								
Analysis of the Multi- Criteria Calibration Approach								
Water-balance Analysis & Identification of Flood prone Area								
LULC prediction								
Identification of Future Flood prone area								
Comparative study between present and Future Flood prone area								
Flood inundation mapping								
Publications			First		Second	Third		Fourth

### **BIO-DATA**

1. Name and full correspondence address: Ankit Singh, 1A, Sarika Vihar, Kalindi Vihar, 100 ft. Road, Tedi Bagiya, Agra, U.P., India, (282001)
2. Email(s) and contact number(s): [asankitsingh2010@gmail.com](mailto:asankitsingh2010@gmail.com)  
9977734807
3. Institution: Indian Institute of Science Education and Research Bhopal (IISERB), Madhya Pradesh, India
4. Date of Birth: 02/09/1991
5. Gender (M/F/T): Male
6. Category Gen/SC/ST/OBC: SC
7. Whether differently abled (Yes/No): No

8. Academic Qualification (Undergraduate Onwards)

	Degree	Year	Subject	University/Institution	% of marks
1.	B.E.	2014	Civil Engineering	Bansal Institute of Science and Technology Bhopal M.P./Affiliated by RGPV, Madhya Pradesh, India	6.59/10
2.	M.Tech.	2017	Water Resources Engineering	Maulana Azad National Institute of Technology (MANIT) Bhopal, Madhya Pradesh, India	7.67/10
3.	Ph.D.	2023	Earth and Environmental Sciences	Indian Institute of Science Education and Research Bhopal (IISERB), Madhya Pradesh, India	7.33/10

9. Ph.D thesis title, Guide's Name, Institute/Organization/University, Year of Award.

**Ph.D. Thesis title:** On the utility of precipitation forecast products, hydrological models, and multi-model approaches for streamflow forecasting.

**Supervisor:** Dr. Sanjeev Kumar Jha.

**Institute:** Indian Institute of Science Education and Research Bhopal, India,

**Year of Award:** 2023

10. Work experience (in chronological order).

S.No.	Positions held	Name of the Institute	From	To	Pay Scale
NA	NA	NA	NA	NA	NA

11. Professional Recognition/ Award/ Prize/ Certificate, Fellowship received by the applicant.

S.No	Name of Award	Awarding Agency	Year
1	AGU Student Travel Grant 2020	American Geophysical Union (AGU)	2020
2	GATE 2014, 2017, and 2018	Department of Higher Education, Ministry of Education (MoE), Government of India (GoI).	2014, 2017, and 2018

12. Publications (*List of papers published in SCI Journals, in year wise descending order*).

S.No.	Author(s)	Title	Name of Journal	Volume	Page	Year
1	Ankit Singh, Soubhik Mondal, Nibedita Samal, Sanjeev Kumar Jha	Evaluation of precipitation forecasts for five-day streamflow forecasting in Narmada River basin	Hydrological Sciences Journal	68/1	1-19	2022
2	Ankit Singh, Shubham Tiwari, Sanjeev Kumar Jha	Evaluation of quantitative precipitation forecast in five Indian river basins	Hydrological Sciences Journal	66/15	2216-2231	2021
3	Ankit Singh, Sanjeev Kumar Jha	Identification of sensitive parameters in daily and monthly hydrological simulations in small to large catchments in Central India	Journal of Hydrology	601	126232	2021
4	Shubham Tiwari, Sanjeev Kumar Jha, Ankit Singh	Quantification of node importance in rain gauge network: influence of temporal resolution and rain gauge density	Scientific Reports	10/1	9761	2020

13. Detail of patents.

S.No	Patent Title	Name of Applicant(s)	Patent No.	Award Date	Agency/Country	Status
NA	NA	NA	NA	NA	NA	NA



14. Books/Reports/Chapters/General articles etc.

S.No	Title	Author's Name	Publisher	Year of Publication
NA	NA	NA	NA	NA

15. Any other Information (maximum 500 words)

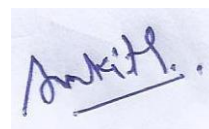
I completed my Ph.D. from the Earth and Environmental Sciences department of the Indian Institute of Science Education and Research, Bhopal. During my Ph.D. studies, I researched the utility of the NWP models in forecasting rainfall and hydrological models in streamflow forecasts. To complete the objectives of my Ph.D. I deal with a large amount of data (entire India) in various formats (.nc, .grib, and .ctl). I used various remote sensing data (LULC, albedo, LAI, and evapotranspiration) and used ARC-Gis for pre-processing before feeding it into the different hydrological models. For completing the multi-model analysis, I explored different mathematical and statistical approaches to combine the simulation of different hydrological models. Also, after completing my Ph.D. I completed a short-term course on machine learning.

Other than Academics I also involved in sports and activities. I was part of my school Handball team and have Passing Certificate of "Tritiya Sopan" (Scout and Guide) (2006), and attending the Rajyapuraskar Camp (2007).

### **Undertaking by the Fellow**

I, **Ankit Singh**, Son/Daughter/Wife of Shri. **Suraj Pal Singh**, resident of **1A, Sarika Vihar, Kalindi Vihar, 100ft Road, Tedibagiya, Rambag, Agra, U.P. (282001)** agree to undertake the following, If I am offered the SERB N-PDF

1. I shall abide by the rules and regulations of SERB during the entire tenure of the fellowship.
2. I shall also abide by the rules, discipline of the institution where I will be implementing my fellowship
3. I shall devote full time to research work during the tenure of the fellowship
4. I shall prepare the progress report at the end of each year and communicate the same to SERB through the mentor
5. I shall send two copies of the consolidated progress report at the end of the fellowship period.
6. I further state that I shall have no claim whatsoever for regular/permanent absorption on expiry of the fellowship.



**(Ankit Singh)**

Signature

Date: **24<sup>th</sup> July 2023**

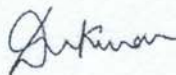
**Endorsement Certificate from the Mentor & Host Institute**

This is to certify that:

- I. The applicant, Dr. Ankit Singh, will assume full responsibility for implementing the project.
- II. The fellowship will start from the date on which the fellow joins University/Institute where he/she implements the fellowship. The mentor will send the joining report to the SERB. SERB will release the funds on receipt of the joining report.
- III. The applicant, if selected as SERB-N PDF, will be governed by the rules and regulations of the University/ Institute and will be under administrative control of the University/ Institute for the duration of the Fellowship.
- IV. The grant-in-aid by the Science & Engineering Research Board (SERB) will be used to meet the expenditure on the project and for the period for which the project has been sanctioned as indicated in the sanction letter/ order.
- V. No administrative or other liability will be attached to the Science & Engineering Research Board (SERB) at the end of the Fellowship.
- VI. The University/ Institute will provide basic infrastructure and other required facilities to the fellow for undertaking the research objectives.
- VII. The University/ Institute will take into its books all assets received under this sanction and its disposal would be at the discretion of Science & Engineering Research Board (SERB).
- VIII. University/ Institute assume to undertake the financial and other management responsibilities of the project.
- IX. The University/ Institute shall settle the financial accounts to the SERB as per the prescribed guidelines within three months from the date of termination of the Fellowship.

Dated: 08-07-2023

Signature of the Mentor:



Name & Designation:



Dr. D. Nagesh Kumar  
Professor  
Department of Civil Engineering  
Indian Institute of Science  
Bangalore - 560 012

Dated: 11-07-2023



Signature of the ~~Registrar of University~~ Head of Institute

Seal of the Institution

सहायक रजिस्ट्रार / Assistant Registrar  
भारतीय विज्ञान संस्थान  
Indian Institute of Science  
बेंगलूरु / Bengaluru - 560 012

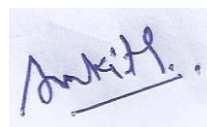
## Undertaking by the Principal Investigator

To

The Secretary  
SERB, New Delhi

Sir

I Ankit Singh hereby certify that the research proposal titled Assessing flood-prone area in an ungauged basin by calibrating a hydrological model using various hydrological components (ET, Surface runoff, Soil moisture) driven from remote sensing submitted for possible funding by SERB, New Delhi is my original idea and has not been copied/taken verbatim from anyone or from any other sources. I further certify that this proposal has been checked for plagiarism through a plagiarism detection tool i.e. Turnitin approved by the Institute and the contents are original and not copied/taken from any one or many other sources. I am aware of the UGCs Regulations on prevention of Plagiarism i.e. University Grant Commission (Promotion of Academic Integrity and Prevention of Plagiarism in Higher Educational Institutions) Regulation, 2018. I also declare that there are no plagiarism charges established or pending against me in the last five years. If the funding agency notices any plagiarism or any other discrepancies in the above proposal of mine, I would abide by whatsoever action taken against me by SERB, as deemed necessary.



(Ankit Singh/SERB NPDF Applicant)

Date: 24<sup>th</sup> July 2023

Signature of PI with date  
Name / designation



क्रमांक S.No. SSE/2007/

केन्द्रीय माध्यमिक शिक्षा बोर्ड

CENTRAL BOARD OF SECONDARY EDUCATION

771576 अंक विवरणिका MARKS STATEMENT

सेकण्डरी स्कूल परीक्षा, 2007

SECONDARY SCHOOL EXAMINATION, 2007

ALL INDIA

नाम Name ANKIT SINGH

अनुक्रमांक Roll No. 1139574

माता का नाम Mother's Name SHRI DEVI

पिता का नाम Father's Name SURAJ PAL SINGH

जन्म तिथि Date of Birth 02/09/1991 02ND SEPTEMBER NINETEEN NINETY ONE

विद्यालय School 03210 KENDRIYA VIDYALAYA KILLAI NAKA DAMOH M P

विषय कोड SUB. CODE	विषय SUBJECT	प्राप्तांक MARKS OBTAINED				स्थितीय ग्रेड POSITIONAL GRADE
		लि. TH	पै/आ.मू PR/IA	योग TOTAL	योग शब्दों में TOTAL IN WORDS	
101	ENGLISH COMM.	052	XXX	052	FIFTY TWO	01
002	HINDI COURSE-A	073	XXX	073	SEVENTY THREE	01
041	MATHEMATICS	052	018	070	SEVENTY	02
086	SCIENCE & TECH.	043	031	074	SEVENTY FOUR	01
	PR.-INTERNAL 019					
	PR.SKLS-TH.EXT 012					
087	SOCIAL SCIENCE	058	016	074	SEVENTY FOUR	02

AB : विषय में अनुपस्थित Absent in the Subject

परिणाम Result PASS

PR : प्रयोगात्मक Practical

IA : आंतरिक मूल्यांकन Internal Assessment

दिल्ली Delhi

दिनांक Dated 28/05/2007

M Sharma  
परीक्षा नियंत्रक

Controller of Examinations



# कार्यालय तहसीलदार टूण्डला, फिरोजाबाद

क्रमांक-161144000162

दिनांक-20-Jan-14



उत्तर प्रदेश के अनुसूचित जाति के लिये जाति प्रमाण पत्र

राजस्व निरीक्षक क्षेत्र-टूण्डला की जाँच आख्या दिनांक-18-Jan-14 के आधार पर प्रमाणित किया जाता है कि-

अंकित सिंह

पिता/पति-श्री सूरजपाल सिंह

निवासी-इमलिया, रामगढ़ उर्फ उम्मरगढ़ तहसील-टूण्डला जनपद-फिरोजाबाद उत्तर प्रदेश की जाटव जाति के व्यक्ति है जिसे संविधान अनुसूचित जाति आदेश-1950 जैसा कि समय-समय पर संशोधित हुआ है अनुसूचित जाति उ0प्र0 आदेश-1967 के अनुसार अनुसूचित जाति/अनुसूचित जनजाति के रूप में शासनादेश सं0-484/क-1/94-1/1994 दिनांक 29.03.1994 के अन्तर्गत है फिरो ज़मीन शासनादेश संख्या-22/16/92 टी0सी0-111-का-2/2002 के अन्तर्गत मान्यता दी गयी है।

अंकित सिंह तथा/अथवा उनका परिवार उ0प्र0 के इमलिया, रामगढ़ उर्फ उम्मरगढ़ तहसील टूण्डला व जिला फिरोजाबाद में सामान्यतः रहता है।



तहसीलदार टूण्डला  
जनपद-फिरोजाबाद

उपरोक्त प्रमाण पत्र का सत्यापन राजस्व परिषद की वेबसाइट <http://www.bor.up.nic.in> पर किया जा सकता है।

## Curriculum Vitae

Name : **D Nagesh Kumar**  
Address : Professor, Department of Civil Engineering  
Indian Institute of Science, Bangalore – 560 012, India  
Phone : +91 80 2293 2666 (O); +91 80 2972 0197 (R)  
Email : nagesh@iisc.ac.in  
Home Page : <http://www.civil.iisc.ac.in/~nagesh>  
Date of Birth : 15 July 1963

### Academic

#### **Doctor of Philosophy (Ph D)**

in Water Resources Systems on "*Integrated Modelling for Optimal Reservoir Operation for Irrigation*" in Civil Engineering Department, Indian Institute of Science, Bangalore. (1987-1992)

#### **Master of Engineering (M E)**

in *Hydrology and Water Resources Engineering* at Centre for Water Resources, Anna University, Madras. First class with Distinction. (1985-1987)

#### **Bachelor of Technology (B Tech)**

in *Civil Engineering*, V R Siddhartha Engineering College, Vijayawada, Nagarjuna University, Andhra Pradesh. First class with Distinction. (1980-1984)

### Experience

**Professor in Dept. of Civil Engg.,** I.I.Sc., Bangalore. (May 2008 to date)

**Prof. Satish Dhawan Chair Professor,** I.I.Sc., Bangalore (Oct 2018 to Oct 2021)

**Chairman,** Centre for Earth Sciences, I.I.Sc., Bangalore. (Mar 2014 to Jan 2020)

**Visiting Professor** in EMSE, Saint-Etienne, France. (Aug to Dec 2012)

**Associate Professor** in Dept. of Civil Engg., I.I.Sc., Bangalore. (May 2002 to May 2008)

**Associate Professor** in Dept. of Civil Engg., I.I.T., Kharagpur. (Aug 2000 to May 2002)

**Visiting Faculty** (BOYSCAST Fellow), Utah State Univ., USA. (Jan to July 1999)

**Assistant Professor** in Civil Engg. Dept., I.I.T., Kharagpur. (Sept 1995 to Aug 2000)

**Visiting Lecturer** in Civil Engg. Dept., I.I.T., Kharagpur. (Feb 1994 to Aug 1995)

**Scientist,** National Remote Sensing Agency, Hyderabad, India. (Sept 1992 to Jan 1994)

### Awards & Distinctions

- ◆ **Fellow,** Indian Academy of Sciences (IASc), Jan 2022
- ◆ **Fellow,** Indian National Academy of Sciences (INSA), Jan 2023
- ◆ **Fellow,** National Academy of Sciences, India (NASI), Nov 2022
- ◆ **Prof. Satish Dhawan Chair Professor Award,** IISc, 2018-21
- ◆ **IBM Faculty Award - 2012**
- ◆ **Editor-in-Chief,** Journal of Water and Climate Change, IWA Publishing, UK
- ◆ **Associate Editor,** Journal of Hydrologic Engineering, ASCE.
- ◆ **Expert Member,** for faculty selections in many IITs, NITs and Univs.
- ◆ **Visitor's Nominee,** for faculty selections in IIT Bombay and Roorkee
- ◆ **Reviewer** for more than 80 International journals and many funding agencies.
- ◆ **Projects Completed/ Ongoing:** Sponsored projects: 14 (~ Rs. 36 Crores); Consultancy projects: 12 (~ Rs. 1 Crore).

## Ph D theses Supervised:

24 (8 in progress) (all funded by MoE Scholarship)

## Post-Doctoral Fellows Mentored:

14 (3 in progress) – Out of 3 –

1 is funded DST NPDF; 1 by UGC Kothiyari Fellowship; 1 by DST-NWO Project

**Publications: 227** (Books: 8; Journals: 138; Book Chapters: 16; In Conf. Proceedings: 63)  
(Complete list of publications is available at <http://civil.iisc.ac.in/~nagesh/publications.htm>)

**Citations : 5500; h-index : 43** (Source: SCOPUS; updated in July 2023)

## Publications in journals during last five years (2018-23)

1. *Estimation of the climate change impact on a catchment water balance using an ensemble of GCMs*, Reshmidevi T V., D Nagesh Kumar, R Mehrotra and A Sharma, **Journal of Hydrology**, Elsevier, Vol. 556, pp. 1192-1204, January 2018, DOI: 10.1016/j.jhydrol.2017.02.016 (Published online on 14 February 2017)
2. *Regional variation of recession flow power-law exponent*, Patnaik S, B Biswal and D Nagesh Kumar and B Sivakumar, **Hydrological Processes**, Wiley InterScience, Vol. 32, No. 7, pp. 866-872, March 2018, DOI: 10.1002/hyp.11441 (Published online on 7 February 2018)
3. *Spectral-Spatial Classification of Hyperspectral Data with Mutual Information based Segmented Stacked Autoencoder Approach*, Subir Paul and D. Nagesh Kumar, **ISPRS Journal of Photogrammetry and Remote Sensing**, Elsevier, Vol. 138, pp. 265-280, April 2018, DOI: 10.1016/j.isprsjprs.2018.02.001 (Published online in February 2018)
4. *Estimation of daily vegetation coefficients using MODIS data for clear and cloudy sky conditions*, Shwetha H R and D Nagesh Kumar, **International Journal of Remote Sensing**, Taylor & Francis, Vol. 39, No. 11, pp. 3776-3800, 2018, DOI: 10.1080/01431161.2018.1448480 (Published online on 15 March 2018)
5. *Assessment of surface water Storage trends for increasing groundwater areas in India*, Chandan Banerjee and D Nagesh Kumar, **Journal of Hydrology**, Elsevier, Vol. 562, pp. 780-788, July 2018, DOI: 10.1016/j.jhydrol.2018.05.052 (Published online on 24 May 2018)
6. *Prioritization of Sub-catchments of a River Basin using DEM and Fuzzy VIKOR*, Srinivasa Raju K, D Nagesh Kumar, Anmol Jalali, **H2 Open Journal**, Open Access, IWA Publishing, UK, Vol. 1, No. 1, pp. 1-11, July 2018, DOI: 10.2166/h2oj.2017.001 (Published online on 01 December 2017)
7. *Trend Detection Analysis of Seasonal Rainfall of Homogeneous Regions and All India, Prepared by Using Individual Month Rainfall Values*, Ganesh D Kale and D. Nagesh Kumar, **Water Conservation Science and Engineering**, Springer, Vol.3, No. 2, pp. 129-138, July 2018, DOI: 10.1007/s41101-018-0047-5 (Published online on 27 June 2018)
8. *Performance evaluation of satellite based approaches for the estimation of daily air temperature and reference evapotranspiration*, Shwetha H R and D Nagesh Kumar, **Hydrological Sciences Journal**, Taylor & Francis, UK, Vol. 63, No. 9, pp. 1347-1367, September 2018, DOI: 10.1080/02626667.2018.1505046 (Published online on 26 July 2018)
9. *Analyzing large-scale hydrologic processes using GRACE and hydrometeorological datasets*, Chandan Banerjee and D. Nagesh Kumar, **Water Resources Management**, Springer, Vol. 32, No. 13, pp. 4409-4423, October 2018, DOI: 10.1007/s11269-018-2070-x
10. *Detection and attribution of climate change signal in South India maximum and minimum temperatures*, P. Sonali, Ravi S. Nanjundiah and D. Nagesh Kumar, **Climate Research**,



- Inter-Research, Germany, Vol. 76, No. 2, pp. 145-160, October 2018, DOI: 10.3354/cr01530 (Published online on 10 October 2018)
11. *Trend Analyses of Seasonal Streamflows of the Tapi Basin*, Ganesh D Kale and D. Nagesh Kumar, **Water Conservation Science and Engineering**, Springer, Vol. 4, No. 1, pp. 1-11, March 2019, DOI: 10.1007/s41101-018-0062-6 (Published online on 07 December 2018)
  12. *Downscaling and Disaggregation of Wind Speed to River Basin in India for IPCC SRES Scenarios*, Anandhi A., V.V. Srinivas, D. Nagesh Kumar and R.S. Nanjundiah, **International Journal of Energy Water Food Nexus**, Vol. 1, No. 1, pp. 29-41, March 2019.
  13. *Multifractal Characterization of Meteorological Drought in India using Detrended Fluctuation Analysis*, Adarsh S, D Nagesh Kumar, Deepthi B, Gayathri G, Aswathy SS, Bhagyasree S, **International Journal of Climatology**, Wiley InterScience on behalf of Royal Meteorological Society (RMetS), Vol. 39, No. 11, pp. 4234-4255, September 2019, DOI: 10.1002/joc.6070
  14. *Partial informational correlation-based band selection for hyperspectral image classification*, Subir Paul and D Nagesh Kumar, **Journal of Applied Remote Sensing**, SPIE, Vol. 13, No. 4, 046505, October 2019, DOI: 10.1117/1.JRS.13.046505
  15. *Evaluation of Feature Selection and Feature Extraction Techniques on Multi-temporal Landsat-8 Images for Crop Classification*, Subir Paul and D Nagesh Kumar, **Remote Sensing in Earth Systems Sciences**, Springer, Vol. 2, No. 4, pp 197-207, December 2019, DOI: 10.1007/s41976-019-00024-8
  16. *Simultaneous retrieval of global scale Vegetation Optical Depth, surface roughness, and soil moisture using X-band AMSR-E observations*, Karthikeyan L, Ming Pan, Alexandra G. Konings, María Piles, Roberto Fernandez-Moran, D. Nagesh Kumar and Eric F. Wood, **Remote Sensing of Environment**, Elsevier, Vol. 234, 111473, pp. 19, December 2019, DOI: 10.1016/j.rse.2019.111473
  17. *Delineation of Flood-Prone Areas using Modified Topographic Index for a River Basin*, Nagesh Kumar D, Apoorva R Shastry and K.Srinivasa Raju, **H2Open Journal**, IWA Publishing, UK, Vol. 3, No. 1, pp. 58-68, January 2020, DOI: 10.2166/h2oj.2020.021
  18. *Effect of Structural Uncertainty in Passive Microwave Soil Moisture Retrieval Algorithm*, Lanka Karthikeyan, Ming Pan, D Nagesh Kumar and Eric F. Wood, Special issue on "Radar and Radiometric Sensors and Sensing", **Sensors**, MDPI, Switzerland, Vol. 20, No. 4, 1225, pp. 12, February 2020, DOI:10.3390/s20041225
  19. *Review of Recent Advances in Climate Change Detection and Attribution Studies: A Large-Scale Hydroclimatological Perspective*, **Invited Review Paper**, Sonali P. and D. Nagesh Kumar, **Journal of Water and Climate Change**, IWA Publishing, UK, Vol. 11, No. 1, pp. 1-29, March 2020, DOI: 10.2166/wcc.2020.091
  20. *Evolutionary Algorithms, Swarm Intelligence Methods and their Applications in Water Resources Engineering: A State-of-the-Art Review*, **Invited Review Paper**, Janga Reddy M and D. Nagesh Kumar, **H2Open Journal**, IWA Publishing, UK, Vol. 3, No. 1, pp. 135-188, January 2020, DOI: 10.2166/h2oj.2020.128
  21. *Review of Approaches for Selection and Ensembling of GCMs*, **Invited Review Paper**, Srinivasa Raju K. and D. Nagesh Kumar, **Journal of Water and Climate Change**, IWA Publishing, UK, Vol. 11, No. 3, pp. 577-599, September 2020, DOI: 10.2166/wcc.2020.128
  22. *Evaluation Framework of Landsat-8 based actual evapotranspiration estimates in data-sparse catchment*, Subir Paul, C. Banerjee and D. Nagesh Kumar, **Journal of Hydrologic Engineering**, American Society of Civil Engineers (ASCE), USA, Vol. 25, No. 9, September 2020, DOI: 10.1061/(ASCE)HE.1943-5584.0001992

23. *Canopy Averaged Chlorophyll Content Prediction of Pear Trees using Convolutional Auto-Encoder on Hyperspectral Data*, Subir Paul, V. Poliyapram, N. Imamoglu, K. Uto, R. Nakamura and D. Nagesh Kumar, **IEEE Journal of Selected Topics in Applied Earth Observations and Remote Sensing (JSTARS)**, IEEE Xplore Digital Library, Vol. 13, No. 1, pp. 1426-1437, December 2020, DOI: 10.1109/JSTARS.2020.2983000
24. *Estimation of daily actual evapotranspiration using vegetation coefficient method for clear and cloudy sky conditions*, Shwetha H.R. and D. Nagesh Kumar, **IEEE Journal of Selected Topics in Applied Earth Observations and Remote Sensing (JSTARS)**, IEEE Xplore Digital Library, Vol. 13, No. 1, pp. 2385-2395, December 2020, DOI: 10.1109/JSTARS.2020.2989422
25. *Transformation of Multispectral Data to Quasi-Hyperspectral Data using Convolutional Neural Network Regression*, Subir Paul and D. Nagesh Kumar, **IEEE Transactions on Geoscience and Remote Sensing**, IEEE, Vol. 59, No. 4, pp. 3352-3368, April 2021, DOI: 10.1109/TGRS.2020.3009290
26. *Decline in terrestrial water recharge with increasing global temperatures*, Chandan Banerjee, Ashish Sharma and D. Nagesh Kumar, **Science of the Total Environment**, Elsevier, Vol. 764, 142913, pp. 1-10, April 2021, DOI: 10.1016/j.scitotenv.2020.142913
27. *Multicriterion decision making in groundwater planning*, Shishir Gaur, K. Srinivasa Raju, D. Nagesh Kumar and Mayank Bajpai, **Journal of Hydroinformatics**, IWA Publishing, Vol. 23, No. 3, pp. 627–638, May 2021, DOI: 10.2166/hydro.2021.122
28. *Estimation of Seasonal Base Flow Contribution to a Tropical River using Stable Isotope Analysis*, Himanshu Bhagat, Prosenjit Ghosh and D Nagesh Kumar, **Journal of Hydrology**, Elsevier, Vol. 601, 126661, Oct 2021, DOI: 10.1016/j.jhydrol.2021.126661
29. *An overview of flood concepts, challenges, and future directions*, Mishra A.K., S. Mukherjee, B. Merz, V.P. Singh, D. Wrights, G. Villarini, Subir Paul, D. Nagesh Kumar, Prakash K, Dev N, G. Schumann, and J.R. Stedinger, **Journal of Hydrologic Engineering**, American Society of Civil Engineers (ASCE), USA, Vol. 27, No. 6, 03122001, pp. 1-30, June 2022, DOI: 10.1061/(ASCE)HE.1943-5584.0002164.
30. *Channel evolution of the Himalayan tributaries in northern Brahmaputra plain in recent centuries*, Rajesh Kumar Sah, D. Nagesh Kumar, and Apurba Kumar Das, **Acta Geophysica**, Springer, pp. 1317-1330, June 2022, DOI: 10.1007/s11600-022-00780-0
31. *Generating pre-harvest crop maps by applying Convolutional Neural Network on Multi-temporal Sentinel-1 Data*, Subir Paul, Mamta Kumari, C S Murthy, and D Nagesh Kumar, **International Journal of Remote Sensing**, Taylor & Francis, Vol. 43, No. 15-16, pp. 6078-6101, 2022, DOI: 10.1080/01431161.2022.2030072
32. *Avulsion distribution on rivers in the Himalayan foreland region*, Rajesh Kumar Sah, D. Nagesh Kumar, and Apurba Kumar Das, **Hydrological Sciences Journal**, Taylor & Francis, UK, Vol. 67, No. 14, pp. 2175-2190, 2022, DOI: 10.1080/02626667.2022.2136000
33. *Streamflow forecasting in a climate change perspective using E-FUSE*, Rishith Kumar Vogeti, Sriman Pankaj Boindala, D Nagesh Kumar, and K Srinivasa Raju, **Journal of Water and Climate Change**, IWA Publishing, UK, Vol. 13, No. 11, pp. 3934-3950, November 2022, DOI:10.2166/wcc.2022.251
34. *Impact of bare soil pixels identification on clay content mapping using airborne hyperspectral AVIRIS-NG data: spectral indices versus spectral unmixing*, George E.B., C. Gomez, D. Nagesh Kumar, S. Dharumarajan and M. Lalitha, **Geocarto International**, Taylor & Francis, Vol. 37, No. 27, pp. 15,912-15,934, 2022, DOI: 10.1080/10106049.2022.2102241
35. *Physics-informed deep learning framework to model intense precipitation events at super*

- resolution*, Teufel B., F. Carmo, L. Sushama, L. Sun, M. N. Khaliq, S. Belair, A. Shamseldin, D. Nagesh Kumar, and J. Vaze, **Geoscience Letters**, Springer Open, Vol. 10, Article No. 9, pp. 1-9, April 2023, DOI: 10.1186/s40562-023-00272-z
36. *Assessment of spectral reduction techniques for endmember extraction in unmixing of hyperspectral images*, George E.B., C.R. Ternikar, R. Ghosh, D. Nagesh Kumar, C. Gomez, T. Ahmad, A.S. Sahadevan, P.K. Gupta, A. Misra, Special Issue on "Parameter Retrieval and Applications with Imaging Spectroscopy Data from AVIRIS-NG", **Advances in Space Research**, Elsevier, 2022, in print, DOI: 10.1016/j.asr.2022.06.028
37. *Endmember Variability based Abundance Estimation of Red and Black Soil over Sparsely Vegetated Area Using AVIRIS-NG Hyperspectral Image*, Sahadevan, A.S., T. Ahmad, R.B. Lyngdoh, D. Nagesh Kumar, Special Issue on "Parameter Retrieval and Applications with Imaging Spectroscopy Data from AVIRIS-NG", **Advances in Space Research**, Elsevier, 2023, in print, DOI: 10.1016/j.asr.2023.05.027 (Published online on 19 May 2023)



## Evaluation of precipitation forecasts for five-day streamflow forecasting in Narmada River basin

Ankit Singh, Soubhik Mondal, Nibedita Samal & Sanjeev Kumar Jha

To cite this article: Ankit Singh, Soubhik Mondal, Nibedita Samal & Sanjeev Kumar Jha (2022): Evaluation of precipitation forecasts for five-day streamflow forecasting in Narmada River basin, Hydrological Sciences Journal, DOI: [10.1080/02626667.2022.2151913](https://doi.org/10.1080/02626667.2022.2151913)

To link to this article: <https://doi.org/10.1080/02626667.2022.2151913>



View supplementary material



Published online: 16 Dec 2022.



Submit your article to this journal



Article views: 23



View related articles



View Crossmark data

# Evaluation of precipitation forecasts for five-day streamflow forecasting in Narmada River basin

Ankit Singh, Soubhik Mondal, Nibedita Samal and Sanjeev Kumar Jha

Department of Earth and Environmental Sciences, Indian Institute of Science Education and Research Bhopal, Madhya Pradesh, India

## ABSTRACT

The accuracy of quantitative rainfall forecasts (QPFs) obtained from numerical weather prediction (NWP) models plays a crucial role in setting up a catchment streamflow forecasting system. Additionally, a suitable hydrological model is required. This study addresses input and model uncertainty in developing a five-day streamflow forecasting system in Narmada River Basin. We use deterministic and ensemble QPFs obtained from the Japan Meteorological Agency (JMA), National Centre for Medium Range Weather Forecasting (NCMRWF), and European Centre for Medium-Range Weather Forecasts (ECMWF). We use two hydrological models, the Soil and Water Assessment Tool (SWAT) and variable infiltration capacity (VIC), to generate streamflow forecasts. By comparing simulated streamflow forecasts with the observed discharge data, our results indicate that the forecast accuracy of NCMRWF is better than other forecasting products for lead times of two to five days. The streamflow generated using VIC produces better results than that obtained from the SWAT hydrological model.

## ARTICLE HISTORY

Received 17 January 2022  
Accepted 7 October 2022

## EDITOR

A. Castellari

## ASSOCIATE EDITOR

M. Ionita

## KEYWORDS

Streamflow Forecasting; hydrological models; numerical weather prediction (NWP); National Centre for Medium Range Weather Forecasting (NCMRWF)

## 1 Introduction

Rainfall-runoff models are used as a standard tool for various hydrological applications, such as flood forecasting and modelling climate change, land-use variability, sediment loading, etc. (Sharma *et al.* 1987, Strasser and Mauser 2001, Zacharias *et al.* 2005, Begou *et al.* 2016, Tiwari *et al.* 2020, Singh *et al.* 2021). Before the model is used for streamflow forecasting, it must undergo calibration and validation to ensure that the model is ready to use. Since the main driver for any hydrological model is rainfall, we rely on the accuracy of quantitative precipitation forecasts (QPFs) obtained from a numerical weather prediction (NWP) model (Dvorak 1975, Roba *et al.* 2000, Cebin *et al.* 2010, Anumeha *et al.* 2017, Honorato *et al.* 2018, Dube *et al.* 2022). Streamflow forecasts generated using a deterministic QPF will significantly impact decision makers as it does not provide information on the associated uncertainty. Hence, researchers and forecast agencies have preferred ensemble QPFs in their streamflow forecasting systems (Zhao *et al.* 2011, Kalra *et al.* 2013, Zhao and Zhao 2014). As forecast centres are improving their NWP models by providing more accurate and high-resolution rainfall forecasts, it is essential to evaluate their utility in generating streamflow forecasts with different lead times (Ferraris *et al.* 2002, Verbunt *et al.* 2006, Xuan *et al.* 2009, Honorato *et al.* 2018). However, past studies show that the skill of QPFs is not uniform in different regions, even within a single river catchment (Ferraris *et al.* 2002, Jasper and Kaufmann 2003, Lokeshwari *et al.* 2018). Thus, comparing the QPFs with the observed data is vital for

determining their reliability across a specific location (Fan *et al.* 2016). Pappenberger *et al.* (2009) noted that using ensembles in predictive analysis offers uncertainty information to forecast users, which helps them in making appropriate decisions. Chen *et al.* (2013) used the Ensemble Square-root-filter (EnSRF) data assimilation method with Hydrological Model (HYMOD) for flash flood forecasting in two basins of China and the USA. Aminyavari and Saghafian (2019) compared the streamflow forecasts obtained from four different NWP products in the Bashar River basin, a major tributary of the Great Karun River basin in southwestern Iran. They applied post-processing methods to determine which NWP model product gives a satisfactory result. Monhart *et al.* (2019) assessed ensemble streamflow prediction (ESP) using the Precipitation–Runoff–Evapotranspiration hydrotope model and rainfall ensembles obtained by the European Centre for Medium-Range Weather Forecasts (ECMWF) in the Verzasca alpine catchment. Jabbari *et al.* (2020) used the Sejong University Rainfall–Runoff hydrological model and the Weather Research and Forecasting (WRF) model for flood forecasting in Imjin River (South and North Korea). They simulated three flood events and checked the effect of spatial resolution of the WRF output in setting up a flood forecasting system. They found that the model's accuracy is not altered up to a spatial resolution of 8 km. Carlberg *et al.* (2020) studied the spatial displacement errors of the QPFs in 17 basins of Iowa, Illinois, and Wisconsin using the Hydrology Laboratory–Research Distributed Hydrologic Model. Siqueira *et al.* (2020)

used ECMWF forecast data for streamflow forecasting over South America with the Modelo Hidrológico de Grandes Bacías hydrological model. They found that at locations with a warm temperate, completely humid climate, forecasts based on the ECMWF were superior to ESP in terms of overall quality and discrimination skill. Since forecast skill varies along streams, finding a simple relationship between forecast skill and basin size has been attempted but was not always found to be valid. Ashrit *et al.* (2020) assessed the accuracy of the Indian National Centre for Medium Range Weather Forecasting (NCMRWF) models (NCMRWF Unified model (NCUM), NCMRWF REGIONAL UNIFIED MODEL (NCUM-R), and NCMRWF Global Ensemble Prediction System (NEPS-G)) in forecasting the August 2018 Kerala (India) flood, which was due to heavy rainfall. Their study finds that the rainfall forecasts by the deterministic NWP models (NCUM and NCUM-R) show high accuracy for shorter lead times (three days), whereas the ensemble forecast shows better accuracy for longer lead times. P. Zhao *et al.* (2021) assessed the accuracy of deterministic and ensemble forecasts of Bureau of Meteorology (BoM) with reference to the Australian Water Availability Project's climate datasets over Australia.

The second critical aspect of streamflow forecasting is selecting an appropriate hydrological model. Data-driven, conceptual, and physics-based are the three categories of hydrological models. Conceptual models are further divided into lumped and distributed models. Detailed and precise datasets are required to set up a fully distributed hydrological model, making it challenging. A lumped model cannot account for the features of a wide range of land uses and hydrological processes. To overcome the issues associated with fully distributed and lumped hydrological models, semi-distributed hydrological models are preferred, in which a watershed is divided into smaller sub-basins, and hydrological units are modelled either separately or together.

Block *et al.* (2009) proposed coupling regional climate models and various hydrological models to predict monthly streamflow in the Jaguaribe basin in Brazil. Randrianasolo *et al.* (2010) compared two hydrological approaches (lumped and distributed) over 211 catchments in France over 17 months. They demonstrated that the skill score of a lead time of two days is more accurate than that of other lead times. Tegegne *et al.* (2017), in their study over Lake Tana Basin in Ethiopia, used lumped and semi-distributed hydrological models to assess water resources in a data-scarce environment. Sharma *et al.* (2019) used a multimodal method to reduce bias in streamflow forecasting in the North Branch Susquehanna River basin in the United States. For the multimodal approach, they used the Global Ensemble Forecast System Reforecast version 2 and three hydrological models (the antecedent precipitation index, National Oceanic and Atmospheric Administration (NOAA)'s Hydrology Laboratory Research Distributed Hydrologic Model, and the Weather Research and Forecasting Hydrological model). They discovered that conditional mutual information indicates that each hydrological model contributes additional information to improve streamflow forecasting skills. Sun *et al.* (2019) compared the accuracy of four models for short-term

streamflow forecasting in two Chinese river basins – autoregressive model, autoregressive moving average model, artificial neural network model, and linear regression model – individually and in combination with wavelet transform. They concluded that wavelet-based hybrid models outperform individual models for long lead times. Ghaith *et al.* (2020) used a machine-learning hydrological and data-driven modelling approach for daily streamflow forecasting in Guadalupe Basin in Texas. Compared to the traditional conceptual hydrological model, the suggested hybrid hydrological data-driven model enhances daily prediction. Wijayarathne and Coulibaly (2020) used three lumped conceptual models and a semi-distributed model to compare flood forecasting results in the Waterford River watershed, St. John's, Newfoundland and Labrador, Canada. They found that some models performed better than others in forecasting the streamflow. Awol, Coulibaly, and Tsanis (2021) combined seven hydrological models with rainfall from Environment and Climate Change Canada and the US National Oceanic and Atmospheric Administration for streamflow forecasting. The studies evaluated the accuracy of various combinations for streamflow forecasting in Canada's Humber River watershed. Hapuarachchi *et al.* (2022) developed a seven-day streamflow forecasting system and tested it on 100 Australian catchments. The Génie Rural à 4 paramètres Journalier (GR4J) hydrological model and the Short-term Water Information Forecasting Tools hydrological modelling package are used for streamflow forecasting, calibrating the rainfall statistical Catchment Hydrologic Pre-Processor, and error reduction and quantification of hydrological uncertainty. They provided a benchmark for accepting forecast locations for public service. Out of 281 possible sites, 209 were chosen for public service. For streamflow forecasting, Kilinc (2022) proposed combining long short-term memory (LSTM) networks and the particle swarm optimization (PSO) algorithm. The study used three hydrological stations along the Orontes River basin. According to their findings, the PSO-LSTM model is more accurate than traditional models.

There are fewer studies in India on streamflow forecasting and on evaluating the accuracy of NWP models from a hydrological perspective. Sana *et al.* (2018) examined the recently developed Indian Monsoon Data Assimilation and Analysis (IMDAA) reanalysis data with India Meteorological Department (IMD) data and European Centre for Medium-Range Weather Forecasts (ECMWF) Re-Analysis Interim (ERA-Interim), Indian gridded observations, and Climate Prediction Center morphing method (CMORPH) data for the whole of India. The study was conducted in 2008 and 2009, and they discovered that the IMDAA can capture the events and intensity of the monsoon period. Goswami *et al.* (2018) forecasted streamflow in the upper and lower sub-basins of the Narmada River basin using the NCUM rainfall forecast and the Soil and Water Assessment Tool (SWAT) hydrological model. Pattanaik *et al.* (2019) investigated the IMD's operational extended-range forecast (ERF) system between 2009 and 2016. The Climate Forecast System version 2 coupled model is used by IMD (CFSv2). The performance of ERF for the southwest monsoon, northeast monsoon, cyclones over the Bay of Bengal, and maximum and minimum temperature were discussed from 2009 to 2018. Long-term forecasts for the southwest monsoon



seasons accurately reflected intra-seasonal variability, such as monsoon delay/early onset, active/break spells, etc. The usage of NWP and WRF model output in streamflow/flood forecasting was tested by Asghar *et al.* (2019). Regional NWP down-scaled rainfall performed well in quantitatively predicting flood waves, and a multimodal approach offered value in giving valid flood warnings as early as six days ahead.

Abinash *et al.* (2019) evaluated the utility of a recurrent neural network (RNN) and radial basis function network (RBFN) for streamflow forecasting in the Mahanadi River basin. They demonstrated that the RNN outperforms the RBFN. In streamflow forecasting, the tansig transfer function with RBFN performed better. Poonia and Lal Tiwari (2020) set up feedforward back-propagation and RBFN models for the Hoshangabad catchment of the Narmada River basin. They demonstrated that the ANN model performs better than the traditional model. Nanditha and Mishra (2021) examined the current state of flood early warning systems in India and proposed improvements for the future. They highlighted the importance of integrating enhanced meteorological forecasting, hydrological and hydraulic modelling, data assimilation, and post-processing to translate ensemble weather and climate forecasts to hydrological ensemble prediction systems. Their findings also highlight the significance of better inflow forecasting with sufficient lead time for reservoir operations, as reservoir operation decisions may be critical for flood management. Nayak and Thomas (2021) used the SWAT model coupled with future General Circulation Models (GCMs) scenarios for streamflow forecast in the Mahanadi River basin, India. Kumari *et al.* (2021) compared GR4J and variable infiltration capacity (VIC) hydrological models for streamflow forecasting in Kangsabati River Basin in eastern India. They selected 13 statistical criteria with which to evaluate the results and recommended the GR4J in the data-scarce region due to its simpler and lower input data requirements. Tiwari *et al.* (2021) examined the influence of bias-corrected rainfall forecast and streamflow. The VIC model was used over the Narmada River basin to calculate runoff, root zone depth, and streamflow. The results suggested that utilizing bias-corrected rainfall improves streamflow forecasting significantly, but that further bias correction is needed.

In India, the NCMRWF provides rainfall forecasts from its UK Met Office Unified Model-based deterministic model (NCUM) and ensemble prediction system (NEPS). To our knowledge, the utility of various QPFs from different NWP

models is still being explored in streamflow forecasting. This study sets up a streamflow forecasting system using the SWAT and VIC hydrological models over the Manot Watershed, a part of the upper Narmada River basin in central India. Deterministic and ensemble QPFs obtained from three global NWP models, namely Japan Meteorological Agency (JMA), NCMRWF, and ECMWF, with  $0.25^\circ \times 0.25^\circ$  resolution are used for streamflow forecasting for the monsoon period (June to September) of the year 2018 with one to five days' lead time. The main objectives of this study are: (i) to compare the performance of two semi-distributed hydrological models (SWAT and VIC) for streamflow forecasting, (ii) to assess the accuracy of three NWP models (JMA, ECMWF, and NCMRWF) for streamflow forecasting in Manot watershed, and (iii) to compare the streamflow forecasts for lead times of one to five days using deterministic and ensemble rainfall forecasts.

## 2 Data and study area

### 2.1 Meteorological forecast data

The precipitation dataset at  $0.25^\circ$  spatial resolution obtained from the Indian Meteorological Department (IMD) was used to calibrate and validate the SWAT model. ERA5 datasets at  $0.25^\circ$  spatial resolution were used to calibrate and validate the VIC model. In terms of spatial resolution, the archived data of different NWP models vary from one to another. Therefore, it was necessary to resample them to a standard spatial grid for their use in the hydrological model. We have chosen  $0.25^\circ$  resolution data from all the NWP models. The Observing System Research and Predictability Experiment (THORPEX) Interactive Grand Global Ensemble (TIGGE) datasets are used for this study (Bougeault *et al.* 2010). NWP data from the TIGGE dataset are continuous, with lead times ranging from 6 to 384 h in 6-h increments. For this study, only 24-h incremental data is used for forecasting one-to five-day streamflow from the different NWP models (ECMWF, JMA, and NCMRWF).

### 2.2 Study area

Manot and Dindori watersheds are selected for this study. Both watersheds are part of central India's upper Narmada River basin (Fig. 1). Central Water Commission of India (CWC) established a discharge monitoring system at the outlet on

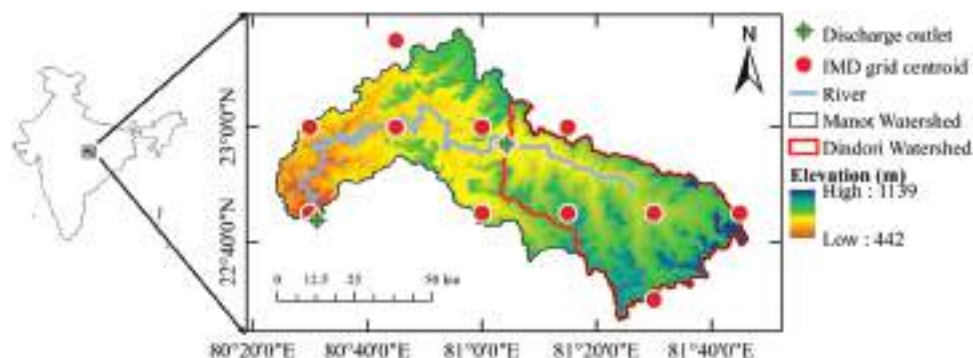


Figure 1. Location of Manot and Dindori watershed. Central Water Commission (CWC) discharge outlets are also shown in the map.

the Narmada River at 22°44'09"N, 80°30'47"E for the Manot watershed and at 22°56'52"N, 81°04'34"E for the Dindori watershed. Manot is the last discharge location downstream of the Narmada River, just before the Bargi dam. The Manot watershed extends geographically from 22°26' to 23°18'N and from 80°24' to 81°47'E, and Dindori ranges from 22°67' to 22°80'N and from 81°11' to 81°40'E. The total area of Manot and Dindori watersheds is 4980 km<sup>2</sup> and 2309 km<sup>2</sup>, respectively. Most of the watershed areas are in the Mandla district, with some parts in the Shadol district of Madhya Pradesh in India. The topography of the study area is primarily hilly, and the region with maximum elevation is 1139 m above mean sea level, while the minimum elevation is 442 m. Most hilly areas are covered by forest, and the low-lying area is fertile and mostly plain. The average annual rainfall in the watershed is approximately 1596 mm. The region receives the majority of its rainfall during the monsoon period (i.e. June to September). The watershed climate is classified as sub-tropical and sub-humid. Most of the soil in this region is loamy and clayey loamy.

### 2.3 Outline of the article

So far, we have discussed the international and national status of streamflow forecasting using different NWP forecast rainfall and hydrological models (in [section 1](#): Introduction). The overall description of the datasets and study area is provided in [section 2](#) (Data and study area). The remainder of this paper is organized as follows: [section 3](#) (Model set-up and methodology) gives details about the SWAT and VIC hydrological models and the datasets that are required to set up these hydrological models ([Section 3.1](#)). [Section 3.2](#) presents the detailed methodology that is adopted for this work. The Results and analysis section ([Section 4](#)) contains the evaluation of skill of the different NWP models ([section 4.1](#)), evaluation of the hydrological models ([section 4.2](#)), evaluation of deterministic forecasts ([section 4.3](#)), and evaluation of ensemble forecasts ([section 4.4](#)). After the results, we summarize and conclude the study in [section 5](#) (Discussion and conclusions).

## 3 Model set-up and methodology

### 3.1 Observed data and model set-up

The SWAT hydrological model is used to obtain the forecasted streamflow from different NWP models. SWAT is a widely

used semi-distributed hydrological model for rainfall-runoff modelling. SWAT requires topographic data for generating streamflow and delineating the sub-basins, along with a Digital Elevation Model (DEM) soil map and land-use map to define the different hydrological response units (HRUs) (Abbaspour *et al.* 2007, Singh and Kumar Jha 2021). Other data sources used for the SWAT model set-up, along with its description, resolution and sources, are provided in [Table 1](#). The meteorological data consisted of daily precipitation and daily minimum and maximum temperature data from the IMD and discharge data from the CWC, which were used to calibrate and validate the model. SWAT auto-simulates the weather generator file's relative humidity, solar radiation, and wind speed. As the SWAT model automatically considers the rainfall grids close to the catchment, 11 IMD grids are considered by the SWAT model for the Manot watershed.

VIC is a semi-distributed, physically-based, and large-scale hydrological model. VIC is an open-source research model that solves both the water and the energy balance. The surface runoff and infiltration scheme were first introduced to generate runoff from excess precipitation concerning the infiltration capacity (Liang *et al.* 1994). This model divides the catchment into cells. Therefore, the catchment is treated as a grid cell. The model consists of multiple soil layers, and each layer has a different bulk density, infiltration capacity, saturated hydraulic conductivity, soil layer depths, and soil moisture diffusion parameters. The VIC model is a grid-based model with variable infiltration soil layers, and each of these layers characterizes the soil hydrological responses and local variability in the form of land-cover classes. The VIC model simulates each grid cell independently with the runoff time series, which is not uniformly distributed. In the routing model, no horizontal flow is allowed, and the flow from the channel back to the grids will not be considered. Once the flow reaches the channel, it will no longer contribute to the water budget. A linear transfer function model is used for the routing within a grid cell, and it is assumed that all runoff will follow a single flow direction and contribute to the outlet point. The meteorological data consisted of daily precipitation, minimum, and maximum temperature and wind speed from ERA5, and discharge data from CWC were used for calibration and validation of the model. The VIC model considers 10 grids of 0.25° × 0.25° for the Manot watershed and five grids of 0.25° × 0.25° for the Dindori watershed, as the VIC model considers only those grids whose centroid lies inside the catchment boundaries. Details of other datasets used in setting up the VIC model are given in [Table 1](#).

**Table 1.** Description of data sets used for setting up the Soil and Water Assessment Tool (SWAT) and Variable Infiltration Capacity (VIC) model.

Data	Resolution	Source	Model
Topography	90 m × 90 m	Shuttle Radar Topography Mission (SRTM)	SWAT/VIC
Land use/land cover	400 m × 400 m	Global Irrigated Area Mapping of International Water Management Institute (GWMI)	SWAT/VIC
Soil		Harmonized World Soil Database (HWSD)	SWAT/VIC
Streamflow	Daily (m <sup>3</sup> /sec)	Central Water Commission of India (CWC)	SWAT/VIC
Precipitation	0.25° × 0.25°	Indian Meteorological Department (IMD)	SWAT
	0.25° × 0.25°	ERA5	VIC
Temperature	0.25° × 0.25°	Indian Meteorological Department (IMD)	SWAT
	0.25° × 0.25°	ERA5	VIC
Wind Speed	0.25° × 0.25°	ERA5	VIC
Leaf area index (LAI)	0.25° × 0.25°	NEO (NASA Earth Observation)	VIC
Albedo	0.25° × 0.25°	NEO (NASA Earth Observation)	VIC



### 3.2 Methodology

After calibrating and validating the hydrological models, the daily simulated streamflow outputs from the SWAT and VIC models were compared against the observed data. The daily discharge data from 1 January 2011 to 31 December 2018 is used for this study. The first two years, from 1 January 2011 to 31 December 2012, are used as a warm-up period. This warm-up period is only used to adapt the basin's hydrological conditions for the model, and this period is not counted further in the performance evaluation of the model. The calibration period is from 2016 to 2018 and the validation period is from 2013 to 2015. Once a well-calibrated and validated model is established, the streamflow forecast for 2018 is generated using the QPFs obtained from three NWP models, namely JMA, NCMRWF, and ECMWF. Each of the QPFs has common spatial and temporal resolutions. The streamflow is forecasted for a five-day lead time. We change the following five-day

rainfall data with predicted rainfall to generate the forecasted streamflow for every day. Eleven parameters from SWAT calibration and uncertainty program (SWAT-CUP) are selected for calibrating the model; detailed descriptions of the parameters are given in Table 2. The detailed methodology applied for this work is shown in Fig. 2. The VIC model is calibrated and validated for the same period as the SWAT model, i.e. from 2013 to 2015 for validation and 2015 to 2018 for calibration. Parameters that are fixed during calibration, along with their description, are shown in Table 3.

Model performance is evaluated using Nash-Sutcliffe efficiency (NSE) as an evaluation criterion. NSE is a popular statistical criterion for measuring model performance in hydrology. Five other statistical criteria – root mean square error (RMSE), normalized root mean square error (NRMSE), absolute bias percentage (ABP), standard regression ( $R^2$ ), and correlation coefficient (CC) – are used along with NSE to

**Table 2.** Descriptions and final ranges of the parameters used for Soil and Water Assessment Tool (SWAT) model calibration.

Parameter	Definition	Process	Default range
ALPHA_BF.gw	Baseflow alpha factor for recession constant (days)	Groundwater	0 to 1
CN2.mgt*	Curve number for moisture condition II	Surface runoff	35 to 98
ESCO.hru	Soil evaporation compensation factor	Evaporation	0 to 1
GW_DELAY.gw	Groundwater delay time (days)	Groundwater	0 to 500
GW_REVAP.gw	Groundwater re-evaporation coefficient	Groundwater	0.02 to 0.2
GWQMN.gw	Threshold depth of water in the shallow aquifer required for return flow to occur (mm)	Groundwater	0–5000
HRU_SLP.hru	Average slope steepness (m/m)	Topographic	0 to 1
OV_N.hru*	Manning's "n" value for overland flow	Overland flow	0.01 to 30
RCHRG_DP.gw	Deep aquifer percolation fraction	Groundwater	0 to 1
REVAPMN.gw	Threshold depth for exchange with deep aquifer	Groundwater	0 to 500
SLSUBBSN.hru	Average slope length (m)	Topographic	10 to 150
SOL_AWC(.).sol*	Available water capacity of the soil layer (mm H <sub>2</sub> O/mm soil)	Soil water	0 to 1
SURLAG.bsn	Surface runoff lag time	Runoff	0.05 to 24

\*means the original value is multiplied by the adjustment factor (1 + given value within the range).

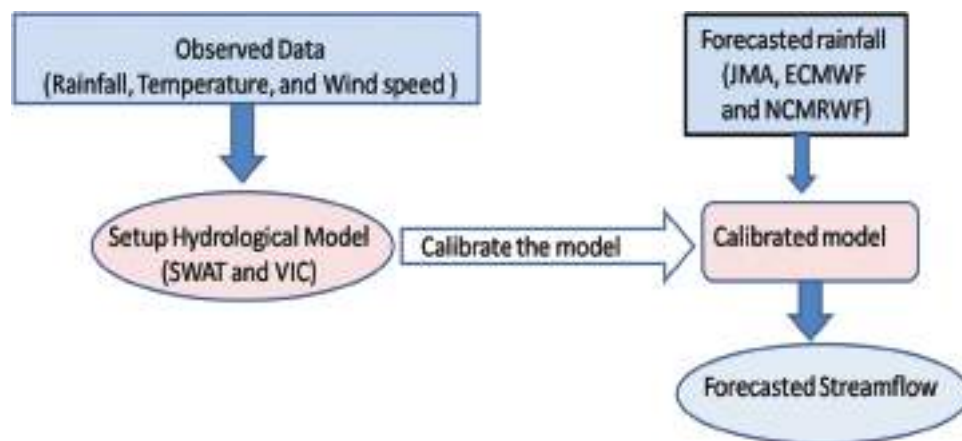


**Figure 2.** Flow chart used for setting up a framework for streamflow forecasting.

**Table 3.** Descriptions and default ranges of the parameters used for Variable Infiltration Capacity (VIC) model calibration European Centre for Medium-Range Forecast (ECMWF) (Se1 to Se5), Japan Metrological Agency (JMA) (Sj1 to Sj5), and National Centre for Medium-Range Weather Forecasting (NCMRWF).

Parameter	Definition	Process	Default range
$D_{max}$	Derived from saturated hydraulic conductivity (ksat) of soil by multiplying with slope.	Non-linear baseflow	>0 to ~30
$D_s$	The fraction of $D_{max}$ where non-linear baseflow takes place.	Non-linear baseflow	>0 to 1
$W_s$	The fraction of the soil moisture of the rock bottom soil layer where non-linear baseflow occurs. This is often analogous to $D_s$ .	Non-linear baseflow	>0 to 1
$b_{infil}$	Describes the quantity of obtainable infiltration capacity as a function of relative saturated grid cell area.	Infiltration	>0 to 0.4

compare forecasted streamflow accuracy. RMSE calculates the difference between observed and simulated values, and serves to aggregate the residuals into a single measure of predictive power. The NRMSE is a better indicator to assess performance because it is scale-free; due to normalizing the RMSE, the range of NRMSE is 0 to 1. ABP is the average tendency of modelled values to be larger or smaller than their observed values. The CC measures the relationship between two variables; 0 shows no connection, 1 shows a high positive relationship, and  $-1$  shows a high negative relationship. NSE is a normalized statistic that compares the quantity of residual variance (“noise”) to measured data variance (“information”). NSE ranges from  $-\infty$  to 1; a negative NSE shows that the observed mean is higher than predicted, and 1 indicates a perfect match between the observed and expected values.  $R^2$  is an index that measures the degree of the linear relationship between observed and simulated streamflow. RMSE, NRMSE, ABP,  $R^2$ , CC, and NSE are expressed by Equations (1–6):

$$RMSE = \sqrt{\frac{\sum_{i=1}^n (Q_o - Q_f)_i^2}{n}} \quad (1)$$

$$NRMSE = \frac{RMSE}{Q_{\max,o} - Q_{\min,f}} \quad (2)$$

$$ABP = \left| \sum_{i=1}^n \frac{(Q_f - Q_o) \times 100}{Q_o} \right| \quad (3)$$

$$R^2 = \frac{\sum_{i=1}^n \{(Q_o - \bar{Q}_o) \times (Q_f - \bar{Q}_f)\}^2}{\sum_{i=1}^n (Q_o - \bar{Q}_o)^2 - (Q_f - \bar{Q}_f)^2} \quad (4)$$

$$\text{Correlation coefficient} = \frac{\text{cov}(Q_f, Q_o)}{\text{sd}_{Q_f} \times \text{sd}_{Q_o}} \quad (5)$$

$$NSE = 1 - \frac{\sum_{i=1}^n (Q_f - \bar{Q}_f)^2}{\sum_{i=1}^n (Q_o - \bar{Q}_o)^2} \quad (6)$$

where  $\bar{Q}$  represents the average discharge, and  $o$  and  $f$  represent the observed and forecasted values. The threshold for RMSE is difficult to define; however, an RMSE of less than 0.5 is considered reasonable.

## 4 Results and analysis

### 4.1 Performance of different rainfall forecasts

Evaluation of rainfall forecasts obtained from various agencies (ECMWF, JMA, and NCMRWF) against the observation data (ERA5 and IMD) is performed by taking the sub-basin average rainfall for Dindori and Manot watersheds. The values of error statistics (RMSE, NRMSE, CC,  $R^2$ , and NSE) with different lead times (one to five days) for Manot and Dindori watersheds are presented in Table 4. It can be seen from Table 4 that the NCMRWF has higher accuracy for all lead times in both watersheds as the RMSE value is approximately 10/12 mm (Manot/Dindori) for IMD and approximately 14/13 mm for ERA5,

**Table 4.** Error statics with 1 to 5-day lead time for National Centre for Medium-Range Weather Forecasting (NCMRWF), Japan Metrological Agency (JMA), and European Centre for Medium-Range Forecast (ECMWF) forecasted rainfall with respect to ECMWF Re-Analysis-5 (ERA5) and Indian Metrological Department (IMD) rainfall for Manot and Dindori watershed.

Obs. vs. NWP rainfall	Lead time	Manot					Dindori				
		RMSE	NRMSE	CC	$R^2$	NSE	RMSE	NRMSE	CC	$R^2$	NSE
ERA5 vs. ECMWF	1 day	13.454	0.349	0.108	0.012	-1.444	14.617	0.345	0.125	0.016	-1.172
	2 days	15.439	0.290	0.047	0.002	-0.961	16.033	0.236	0.099	0.010	-0.874
	3 days	14.209	0.278	0.057	0.003	-1.371	14.993	0.244	0.050	0.003	-1.451
	4 days	21.370	0.125	-0.030	0.001	-0.441	20.453	0.174	-0.036	0.001	-0.623
	5 days	15.203	0.243	0.055	0.003	-1.041	15.427	0.251	0.044	0.002	-1.307
IMD vs. ECMWF	1 day	12.205	0.283	0.315	0.099	-0.452	13.391	0.326	0.217	0.047	-1.087
	2 days	15.914	0.179	0.183	0.033	-0.370	15.609	0.227	0.145	0.021	-0.745
	3 days	12.588	0.210	0.307	0.094	-0.315	15.250	0.229	0.224	0.050	-0.483
	4 days	14.867	0.211	0.199	0.040	-0.321	18.588	0.122	0.182	0.033	-0.258
	5 days	29.575	0.109	0.066	0.004	-0.107	21.430	0.127	0.110	0.012	-0.269
ERA5 vs. JMA	1 day	14.257	0.294	0.130	0.017	-1.113	14.821	0.314	0.155	0.024	-1.145
	2 days	13.621	0.310	0.140	0.020	-1.147	14.224	0.315	0.164	0.027	-1.157
	3 days	12.412	0.387	0.215	0.046	-1.344	13.041	0.386	0.221	0.049	-1.432
	4 days	11.987	0.339	0.259	0.067	-1.337	12.738	0.356	0.250	0.062	-1.422
	5 days	11.932	0.354	0.284	0.080	-1.145	12.516	0.349	0.282	0.080	-1.301
IMD vs. JMA	1 day	11.871	0.329	0.363	0.132	-0.503	13.529	0.380	0.276	0.076	-0.982
	2 days	13.104	0.272	0.258	0.067	-0.635	14.598	0.294	0.191	0.037	-1.063
	3 days	14.163	0.294	0.139	0.019	-0.803	15.525	0.329	0.086	0.007	-1.242
	4 days	12.702	0.263	0.186	0.035	-0.827	14.265	0.312	0.132	0.017	-1.354
	5 days	12.341	0.372	0.149	0.022	-1.090	14.018	0.420	0.092	0.009	-1.756
ERA5 vs. NCMRWF	1 day	15.410	0.188	0.090	0.008	-0.781	13.271	0.316	0.176	0.031	-1.713
	2 days	17.889	0.157	0.068	0.005	-0.501	15.305	0.181	0.126	0.016	-0.897
	3 days	13.938	0.315	0.111	0.012	-1.225	12.350	0.411	0.269	0.072	-2.152
	4 days	14.406	0.321	0.066	0.004	-1.274	13.683	0.353	0.140	0.019	-1.755
	5 days	14.865	0.323	0.019	0.000	-1.416	13.905	0.491	0.063	0.004	-2.754
IMD vs. NCMRWF	1 day	10.233	0.208	0.414	0.171	-0.386	12.076	0.206	0.301	0.090	-1.269
	2 days	10.467	0.272	0.394	0.155	-0.420	12.221	0.185	0.300	0.090	-1.136
	3 days	10.841	0.277	0.344	0.118	-0.516	12.577	0.265	0.275	0.076	-1.121
	4 days	10.180	0.260	0.375	0.141	-0.742	11.929	0.416	0.294	0.087	-2.552
	5 days	10.702	0.191	0.367	0.135	-0.527	11.712	0.347	0.367	0.135	-2.121

which is less compared to other forecasts. For IMD, CC is more than 0.35/0.3, and  $R^2$  is more than 0.1/0.75. For ERA5, CC is more than 0.66/0.14, which is relatively higher than the value for other NWP models. As expected, a lead time of one day for all of the models shows higher accuracy than longer lead times. The lowest accuracy is shown for four days' lead time, followed by two days' lead time, in the case of almost all the NWP models. However, the maximum values of CC (0.414) and  $R^2$  (0.171) are achieved by NCMRWF at a one-day lead time with respect to IMD, and the maximum value of NSE (−0.1065) is achieved by ECMWF for a five-day lead time with IMD. The minimum values of RMSE (10.18) and NRMSE (0.1094) are obtained for NCMRWF for a four-day lead time and for ECMWF with a five-day lead time, respectively, with respect to IMD for the Manot watershed. The minimum values of RMSE (10.18) and NRMSE (0.1094) are associated with a five-day lead time for NCMRWF and a four-day lead time for ECMWF, respectively, with respect to IMD. The maximum values of CC (0.367) and  $R^2$  (0.135) are associated with NCMRWF for a five-day lead time with respect to IMD; the minimum value of NSE (−0.2581) is associated with ECMWF for a four-day lead time with respect to IMD. The minimum values of RMSE (11.712) and NRMSE (0.122) are associated with NCMRWF for a five-day lead time and ECMWF for a four-day lead time, respectively, with respect to IMD for Dindori watershed. Of the 30 Dindori watersheds, 21 show higher maximum RMSE and NRMSE than the Manot watershed. Eleven times out of 30 for CC and  $R^2$ , and only 2 times out of 30 for NSE, Dindori watershed shows higher values than the Manot watershed. These observations imply that the NWP models' forecast rainfall is more reliable for large areas than for small areas.

#### 4.2 Evaluation of the SWAT and VIC hydrological models

Figure 3 compares the observed streamflow with the simulated streamflow for the validation and calibration periods (January 2013 to December 2018) obtained from the SWAT and VIC models for Dindori and Manot watershed. The black line

indicates the observed discharge, and red and blue lines show the simulated discharge from the VIC and SWAT models, respectively. Our results show that there is a similar trend between the observed and the simulated streamflow. The SWAT model seems to overestimate the peaks, while the VIC model estimates are close to the observations for Dindori watershed. For Manot watershed, discharge simulated by the hydrological models (SWAT and VIC) is close to the observed discharge data. Moreover, the VIC model simulates the low flows well, but the SWAT model shows a higher low flow than the VIC model during simulation.

NRMSE, CC,  $R^2$ , and NSE error statistics are used to evaluate the performance of the hydrological models, as shown in Fig. 3. In calibration and validation, both NSE and  $R^2$  values are more than 0.45 for the VIC and the SWAT model for both watersheds. The VIC model shows higher values of CC,  $R^2$ , and NSE (0.68/0.73, 0.47/0.53, 0.48/0.34) than the SWAT model (0.66/0.59, 0.44/0.34, 0.46/0.39) for the calibration and validation periods, respectively, for Dindori watershed. The simulated results for Manot watershed are almost the same for both SWAT (CC,  $R^2$ , and NSE: 0.61/0.69, 0.64/0.61, and 0.56/0.54) and VIC (CC,  $R^2$ , and NSE: 0.62/0.65, 0.60/0.60, and 0.57/0.55).

#### 4.3 Deterministic streamflow forecast comparison

##### 4.3.1 Dindori watershed

Figures 4 and 5 show the streamflow forecasted by using rainfall forecasts from three different agencies (ECMWF, JMA, and NCMRWF) in the SWAT and VIC hydrological models for the Dindori watershed from 1 June to 30 September. By comparing with the observed streamflow, we find that the streamflow generated by rainfall forecasts with a one-day lead time provides more accurate information than with a four- to five-day lead time. In Fig. 4, it can be seen that the peak values from 15 July to 1 August and from 15 August to 1 September are overestimated by two to three times by all NWP models for lead times of two to five days, particularly by the SWAT model

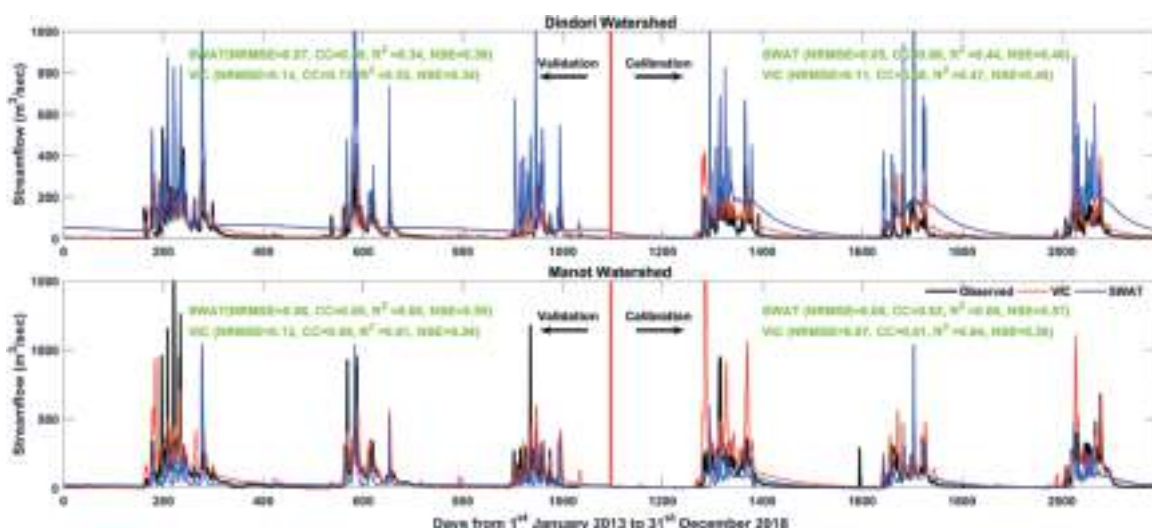


**Figure 3.** Time series plots of observed and simulated streamflow for Dindori and Manot Watershed. Simulations were performed using the Variable Infiltration Capacity (VIC) and Soil and Water Assessment Tool (SWAT) hydrological model.

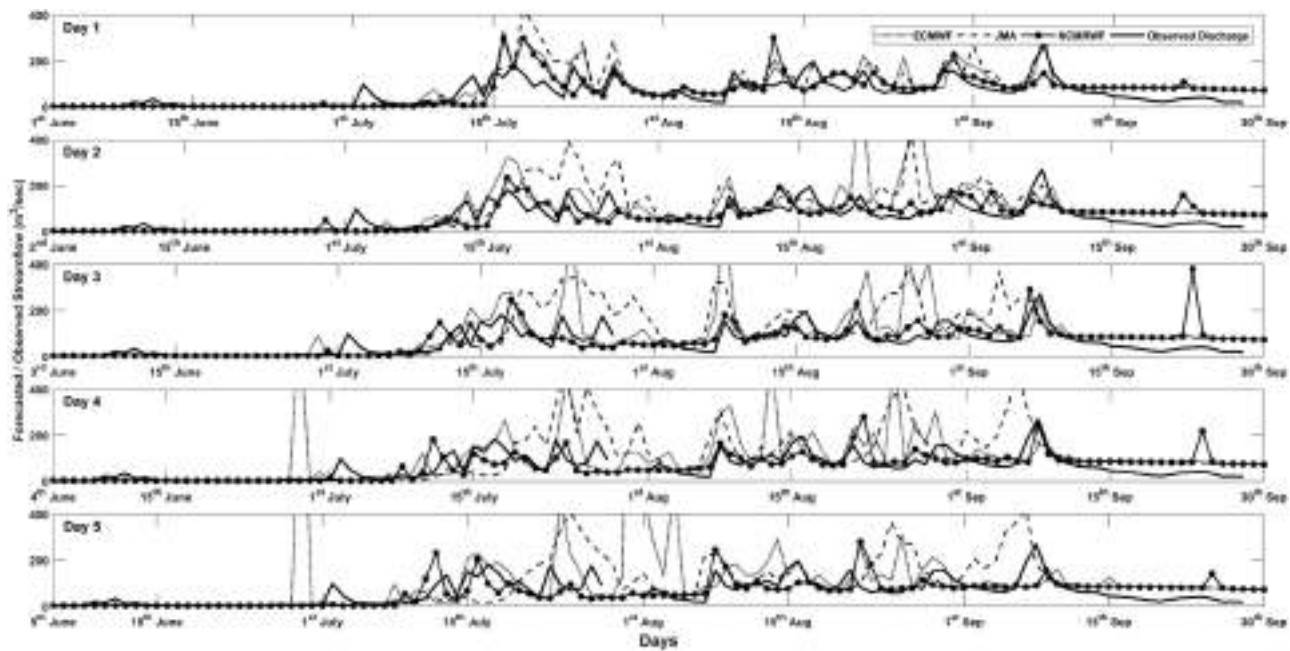


**Figure 4.** 1 to 5-day streamflow forecast generated from Soil and Water Assessment Tool (SWAT) hydrological model using the Japan Metrological Agency (JMA), the European Centre for Medium-Range Forecast (ECMWF), and the National Centre for Medium-Range Weather Forecasting (NCMRWF) rainfall forecasts for Dindori watershed.

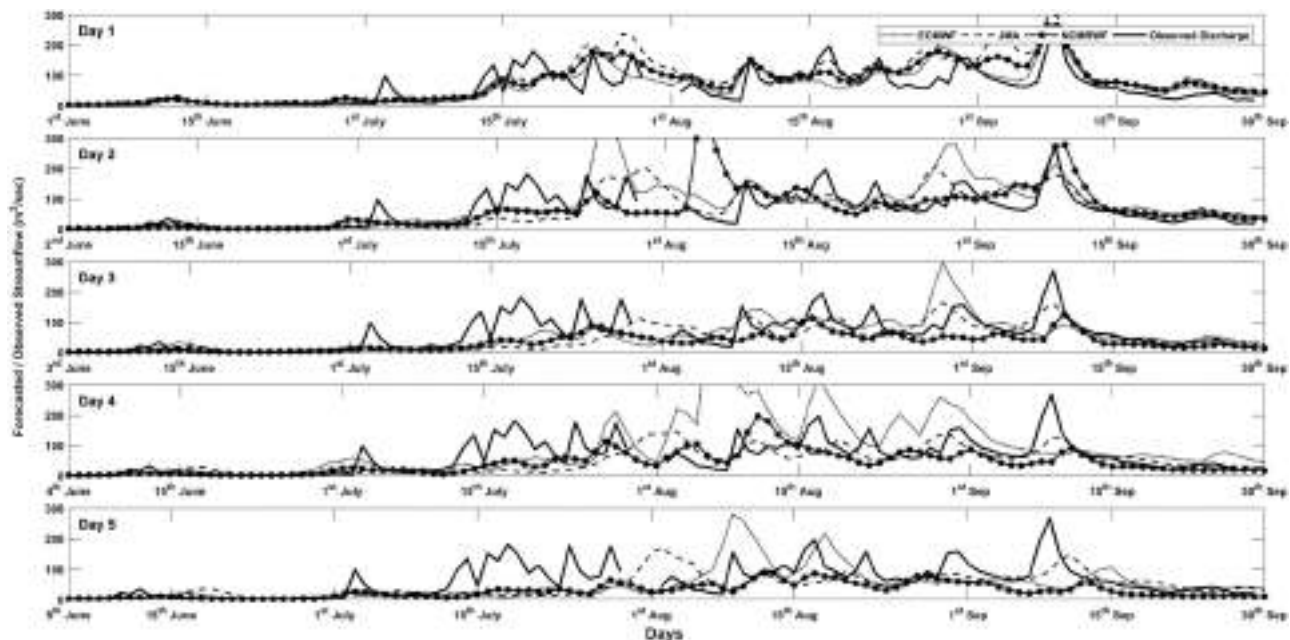


**Figure 5.** 1 to 5-day streamflow forecast generated from Variable Infiltration Capacity (VIC) hydrological model with the Japan Metrological Agency (JMA), the European Centre for Medium-Range Forecast (ECMWF), and the National Centre for Medium-Range Weather Forecasting (NCMRWF) rainfall forecasts for Dindori watershed.

using rainfall forecasts from ECMWF and JMA. Looking at the output from the VIC model (Fig. 5), we observe that the initial peak around 15 July is not at all captured by the VIC model for all lead times. Moreover, streamflow forecasted by the VIC hydrological model using the ECMWF rainfall forecast sometimes shows very high values (for instance, between 1 and 15 August). We can see that the forecasted streamflow is more

than four times higher compared to observed discharge data (Fig. 5, day 4 and day 5).

#### 4.3.2 Manot watershed

Figures 6 and 7 present the forecasted streamflow from SWAT and VIC hydrological models using rainfall forecasts from ECMWF, JMA, and NCMRWF for the Manot watershed from



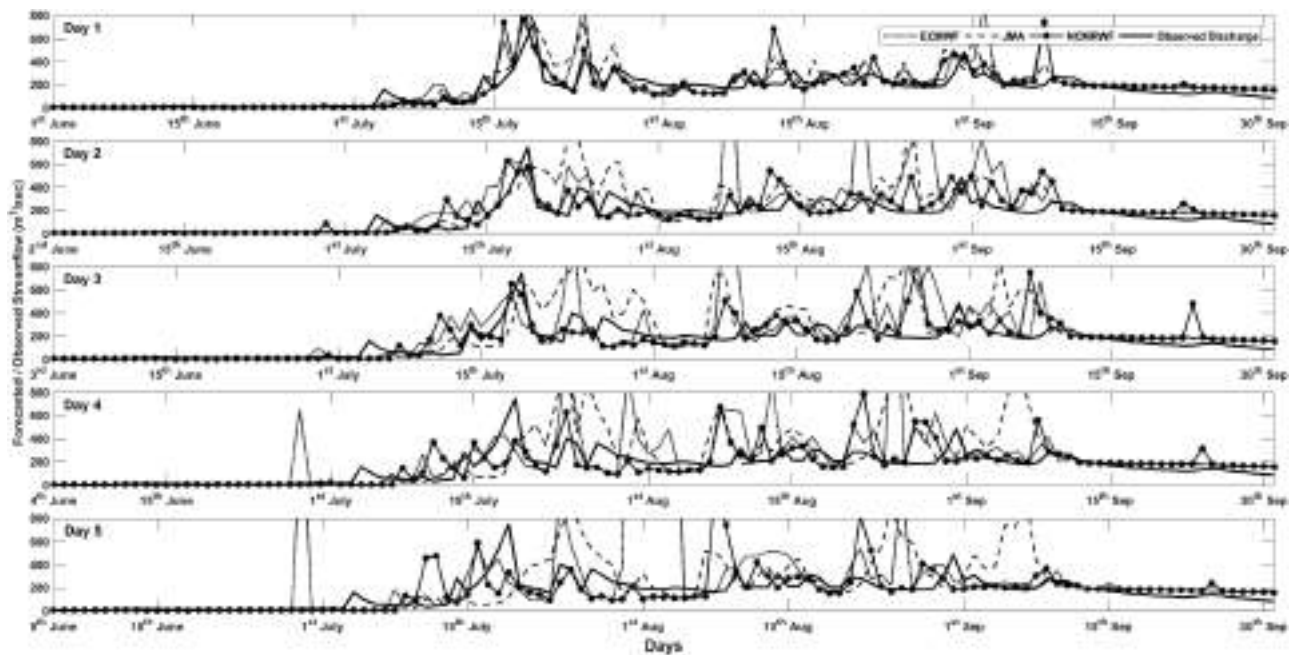


**Figure 6.** 1 to 5-day streamflow forecast generated by using the Soil and Water Assessment Tool (SWAT) hydrological model by using the Japan Metrological Agency (JMA), the European Centre for Medium-Range Forecast (ECMWF), and the National Centre for Medium-Range Weather Forecasting (NCMRWF) rainfall forecasts for Manot watershed.

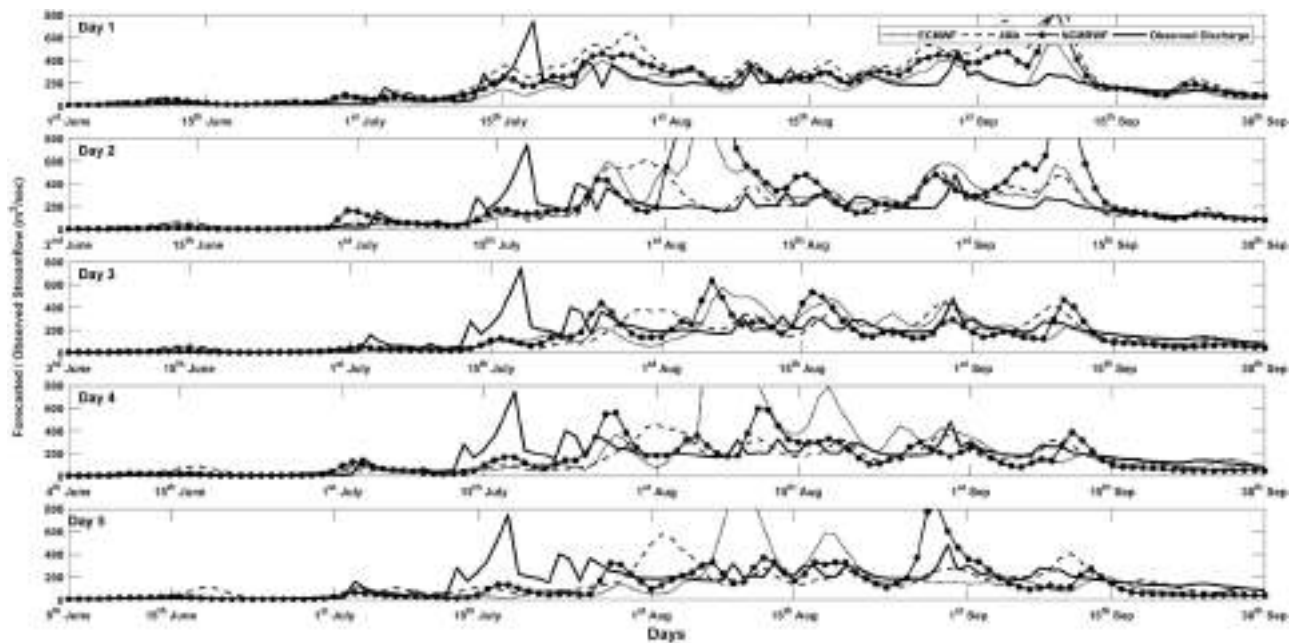


**Figure 7.** 1 to 5-day streamflow forecast obtained from Variable Infiltration Capacity (VIC) hydrological model using rainfall forecast from the Japan Metrological Agency (JMA), the European Centre for Medium-Range Forecast (ECMWF), and the National Centre for Medium-Range Weather Forecasting (NCMRWF) for Manot watershed.

1 June to 30 September (monsoon period). It is evident that for the lead time of one day, streamflow generated by both SWAT and VIC hydrological models using the rainfall forecasts from three agencies matches with the observations. In Fig. 6, it can be seen that the overestimation of the peak values for lead times of two to five days, from 15 July to 1 August and from 15 August to 1 September, for Manot watershed is similar to what we

observed in the case of Dindori watershed (Fig. 4). From Figs 6 and 7, it is evident that the first peak, around 15 July, is well captured by SWAT using rainfall from all the forecast agencies (Fig. 6), but not by VIC (half of the discharge data) (Fig. 7). From Figs 6 and 7, it is evident that the peak value around 10 September forecasted by the SWAT and VIC hydrological models using rainfall forecasts from all three agencies shows high

values (almost three times) compared to observed discharge for all lead times.

Figures 6 and 7 show that the streamflow forecast using the NCMRWF data performed better than that with the other two datasets (i.e. JMA and ECMWF), as the bulleted lines are close to the observed data for all lead times. JMA also captured three- to five-day forecasts well. However, sometimes the streamflow prediction using JMA and NCMRWF is inaccurate. Figures 5 and 6 show that the streamflow forecast using ECMWF data produces highly overestimated results.

The streamflow forecasts using the SWAT (Figs 4 and 6) hydrological model mostly show overestimation in comparison to the VIC (Figs 5 and 7) simulation. However, the VIC (Figs 5 and 7) simulated discharge is underestimated for some peaks. Supplementary Figure S1 also shows that the average streamflow for the June to September period is higher with SWAT than with the VIC model. Average streamflow (173.9/69.25, 178.22/65.11, 182.94/68.20, 173.48/63.13, 171.46/60.64) generated from NCMRWF rainfall by the SWAT model for Manot/Dindori watershed is close to the average of observed discharge data (153.82/59.50). For the VIC hydrological model, in contrast, streamflow forecasted using the ECMWF rainfall forecasts shows values that are closer to the average observed discharge data.

#### 4.3.3 Error statistics

We used six error statics to evaluate the performance of streamflow produced using rainfall forecasts from three

different agencies for Manot and Dindori watersheds. The error statistics calculated for the one- to five-day lead times, with the three datasets, obtained from the SWAT and VIC hydrological models, are shown in Table 5. From the table, it can be seen that the Dindori watershed shows lower RMSE and ABP compared to those for the Manot watershed, because these error statistics do not normalize the values.

The SWAT model results for Dindori and Manot watershed in Table 5 show that the RMSE value is low for NCMRWF and high for ECMWF for all lead times. For instance, the lowest value of RMSE is 47.009/104.99 for a two-day lead time with the NCMRWF data for Dindori/Manot watershed, and the highest value (129.575/787.12) is associated with the ECMWF model for a five-day lead time. The NRMSE shows low values for the NCMRWF data and high values for the JMA data for all lead times. An interesting observation is that the 3-day lead time shows the highest NRMSE (0.221, 0.192, and 0.185) for all the NWP model data for the Manot watershed. Also, for  $R^2$ , NSE, and CC, JMA shows high values and ECMWF shows low values for Manot watersheds. JMA shows high values of  $R^2$  (0.671), NSE (0.623), and CC (0.819) for a one-day lead time. ECMWF shows low values of  $R^2$  (0.065) and CC (0.225) for a five-day lead time. For Dindori watershed, high values of CC (0.632) are associated with NCMRWF for a one-day lead time, high values of  $R^2$  (0.400) are associated with NCMRWF for a two-day lead time, and high values of NSE (0.255) are associated with NCMRWF for a one-day lead time.

Error statistics associated with the streamflow forecasted by VIC using the forecast rainfall from the different agencies

**Table 5.** Error statics with 1 to 5-day lead time for National Centre for Medium-Range Weather Forecasting (NCMRWF), Japan Metrological Agency (JMA), and European Centre for Medium-Range Forecast (ECMWF) with respect to Soil and Water Assessment Tool (SWAT) and Variable Infiltration Capacity (VIC) model for the deterministic forecast for Manot and Dindori watershed.

Models	Lead time	Dindori						Manot					
		RMSE	NRMSE	ABP	CC	R2	NSE	RMSE	NRMSE	ABP	CC	R2	NSE
VIC with ECMWF	DAI 1	102.526	0.188	17919.558	0.662	0.438	0.307	39.511	0.165	7470.410	0.744	0.553	0.469
	DAY 2	191.198	0.173	25561.307	0.518	0.268	0.196	61.632	0.159	9141.866	0.613	0.376	0.288
	DAY 3	126.907	0.223	17201.943	0.549	0.302	0.174	50.217	0.170	6106.021	0.558	0.312	-0.002
	DAY 4	340.749	0.141	26479.929	0.318	0.101	0.069	103.752	0.169	10774.745	0.356	0.127	-0.006
	DAY 5	187.917	0.176	15862.179	0.337	0.114	-0.011	60.806	0.218	5332.077	0.394	0.155	-0.346
SWAT with ECMWF	DAI 1	122.56	0.133	22606.68	0.57	0.755	0.536	66.438	0.202	9352.767	0.554	0.307	0.189
	DAY 2	242.36	0.143	27888.08	0.216	0.465	0.133	96.034	0.144	10722.839	0.439	0.192	0.073
	DAY 3	228.31	0.185	27163.23	0.163	0.404	0.06	106.871	0.169	10856.332	0.337	0.114	-0.022
	DAY 4	239.95	0.133	27698.34	0.187	0.433	0.099	113.493	0.179	11197.012	0.323	0.105	-0.031
	DAY 5	787.12	0.095	37575.4	0.065	0.255	0.018	129.575	0.118	10900.723	0.261	0.068	-0.032
VIC with JMA	DAI 1	194.135	0.180	31678.506	0.651	0.424	0.174	53.713	0.182	10252.656	0.754	0.568	0.396
	DAY 2	136.816	0.227	21507.573	0.567	0.322	0.253	47.362	0.227	7165.559	0.626	0.392	0.235
	DAY 3	119.016	0.264	17167.811	0.541	0.293	0.050	45.559	0.279	5340.216	0.625	0.390	-0.246
	DAY 4	127.411	0.284	16034.062	0.437	0.191	-0.324	49.295	0.341	5159.167	0.546	0.298	-0.649
	DAY 5	139.438	0.246	16247.272	0.334	0.111	-0.493	54.717	0.322	4867.715	0.410	0.168	-1.421
SWAT with JMA	DAI 1	107.35	0.119	22907.82	0.671	0.819	0.623	70.539	0.168	9971.339	0.602	0.362	0.254
	DAY 2	156.34	0.152	25987.12	0.474	0.689	0.382	82.603	0.188	10983.699	0.557	0.311	0.160
	DAY 3	193.85	0.221	28894.83	0.446	0.668	0.302	98.151	0.265	11969.021	0.506	0.256	0.078
	DAY 4	209.89	0.183	28166.35	0.364	0.603	0.256	109.115	0.225	11573.455	0.375	0.141	-0.010
	DAY 5	176.01	0.182	25938.47	0.4	0.633	0.322	96.195	0.232	10773.165	0.418	0.175	0.042
VIC with NCMRWF	DAI 1	132.048	0.163	24799.032	0.673	0.452	0.352	42.959	0.163	8861.533	0.768	0.590	0.490
	DAY 2	382.783	0.156	33361.309	0.330	0.109	0.013	63.062	0.157	7784.112	0.509	0.259	0.161
	DAY 3	128.927	0.204	16332.878	0.533	0.284	0.123	47.853	0.390	3829.088	0.725	0.525	-2.082
	DAY 4	133.601	0.226	16704.352	0.484	0.234	0.027	50.295	0.256	4808.850	0.543	0.295	-0.750
	DAY 5	153.449	0.188	15249.121	0.395	0.156	-0.087	55.084	0.645	3163.194	0.608	0.370	-4.634
SWAT with NCMRWF	DAI 1	104.99	0.138	21115.88	0.598	0.773	0.583	56.012	0.187	8132.864	0.591	0.349	0.255
	DAY 2	112.82	0.181	21643.36	0.48	0.693	0.433	47.009	0.204	7616.758	0.632	0.400	0.223
	DAY 3	149.35	0.192	22218.7	0.252	0.502	0.144	64.898	0.171	7998.701	0.413	0.171	-0.071
	DAY 4	150.61	0.175	21065.04	0.195	0.442	0.038	58.642	0.211	7385.129	0.429	0.184	-0.173
	DAY 5	169.91	0.161	20818.22	0.126	0.355	-0.045	58.075	0.210	7074.445	0.435	0.189	-0.160

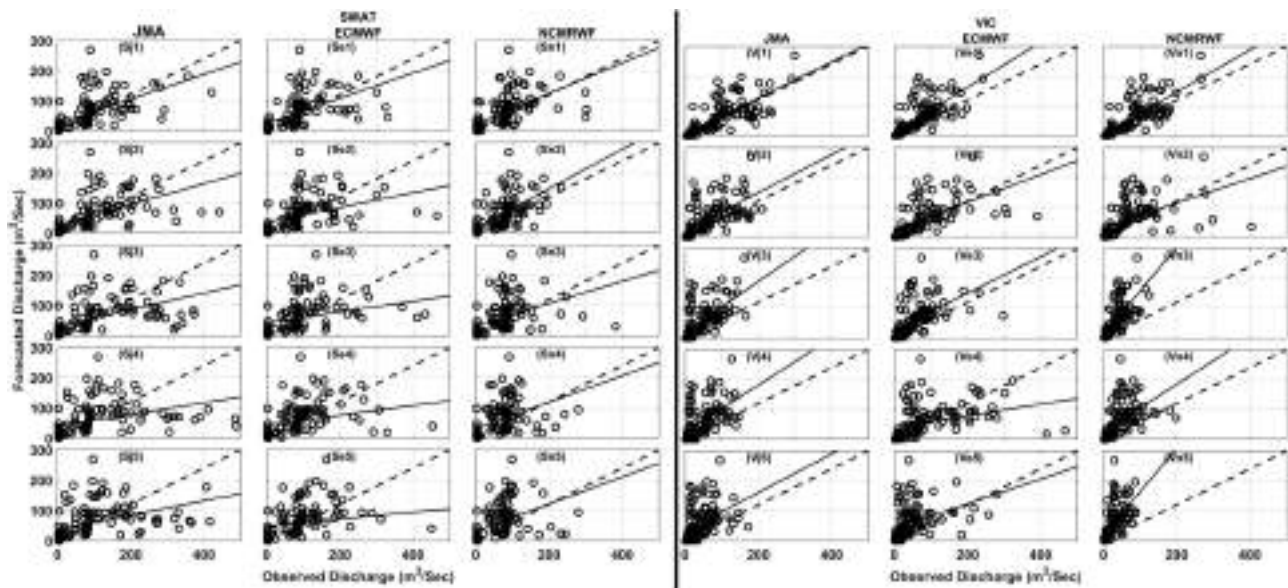


**Figure 8.** Scatter plot of forecasted and observed streamflow obtained from Soil and Water Assessment Tool (SWAT) and Variable Infiltration Capacity (VIC) hydrological models for the Dindori watershed. The rainfall forecasts of the Japan Meteorological Agency (JMA) (Sj1 to Sj5 for SWAT and Vj1 to Vj5 for VIC), the European Centre for Medium-Range Forecast (ECMWF) (Se1 to Se5 for SWAT and Ve1 to Ve5 for VIC), and the National Centre for Medium-Range Weather Forecasting (NCMRWF) (Sn1 to Sn5 for SWAT and Vn1 to Vn5 for VIC) for 1-day to 5-day lead times were used. The dotted line represents the  $X=Y$  line, and the solid line shows the best fit line.

(ECMWF, JMA, and NCMRWF) for different lead times are also shown in Table 5. The RMSE value is low for NCMRWF, while NRMSE is low for ECMWF, for all lead times. The ABP value is almost the same for forecasts with all the model data at all lead times. The  $R^2$ , CC, and NSE are high for NCMRWF and low for the ECMWF model at all lead times for both watersheds. The highest values for  $R^2$  (0.590/0.452), CC (0.768/0.673), and NSE (0.490/0.352) are associated with NCMRWF for a lead time of one day for Dindori and Manot watersheds. Generally, the highest values of NSE are associated with lead times of one and two days for all the NWP models.

When the forecasting results from both hydrological models using the three datasets are compared, it can be seen that the VIC model shows more accuracy in comparison to the SWAT model. For instance, Supplementary Fig. S2 shows high values of RMSE and ABP and low values of CC and NSE for both watersheds with the SWAT model. However, VIC only shows high values of NRMSE for both watersheds and low  $R^2$  values for only Manot watershed.

#### 4.3.4 Scatter plots

Figure 8 presents a scatter plot of the streamflow forecasts from the SWAT and VIC hydrological models using rainfall forecasts from the three agencies and observed streamflow for one to five days' lead time for the 2018 monsoon period (June to September) for Dindori watersheds. The right panel of Fig. 8 (streamflow forecasted by VIC) shows that the best-fit lines are closer to the  $x = y$  line than those in the left panel (streamflow forecasted by SWAT). A close inspection of Fig. 8 reveals that the streamflow forecasted by VIC using the NCMRWF forecast rainfall (Fig. 8, Vn3 and Vn5) shows high overprediction in comparison to other NWP models and the other hydrological model. There is a close resemblance between observed and forecasted streamflow for the one-day lead time as the best-fit line is close to the  $x = y$  line in the top row of Fig. 8. The

SWAT model shows better compatibility for NCMRWF (Fig. 8, Sn1 to Sn8) data as  $x = y$  line is closer to best-fit line in comparison to JMA (Fig. 8, Sj1 to Sj5) and ECMWF (Fig. 8, Se1 to Se5) data. From Fig. 8 (Se3 to Se5, and Sj3 to Sj5), it is evident that the streamflow forecasted using ECMWF data and JMA data is highly underpredicted for three- to five-day lead times using the SWAT hydrological model.

The streamflow generated from the VIC model shows more confidence in the ECMWF data (Fig. 8, Ve1 to Ve5) with all lead times except for four days (Fig. 8, Ve4). The VIC model using the JMA (Fig. 8, Vj1 to Vj5) rainfall forecast shows overestimation for all lead times, but less than with the NCMRWF data (Fig. 8, Ve3 to Ve5) for three to five days' lead time. Overall, the VIC model (Fig. 8, right panel) shows overestimation using rainfall forecasts from all three agencies for all lead times in comparison to SWAT (Fig. 8, left panel).

Figure 9 shows a scatter plot of observed streamflow versus forecasted streamflow for JMA, ECMWF, and NCMRWF as generated by the SWAT and VIC hydrological models (left and right panel, respectively) for the Manot watershed. Figure 9 shows that overall, streamflow forecasts from both hydrological models using rainfall forecasts from different agencies are underpredicting. The streamflow forecast for a lead time of one day (top row) shows more accuracy than the other lead times, as the best-fit line is closer to the  $x = y$  line. Streamflow simulated by the SWAT hydrological model shows good agreement with the NCMRWF (Fig. 9, Sn1 to Sn5) as the best-fit line is closer to the  $x = y$  line than in JMA and ECMWF. Moreover, the ECMWF data (Fig. 9, Se2 to Se5) shows higher underprediction for two- to five-day lead times than JMA and NCMRWF.

Streamflow simulated by the VIC model shows that JMA data (Fig. 9, Vj1 to Vj5) produces better results than the ECMWF and NCMRWF data, as the best-fit line is closer to the  $x = y$  line. Moreover, the ECMWF data (Fig. 9, Ve2



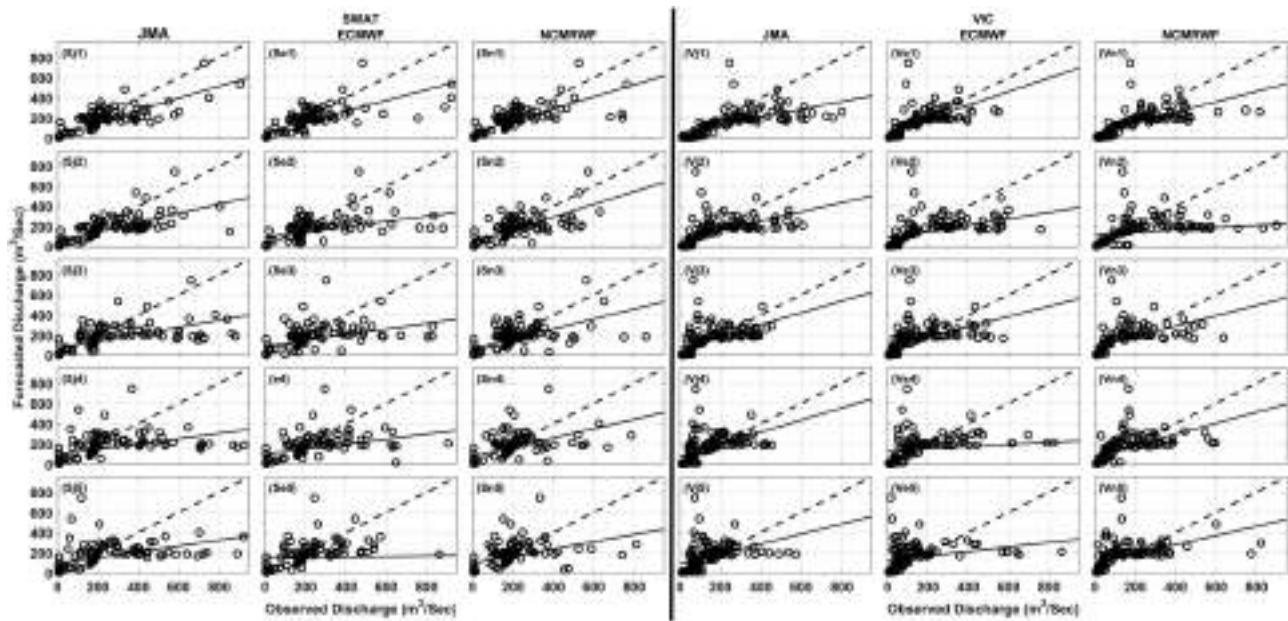


**Figure 9.** Scatter plot of forecasted and observed streamflow obtained from Soil and Water Assessment Tool (SWAT) and Variable Infiltration Capacity (VIC) hydrological model for Manot watershed using the rainfall forecast for 1-day to 5-day lead times from the Japan Metrological Agency (JMA), the European Centre for Medium-Range Forecast (ECMWF), and the National Centre for Medium-Range Weather Forecasting (NCMRWF).

to Ve5) shows high underprediction compared to JMA and NCMRWF data. The best simulation is achieved by the ECMWF data (Fig. 9, Ve1) for a one-day lead time, as its best-fit line is closest to  $x = y$  line in comparison to others. The NCMRWF data for a lead time of two days (Fig. 9, Vn2) shows more underprediction as the best-fit line is closer to the x-axis than the others.

From Figs 8 and 9 it is evident that the streamflow simulated by the VIC hydrological model shows relatively more accurate results than that of the SWAT hydrological model.

However, the VIC model shows more accuracy with JMA data (Figs 8 and 9, Vj1 to Vj5) data and the SWAT model shows more accuracy with NCMRWF data (Figs 8 and 9, Sn1 to Sn5).

#### 4.4 Analysis of ensemble streamflow forecasts

##### 4.4.1 Manot watershed

Streamflow ensembles obtained from the SWAT hydrological model using ECMWF data for the Manot watershed for a lead time of one to five days are shown in Fig. 10(a–e). The

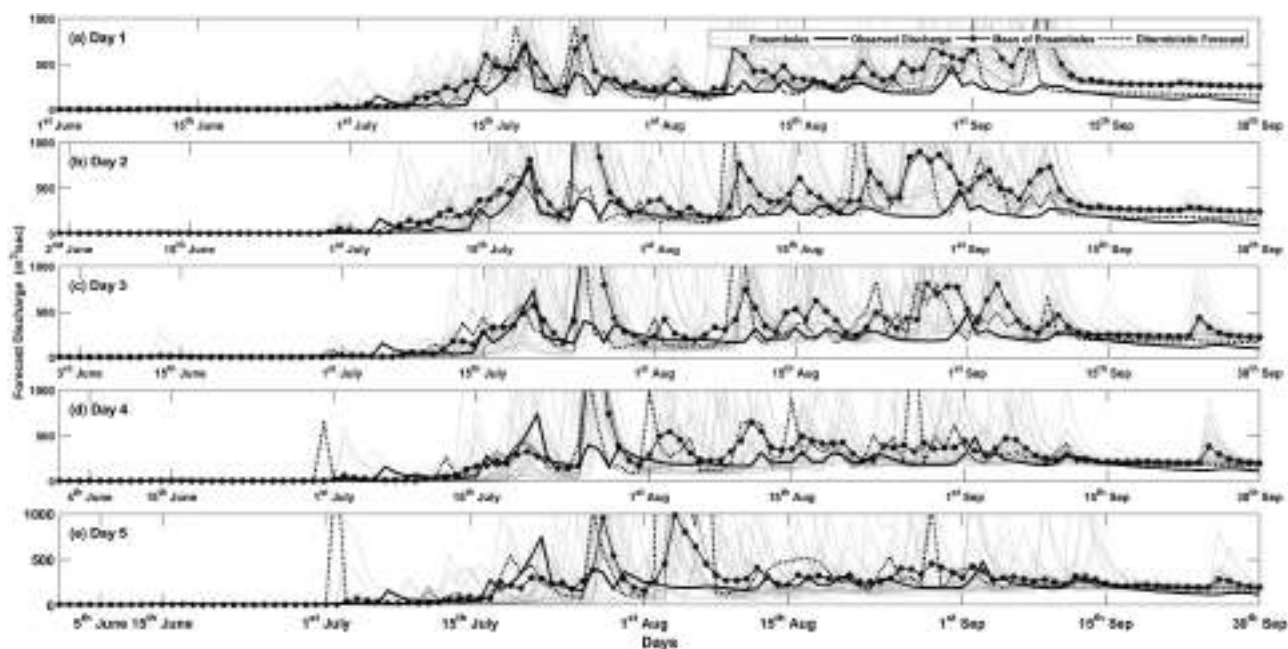


**Figure 10.** 1 to 5-days (a to e) ensembles streamflow forecasts for the Manot watershed from the Soil and Water Assessment Tool (SWAT) hydrological model using the European Centre for Medium-Range Forecast (ECMWF) rainfall forecasts. In the figure, thin lines show ensembles, the (---) line shows the mean of ensembles, the (....) line represents the deterministic, and the dark thick line shows the observed discharge.



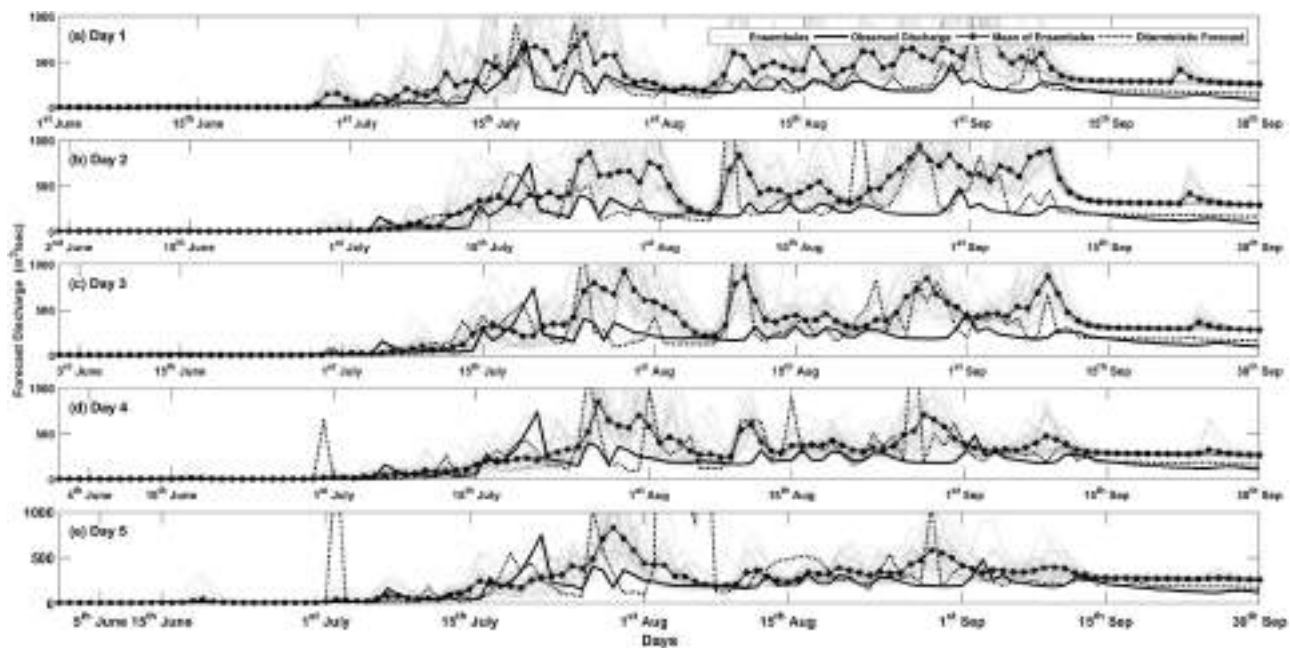


**Figure 11.** Soil and Water Assessment Tool (SWAT) hydrological model forecasts streamflow ensemble for the Manot watershed for 1 to 5 days (a to e) using the Japan Meteorological Agency (JMA) rainfall forecasts.

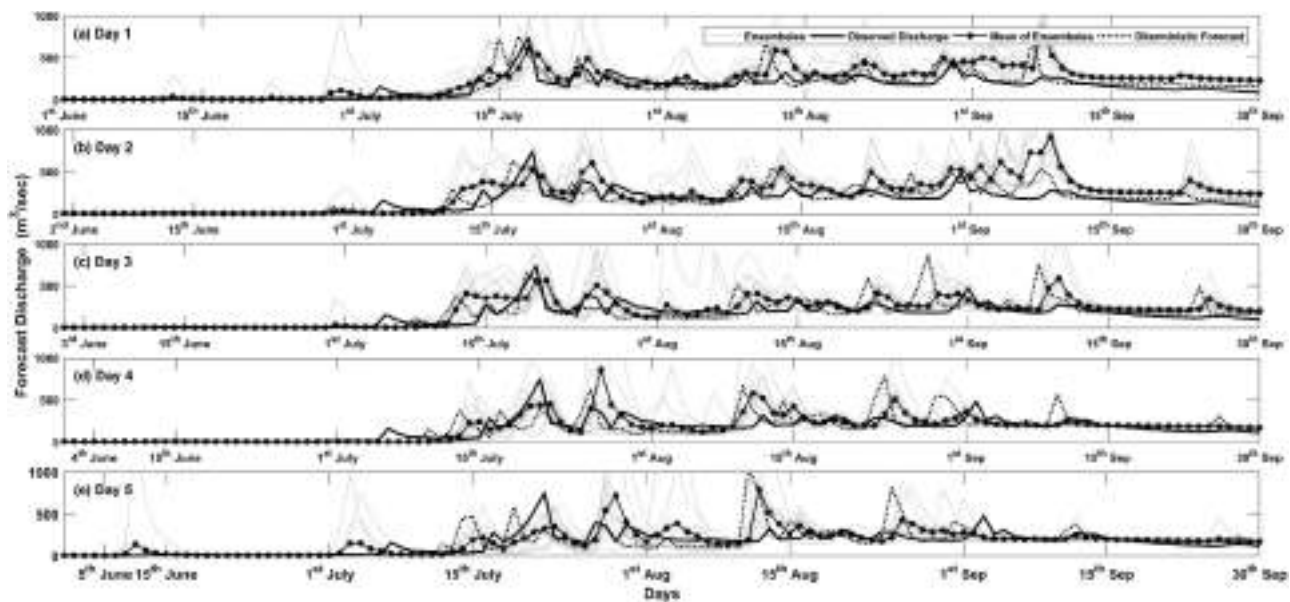


**Figure 12.** Using National Centre for Medium-Range Weather Forecasting (NCMRWF) rainfall forecasts, the Soil and Water Assessment Tool (SWAT) hydrological model forecasts streamflow ensemble for the Manot watershed for the 1 to 5 days (a to e).

streamflow ensembles generated using the SWAT hydrological model with JMA and NCMRWF data are shown in Figs 11 and 12, respectively. Figures 10–12 indicate that the high and low peaks of ensembles and the means of ensembles match closely with the observed data. One-day ensembles are closer to the observation data in comparison to other lead times. It is clear that all the streamflow ensembles obtained from NCMRWF forecasts match the observed values more closely than the forecasts from JMA and ECMWF data. It is evident from Figs 10–12 that the ensemble means obtained from NCMRWF data are closer to the observation than the mean ensemble forecast of the other two data sources (JMA and ECMWF). The

deterministic line is close to the mean ensemble line in most of the cases (except for three days' lead time with JMA data (Fig. 11(c)).

Streamflow ensembles obtained from the VIC hydrological model using ECMWF, JMA, and NCMRWF data for Manot watershed for lead times of one to five days are shown in Figs 13–15. The ensemble peak and mean of ensembles match with the observed discharge for all models for every lead time. However, the JMA (Fig. 13(b–e)) shows an overprediction (around twice the observed data) in streamflow for two to five days' lead time around 1 August. ECMWF (Fig. 14(b) and (c)) shows overprediction throughout the sampled time

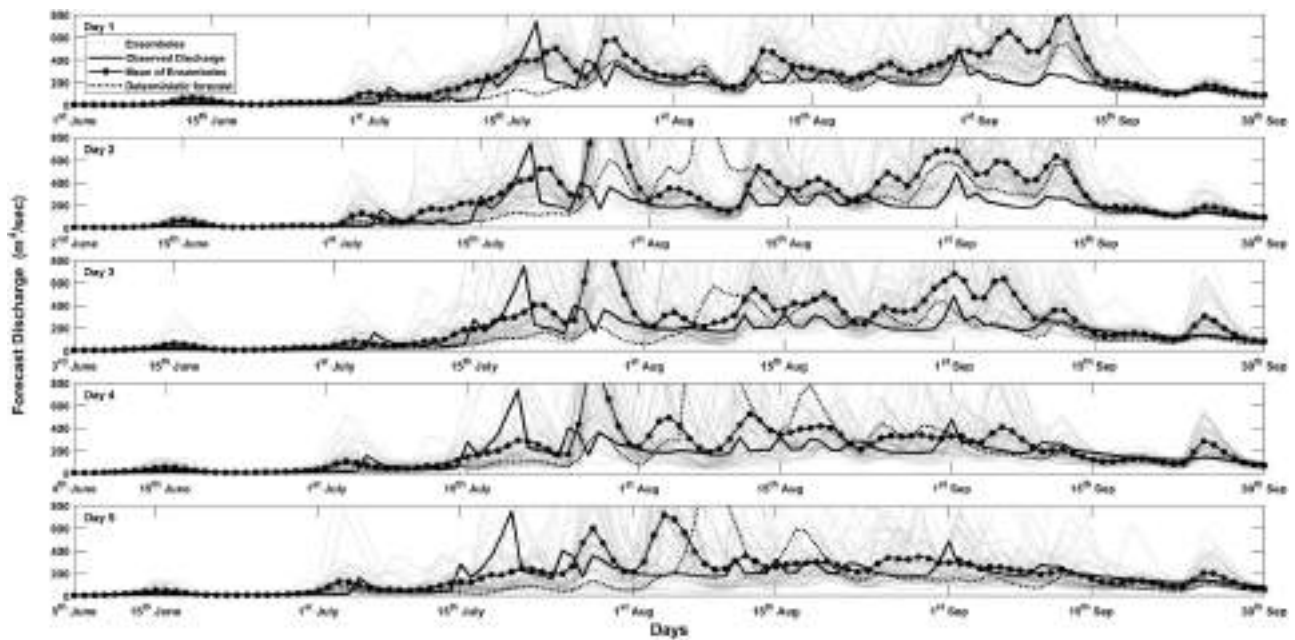


**Figure 13.** 1 to 5-day ensembles streamflow forecasts for Manot watershed from Variable Infiltration Capacity (VIC) hydrological model using the European Centre for Medium-Range Forecast (ECMWF) rainfall forecasts.

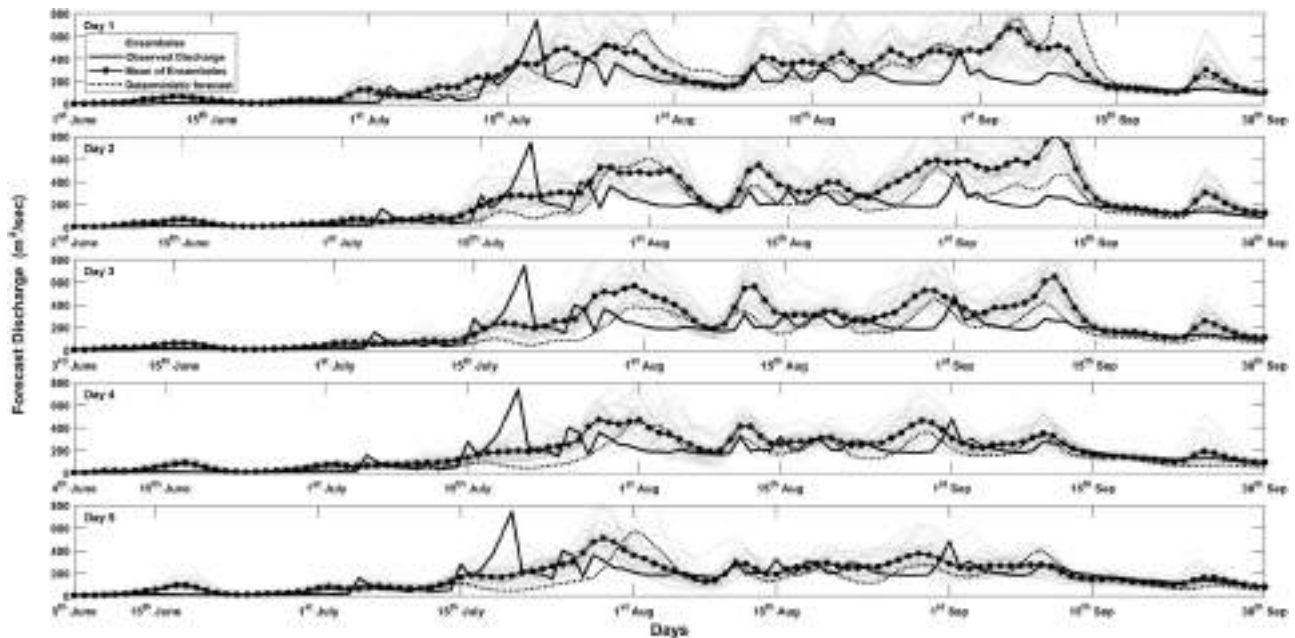


**Figure 14.** VIC hydrological model used for forecasting streamflow ensemble for 1 to 5 days for the Manot watershed by using Japan Metrological Agency (JMA) rainfall forecasts.

period for two- and three-day lead times. A peak before 1 August is highly overestimated (by more than three times compared to the observed data) by ECMWF (Fig. 14) for all lead times. Moreover, the streamflow generated using ensemble rainfall forecasts from NCMRWF (Fig. 15(a-e)) show less overprediction than ECMWF and JMA models. The forecasted streamflow ensemble mean matches well with the observed discharge and deterministic forecast using forecasted rainfall from the different global agencies.

Supplementary Figures S3 to S8 show the forecasted streamflow ensembles generated by the SWAT and VIC hydrological models using different rainfall forecasts for the Dindori watershed. The results are similar to the results obtained for the Manot watershed.

#### 4.4.2 Error statistics

Table 6 shows six error statistics (RMSE, NRMSE, ABP,  $R^2$ , CC, and NSE) associated with the mean ensemble streamflow

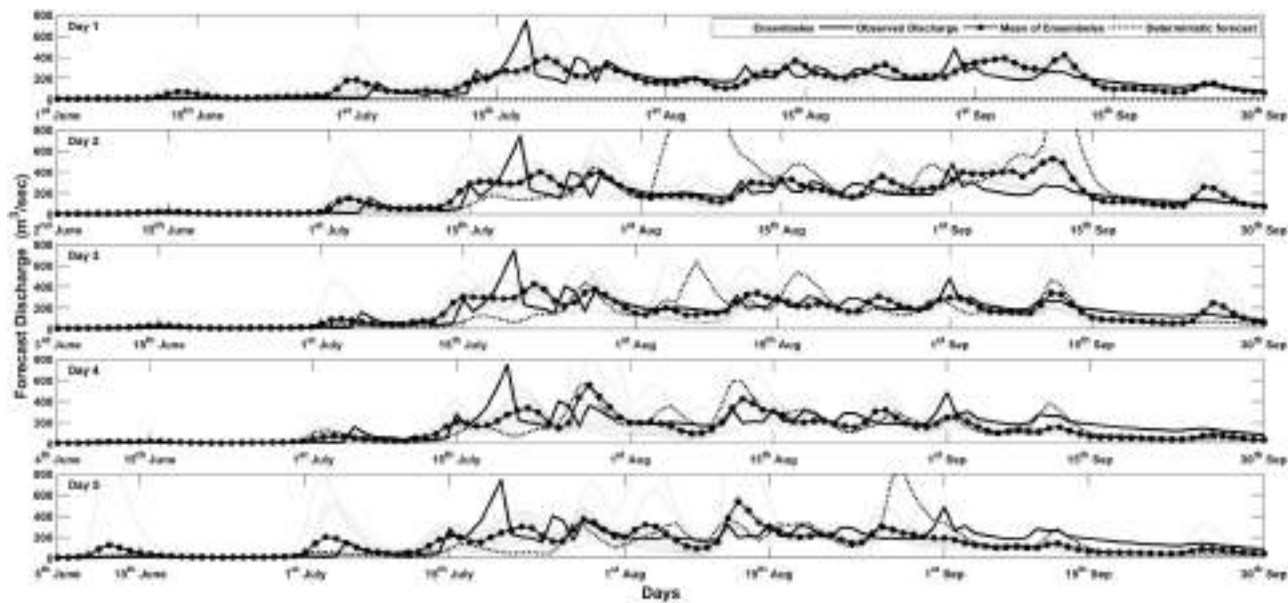


**Figure 15.** Using National Centre for Medium-Range Weather Forecasting (NCMRWF) rainfall forecasts and Variable Infiltration Capacity (VIC) hydrological model for forecasts streamflow ensemble up to 5 days for the Manot watershed.

**Table 6.** Error statics with 1 to 5-day lead time for National Centre for Medium-Range Weather Forecasting (NCMRWF), Japan Metrological Agency (JMA), and European Centre for Medium-Range Forecast (ECMWF) with respect to Soil and Water Assessment Tool (SWAT) and Variable Infiltration Capacity (VIC) model for a mean of ensembles forecast for the Manot watersheds.

Models	Lead time	Manot					
		RMSE	NRMSE	BP	CC	R2	NSE
VIC with ECMWF	1 day	151.198	0.188	28 467.531	0.722	0.521	0.334
	2 days	210.223	0.163	32 527.182	0.689	0.474	0.224
	3 days	179.729	0.164	29 402.092	0.692	0.479	0.303
	4 days	139.873	0.151	24 211.778	0.65	0.423	0.35
	5 days	123.282	0.173	21 777.554	0.617	0.381	0.295
SWAT with ECMWF	1 day	216.95	0.177	34 880.25	0.487	0.698	0.142
	2 days	293.79	0.148	37 914.91	0.362	0.602	0.058
	3 days	242.93	0.155	33 639.67	0.392	0.626	0.156
	4 days	192.35	0.128	27 925.49	0.357	0.598	0.24
	5 days	151.29	0.154	25 344.38	0.402	0.634	0.311
VIC with JMA	1 day	152.514	0.228	29 753.214	0.725	0.526	0.27
	2 days	180.425	0.223	31 198.052	0.687	0.471	0.215
	3 days	145.972	0.227	27 239.09	0.679	0.461	0.3
	4 days	106.347	0.226	22 661.001	0.689	0.475	0.344
	5 days	94.886	0.188	20 568.786	0.703	0.495	0.338
SWAT with JMA	1 day	215.77	0.269	37 674.02	0.597	0.773	0.072
	2 days	275.89	0.294	40 880.15	0.442	0.665	-0.052
	3 days	240.24	0.261	36 607.51	0.403	0.635	0.028
	4 days	174.79	0.207	30 912.29	0.45	0.671	0.183
	5 days	147.3	0.178	28 481.11	0.493	0.702	0.281
VIC with NCMRWF	1 day	88.733	0.213	19 882.599	0.734	0.539	0.4
	2 days	98.5	0.19	21 583.974	0.736	0.541	0.477
	3 days	82.518	0.197	18 204.472	0.766	0.587	0.463
	4 days	98.413	0.18	15 631.343	0.693	0.48	0.278
	5 days	107.263	0.202	16 178.001	0.601	0.361	-0.008
SWAT with NCMRWF	1 day	127.74	0.153	27 275.08	0.605	0.778	0.433
	2 days	165.06	0.182	28 888.97	0.456	0.675	0.27
	3 days	112.22	0.191	24 286.26	0.551	0.742	0.454
	4 days	103.1	0.121	20 974.91	0.545	0.738	0.518
	5 days	112.67	0.142	21 455.94	0.433	0.658	0.349

forecasts from the ECMWF, JMA, and NCMRWF rainfall data with observed discharge for a lead time of one to five days, obtained from the SWAT and VIC models for the Manot watershed. The mean of streamflow ensembles obtained

using QPFs from NCMRWF shows high accuracy compared to JMA and ECMWF using the SWAT model for streamflow forecasting. Table 6 shows that NCMRWF has low RMSE and NRMSE, and high  $R^2$ , CC, and NSE values for all lead times,



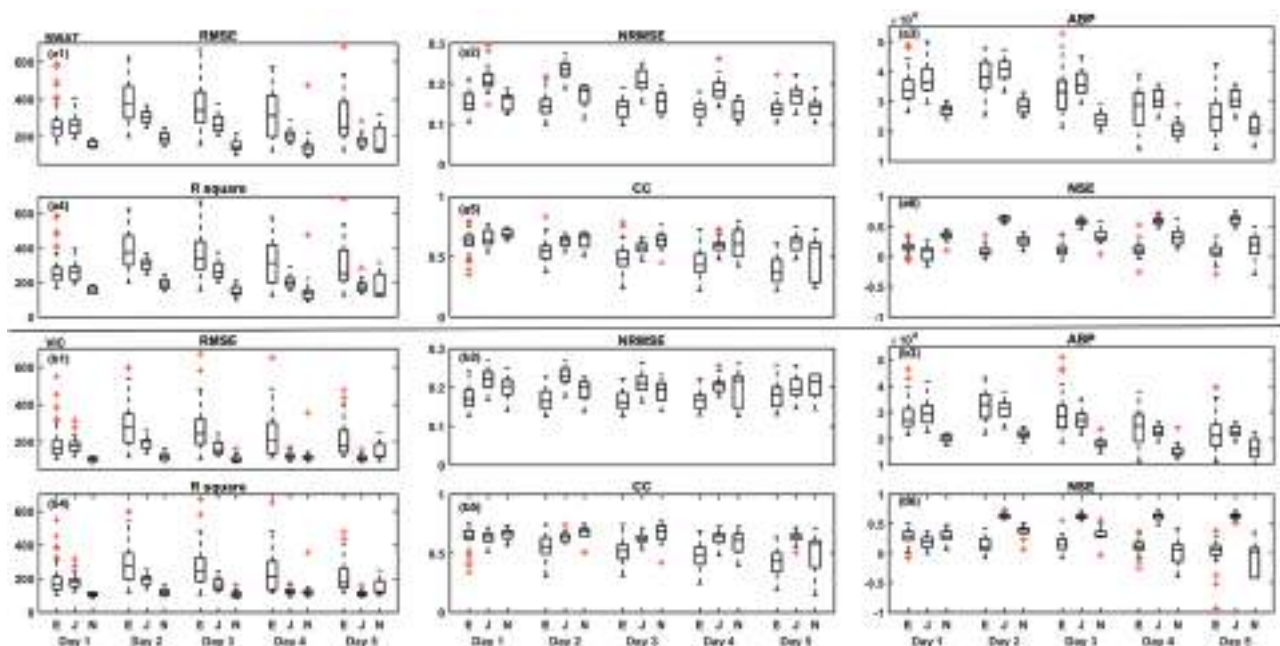


**Figure 16.** Box plots of the error statistics (RMSE, NRMSE, ABP, R square, CC, and NSE) for forecasted streamflow ensemble at Manot watershed using Soil and Water Assessment Tool (SWAT) (a1 to a6) and Variable Infiltration Capacity (VIC) (b1 to b6) hydrological models. The rainfall forecasts from the European Centre for Medium-Range Forecast (ECMWF) (E), Japan Meteorological Agency (JMA) (J), and National Centre for Medium-Range Weather Forecasting (NCMRWF) (N) for a lead time of 1 to 5 days has been used.

while JMA has high RMSE and NRMSE and ECMWF has low  $R^2$ , CC, and NSE. For instance, NCMRWF has the lowest RMSE (103.10) for Manot for a four-day lead time. Moreover, NCMRWF has the highest  $R^2$  (0.605) and NSE (0.581) for a lead time of four days, and has the highest CC (0.778) for a lead time of one day for the Manot watershed.

Streamflow forecasted by the VIC model shows high accuracy with NCMRWF data for two to five days' lead time, having low RMSE, NRMSE, and ABP, and high  $R^2$ , CC, and

NSE. However, for a one-day lead time, the accuracy of ECMWF is better than that of NCMRWF and JMA for the Dindori watershed. For the Manot watershed, the lowest RMSE (82.518) and ABP (15 631), and the highest CC (0.766),  $R^2$  (0.587), and NSE (0.477) are associated with NCMRWF data for lead times of three, four, three, three and two days, respectively. NCMRWF has RMSE values of less than ~90 and ABP values of less than ~20 000 for Manot watershed. The performance of streamflow generated from

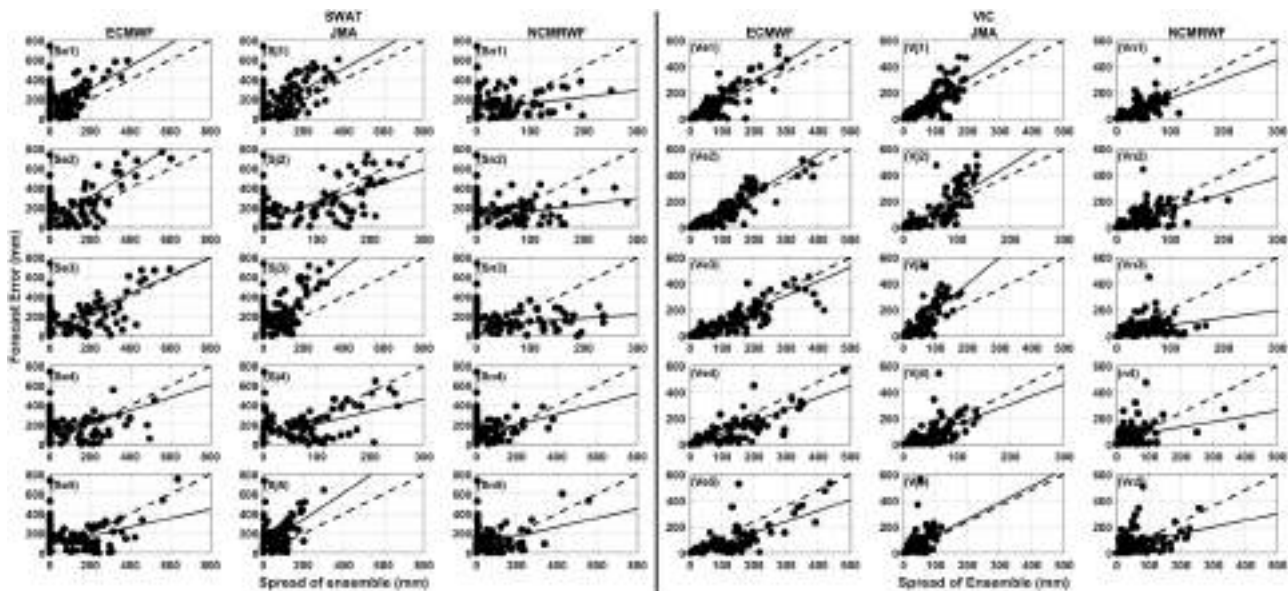


**Figure 17.** The plot of ensemble spread of streamflow generated by Soil and Water Assessment Tool (SWAT) hydrological models using European Centre for Medium-Range Forecast (ECMWF) (Se1 to Se5), Japan Meteorological Agency (JMA) (Sj1 to Sj5), and National Centre for Medium-Range Weather Forecasting (NCMRWF) (Sn1 to Sn5) rainfall forecasts, and Variable Infiltration Capacity (VIC) hydrological models using ECMWF (Ve1 to Ve5), JMA (Vj1 to Vj5), and NCMRWF (Vn1 to Vn5) rainfall forecasts, for the Manot watershed.

the SWAT and VIC hydrological models with the rainfall forecasts from different agencies are shown for the Dindori watershed (Supplementary Table S1).

Comparing the streamflow forecasts from both hydrological models (SWAT and VIC) using rainfall forecasts from the three agencies, we noticed that the VIC model is producing more accurate results than the SWAT model. SWAT produced the highest values of RMSE and ABP and the lowest values of CC and NSE for both watersheds, as shown in Supplementary Fig. S9.

#### 4.4.4 Box plots of errors for the ensemble streamflow forecasts

Figure 16 shows the box plots for the six error statistics (RMSE, NRMSE, ABP,  $R^2$ , CC, and NSE) used to assess the performance of streamflow ensembles obtained from the SWAT (top) and VIC (bottom) hydrological models by using ensemble rainfall forecasts from ECMWF (50 ensembles), JMA (26 ensembles) and NCMRWF (11 ensembles). From the figure, we can see that the spread in the case of NCMRWF is less than that of JMA and ECMWF for all error statistics for SWAT (Fig. 16, top). The box plots show that the medians of RMSE (<200) and ABP (< 3000) related to NCMRWF are lower compared to those of JMA and ECMWF for all lead times. The median of ECMWF is less for NRMSE (less than 0.15), as shown in Fig. 16 (top). The spread of the box plot of JMA and NCMRWF for  $R^2$  and CC is almost the same, and lower than that of ECMWF. However, for a lead time of five days, the spread of NCMRWF is greater than that of JMA for  $R^2$  and CC. The highest value (more than 600) of  $R^2$  for all lead times is observed with ECMWF. The highest value of  $R^2$  observed with NCMRWF is more than 0.8 for lead times of one and two days, whereas it is approximately 0.7 for a lead time of three days. JMA shows the highest values (more than 0.7) and less spread for NSE values than ECMWF and NCMRWF. It can be concluded that the performance of the NCMRWF rainfall ensembles (in comparison to JMA and ECMWF) is reliable in generating streamflow with the SWAT and VIC models. We demonstrate the accuracy of the models for the Dindori watershed in Supplementary Fig. S10.

#### 4.4.5 Ensemble spread

Figure 17 shows the ensemble spread of the streamflow ensemble forecasts produced by the SWAT (left panel) and VIC (right panel) hydrological models using rainfall forecasts from ECMWF, JMA, and NCMRWF for Manot watershed. The streamflow ensembles produced from SWAT and VIC using ECMWF rainfall forecast show a good agreement between the forecast error and ensemble spread as the best-fit line is close to the  $x = y$  line (Fig. 17, e1 to e5). The forecast error of ensemble spread for NCMRWF data is lower as the best-fit line is inclined towards the x-axis for the Manot watershed (Fig. 17, n1 to n5). The JMA forecast error is always higher in comparison to that of other agencies' data (Fig. 17, j1 to j5), except for the five-day lead time with the VIC model (Fig. 17, vj5 right panel), where the

best-fit line is closer to the  $x = y$  line, and for the four-day lead time, where the best-fit line tends towards the x-axis.

Figure 17 shows that the forecast error decreases with an increase in the lead time, as we can see that the best-fit line moves towards the x-axis when the lead time is increased (Fig. 17 and Supplementary Fig. S11).

## 5 Discussion and conclusions

Coupling the NWP and hydrological models to generate streamflow forecasts is a vital research area for hydrologists. According to recent studies, these coupled models need to be evaluated and analysed robustly to understand their pros and cons. Factors such as parameterization, schemes, spin-up time, spatial and temporal resolution, and forecast lead time affect the precipitation prediction accuracy of different NWP models. As expected, our results indicate that the streamflow forecasts are more accurate for shorter lead times than longer ones. The accuracy assessments indicated an increase in RMSE, NRMSE, and ABP and a decrease in error measurement ( $R^2$ , CC, and NSE) with increasing lead times (from one day to five days). This trend was observed in the forecasts from all three agencies – NCMRWF, JMA, and ECMWF.

The uncertainties in streamflow forecasting could be related to using observed rainfall and streamflow in calibrating the hydrological model. Also, the sources of rainfall used as input to the hydrological model may vary. Therefore, it is expected that the hydrological response in forecasting the streamflow will not match the simulated streamflow perfectly. Our results also suggest that using ensemble rainfall forecasts produces more promising results than using the deterministic rainfall forecast.

SWAT and VIC hydrological models are also compared in this study to evaluate the effect of different model structures on streamflow forecasts. Our study suggests that both hydrological models can capture the high peaks in forecasting. However, the error statistics indicate less error in streamflow forecasting with the VIC hydrological model than the SWAT hydrological model. The comparison of several combinations of rainfall forecasts from three agencies and two hydrological models help determine the optimal combination that can produce the most reliable streamflow forecasts.

From the above results and discussion, we conclude that:

- Rainfall forecasts with a lead time of one day perform better than those with other lead times; also, the performance of the rainfall forecasts over the Dindori watershed was lower compared to that of the Manot watershed.
- RMSE, NRMSE, and ABP increase with increasing lead time;  $R^2$ , CC, and NSE decrease with increasing lead time. This shows that the accuracy of the generated streamflow forecast decreases with increasing lead time.
- The line plots and scatter plots of the results show that the forecasted streamflow underpredicts the low flows and overpredicts the higher flows in the case of higher lead times.
- The streamflow forecast using rainfall forecast data from NCMRWF is more accurate than that of JMA and

ECMWF for two- to five-day lead times. For a lead time of one day, JMA more accurately forecasts the streamflow than NCMRWF and ECMWF.

- The VIC hydrological model is more accurate than the SWAT hydrological model in forecasting the streamflow in this study area.
- We noticed that the combination of a QPF and a hydrological model produced better results than the other combinations. For instance, VIC gives better forecasts with JMA and NCMRWF, and SWAT gives better forecasts with ECMWF and NCMRWF.
- Ensembles are more reliable than deterministic forecasts as they give a range of forecasted streamflow. In most cases, there is a match between the streamflow forecast obtained using the ensembles' mean and deterministic QPF.
- The ensemble spread plots show that the forecast error of the ensemble decreases with increasing lead time in this study.
- The number of ensemble members also plays an important role as the ECMWF, with a high number of ensembles (50), shows high forecast error while NCMRWF, with a low number of ensembles (11), shows low forecast error in terms of spread of ensembles.
- In some cases, it is extremely challenging to capture all the peaks in the observed streamflow data. Our results show that some peaks are not captured by any combination of rainfall forecasts and hydrological models in the case of the Manot watershed while they are perfectly simulated for the Dindori watershed.

Our future work will involve pre-processing raw rainfall forecasts to remove the inherent bias before using them in any hydrological model. We also plan to overcome the uncertainty due to hydrological model selection by applying multimodal approaches. The combination of improved forecasts with a multimodal system is expected to further improve the streamflow forecasts.

## Acknowledgements

This research was completed thanks to the support of the Science and Engineering Research Board (SERB), project number CRG/2018/000649, awarded to Sanjeev Kumar Jha.

## Funding

This work was supported by the Science and Engineering Research Board (SERB) (<http://www.serb.gov.in/>) of India [CRG/2018/000649].

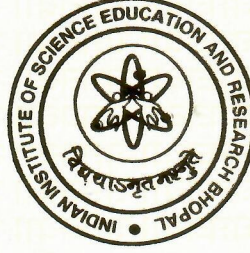
## References

- Abbaspour, K.C., et al., 2007. Modelling hydrology and water quality in the pre-alpine/alpine thur watershed using SWAT. *Journal of Hydrology*, 333 (2–4), 413–430. doi:10.1016/j.jhydrol.2006.09.014.
- Abinash, S., Samantaray, S., and Ghose, D.K., 2019. Stream flow forecasting in Mahanadi River Basin using artificial neural networks. *Procedia Computer Science*, 157, 168–174. doi:10.1016/j.procs.2019.08.154
- Aminyavari, S. and Saghaian, B., 2019. Probabilistic streamflow forecast based on spatial post-processing of TIGGE precipitation forecasts. *Stochastic Environmental Research and Risk Assessment*, 33 (11–12), 1939–1950. doi:10.1007/s00477-019-01737-4.
- Anumeha, D., et al., 2017. Evaluating the performance of two global ensemble forecasting systems in predicting rainfall over India during the southwest monsoons. *Meteorological Applications*, 24 (2), 230–238. doi:10.1002/MET.1621.
- Asghar, M.R., et al., 2019. Flood and inundation forecasting in the sparsely gauged transboundary chenab river basin using satellite rain and coupling meteorological and hydrological models. *Journal of Hydrometeorology*, 20 (12), 2315–2330. doi:10.1175/JHM-D-18-0226.1.
- Ashrit, R., et al., 2020. Prediction of the august 2018 heavy rainfall events over Kerala with high-resolution NWP models. *Meteorological Applications*, 27 (2). doi:10.1002/MET.1906.
- Awol, F.S., Coulibaly, P., and Tsanis, I., 2021. Identification of Combined Hydrological Models and Numerical Weather Predictions for Enhanced Flood Forecasting in a Semiurban Watershed. *J. Hydrol. Eng.*, 26, 04020057. doi:10.1061/(asce)he.1943-5584.0002018.
- Begou, J.C., et al., 2016. Multi-site validation of the SWAT model on the bani catchment: model performance and predictive uncertainty. *Water (Switzerland)*, 8 (5). doi:10.3390/w8050178.
- Block, P.J., et al., 2009. A streamflow forecasting framework using multiple climate and hydrological models. *Journal of the American Water Resources Association*, 45 (4), 828–843. doi:10.1111/j.1752-1688.2009.00327.x.
- Bougeault, P., et al., 2010. The thorpe interactive grand global ensemble. *Bulletin of the American Meteorological Society*, 91 (8), 1059–1072. doi:10.1175/2010BAMS2853.1.
- Carlberg, B., Franz, K., and Gallus, W., 2020. A method to account for qpf spatial displacement errors in short-term ensemble streamflow forecasting. *Water (Switzerland)*, 12 (12), 1–18. doi:10.3390/w12123505.
- Chen, H., et al., 2013. Hydrological data assimilation with the ensemble square-root-filter: use of streamflow observations to update model states for real-time flash flood forecasting. *Advances in Water Resources*, 59, 209–220. doi:10.1016/J.ADVWATRES.2013.06.010
- Cibin, R., Sudheer, K.P., and Chaubey, I., 2010. Sensitivity and identifiability of stream flow generation parameters of the SWAT model. *Hydrological Processes*, 24 (9), 1133–1148. doi:10.1002/hyp.7568.
- Dube, A., et al., 2022. Spatial verification of ensemble rainfall forecasts over India. *Atmospheric Research*, 273, 106169. doi:10.1016/J.ATMOSRES.2022.106169
- Dvorak, V.F., 1975. Tropical cyclone intensity analysis and forecasting from satellite imagery. *Monthly Weather Review*, 103 (5), 420–430. doi:10.1175/1520-0493(1975)103<0420:tciaaf>2.0.co;2.
- Fan, F.M., et al., 2016. Flood forecasting on the tocantins river using ensemble rainfall forecasts and real-time satellite rainfall estimates. *Journal of Flood Risk Management*, 9 (3), 278–288. doi:10.1111/jfr3.12177.
- Ferraris, L., Rudari, R., and Siccaldi, F., 2002. The uncertainty in the prediction of flash floods in the Northern Mediterranean environment. *Journal of Hydrometeorology*, 3 (6), 714–727. doi:10.1175/1525-7541(2002)003<0714:TUITPO>2.0.CO;2.
- Ghaith, M., et al., 2020. Hybrid hydrological data-driven approach for daily streamflow forecasting. *Journal of Hydrologic Engineering*, 25 (2), 04019063. doi:10.1061/(asce)he.1943-5584.0001866.
- Goswami, S.B., Kumar Bal, P., and Mitra, A.K., 2018. Use of rainfall forecast from a high-resolution global NWP model in a hydrological stream flow model over Narmada River Basin during monsoon. *Modeling Earth Systems and Environment*, 4 (3), 1029–1040. doi:10.1007/s40808-018-0436-y.
- Hapuarachchi, H.A.P., et al., 2022. Development of a National 7-day ensemble streamflow forecasting service for Australia. *Hydrology and Earth System Sciences*, (March), 1–35.
- Honorato, A.G.D.S.M., da Silva, G.B.L., and Augusto Guimarães Santos, C., 2018. Monthly streamflow forecasting using neuro-wavelet techniques and input analysis. *Hydrological Sciences Journal*, 63 (15–16), 2060–2075. doi:10.1080/02626667.2018.1552788.
- Jabbari, A., Jae Min, S., and Hyo Bae, D., 2020. Precipitation forecast contribution assessment in the coupled meteo-hydrological models. *Atmosphere*, 11 (1). doi:10.3390/ATMOS11010034.
- Jasper, K. and Kaufmann, P., 2003. Coupled runoff simulations as validation tools for atmospheric models at the regional scale. *Quarterly*



- Journal of the Royal Meteorological Society*, 129 (588), 673–692. doi:10.1256/qj.02.26.
- Kalra, A., Ahmad, S., and Nayak, A., 2013. Increasing streamflow forecast lead time for snowmelt-driven catchment based on large-scale climate patterns. *Advances in Water Resources*, 53, 150–162. doi:10.1016/J.ADVWATRES.2012.11.003
- Kilinc, H.C., 2022. Daily streamflow forecasting based on the hybrid particle swarm optimization and long short-term memory model in the orontes basin. *Water (Switzerland)*, 14, 3. doi:10.3390/w14030490
- Kumari, N., et al., 2021. Identification of suitable hydrological models for streamflow assessment in the Kangsabati River Basin, India, by using different model selection scores. *Natural Resources Research*, 30 (6), 4187–4205. doi:10.1007/s11053-021-09919-0.
- Liang, X., et al., 1994. A simple hydrologically based model of land surface water and energy fluxes for general circulation models. *Journal of Geophysical Research: Atmospheres*, 99 (D7), 14415–14428. doi:10.1029/94JD00483.
- Lokeshwari, M., Mendi, V., and Reddy, N.A. 2018. Peak flood estimation along southern coast: Kerala, India. In *ASIAN AND PACIFIC COASTS 2017: Proceedings of the 9th International Conference on APAC*, SMX Convention Centre, Pasay City, Philippines, 19–21 October (pp. 19–21). doi:10.1142/9789813233812\_0017.
- Monhart, S., et al., 2019. Subseasonal hydrometeorological ensemble predictions in small- and medium-sized mountainous catchments: benefits of the NWP approach. *Hydrology and Earth System Sciences*, 23 (1), 493–513. doi:10.5194/hess-23-493-2019.
- Nanditha, J.S. and Mishra, V., 2021. On the need of ensemble flood forecast in India. *Water Security*, 12, 100086. doi:10.1016/J.WASEC.2021.100086
- Nayak, P.C. and Thomas, T., 2021. Statistical downscaling of precipitation for Mahanadi Basin in India - prediction of future stream flows. 0–40.
- Pappenberger, F., et al., 2009. The skill of probabilistic precipitation forecasts under observational uncertainties within the generalized likelihood uncertainty estimation framework for hydrological applications. *Journal of Hydrometeorology*, 10 (3), 807–819. doi:10.1175/2008JHM956.1.
- Pattanaik, D.R., et al., 2019. Evolution of operational extended range forecast system of IMD: prospects of its applications in different sectors. *Mausam*, 70 (2), 233–264. doi:10.54302/mausam.v70i2.170.
- Poonia, V. and Lal Tiwari, H., 2020. Rainfall-runoff modeling for the hoshangabad basin of Narmada River using artificial neural network. *Arabian Journal of Geosciences*, 13 (18), 18. doi:10.1007/s12517-020-05930-6.
- Randrianasolo, A., et al., 2010. Comparing the scores of hydrological ensemble forecasts issued by two different hydrological models. *Atmospheric Science Letters*, 11 (2), 100–107. doi:10.1002/asl.259.
- Roba, F.G., Arya, D.S., and Goel, N.K., 2000. Streamflow forecasting using artificial neural network. *Water and Energy International*, 57 (1), 30–37.
- Sana, M., et al., 2018. Indian monsoon data assimilation and analysis regional reanalysis: configuration and performance. *Atmospheric Science Letters*, 19 (3), 1–7. doi:10.1002/asl.808.
- Sharma, M.L., et al., 1987. Subsurface water flow simulated for hillslopes with spatially dependent soil hydraulic characteristics. *Water Resources Research*, 23 (8), 1523–1530. doi:10.1029/WR023i08p01523.
- Sharma, S., et al., 2019. Hydrological model diversity enhances streamflow forecast skill at short-to medium-range timescales. *Water Resources Research*, 55 (2), 1510–1530. doi:10.1029/2018WR023197.
- Singh, A. and Kumar Jha, S., 2021. Identification of sensitive parameters in daily and monthly hydrological simulations in small to large catchments in Central India. *Journal of Hydrology*, 601, 126632. doi:10.1016/J.JHYDROL.2021.126632
- Singh, A., Tiwari, S., and Kumar Jha, S., 2021. Evaluation of quantitative precipitation forecast in five Indian river basins. 1–16. doi:10.1080/02626667.2021.1982138.
- Siqueira, V.A., et al., 2020. Potential skill of continental-scale, medium-range ensemble streamflow forecasts for flood prediction in South America. *Journal of Hydrology*, 590 (February), 125430. doi:10.1016/j.jhydrol.2020.125430.
- Strasser, U. and Mauser, W., 2001. Modelling the spatial and temporal variations of the water balance for the weser catchment 1965–1994. *Journal of Hydrology*, 254 (1–4), 199–214. doi:10.1016/S0022-1694(01)00492-9.
- Sun, Y., Niu, J., and Sivakumar, B., 2019. A comparative study of models for short-term streamflow forecasting with emphasis on wavelet-based approach. *Stochastic Environmental Research and Risk Assessment*, 33 (10), 1875–1891. doi:10.1007/s00477-019-01734-7.
- Tegegne, G., Kwan Park, D., and Oh Kim, Y., 2017. Comparison of hydrological models for the assessment of water resources in a data-scarce region, the upper blue Nile river basin. *Journal of Hydrology: Regional Studies*, 14 (October), 49–66. doi:10.1016/j.ejrh.2017.10.002.
- Tiwari, S., Kumar Jha, S., and Singh, A., 2020. Quantification of node importance in rain gauge network: influence of temporal resolution and rain gauge density. *Scientific Reports*, 10 (1). doi:10.1038/s41598-020-66363-5.
- Tiwari, A.D., Mukhopadhyay, P., and Mishra, V., 2021. Influence of bias correction of meteorological and streamflow forecast on hydrological prediction in India. *Journal of Hydrometeorology*, 1(aop). doi:10.1175/JHM-D-20-0235.1.
- Verbunt, M., et al., 2006. Verification of a coupled hydrometeorological modelling approach for alpine tributaries in the rhine basin. *Journal of Hydrology*, 324 (1–4), 224–238. doi:10.1016/j.jhydrol.2005.09.036.
- Wijayarathne, D.B. and Coulibaly, P., 2020. Identification of hydrological models for operational flood forecasting in St. John's, Newfoundland, Canada. *Journal of Hydrology: Regional Studies*, 27 (November 2019), 100646. doi:10.1016/j.ejrh.2019.100646.
- Xuan, Y., Cluckie, I.D., and Wang, Y., 2009. Uncertainty analysis of hydrological ensemble forecasts in a distributed model utilising short-range rainfall prediction. *hydrology and earth system sciences*, 13 (3), 293–303. <http://www.hydrol-earth-syst-sci.net/13/293/2009/>
- Zacharias, I., Dimitriou, E., and Koussouris, T., 2005. Integrated water management scenarios for wetland protection: application in Trichonis lake. *Environmental Modelling and Software*, 20 (2), 177–185. doi:10.1016/j.envsoft.2003.09.003.
- Zhao, P., et al., 2021. Which precipitation forecasts to use? Deterministic versus coarser-resolution ensemble NWP models. *Quarterly Journal of the Royal Meteorological Society*, 147 (735), 900–913. doi:10.1002/qj.3952.
- Zhao, T., Cai, X., and Yang, D., 2011. Effect of streamflow forecast uncertainty on real-time reservoir operation. *Advances in Water Resources*, 34 (4), 495–504. doi:10.1016/J.ADVWATRES.2011.01.004.
- Zhao, T. and Zhao, J., 2014. Forecast-skill-based simulation of streamflow forecasts. *Advances in Water Resources*, 71, 55–64. doi:10.1016/J.ADVWATRES.2014.05.011

**भारतीय विज्ञान शिक्षा एवं अनुसंधान संस्थान भोपाल**  
**Indian Institute of Science Education and Research Bhopal**



विद्या परिषद् की अनुशंसा पर  
भारतीय विज्ञान शिक्षा एवं अनुसंधान संस्थान भोपाल के शासक मंडल द्वारा

**अंकित सिंह**

को पीएच. डी. उपाधि कार्यक्रम की  
अर्हताएं पूर्ण कर लेने पर  
**पृथ्वी एवं पर्यावरण विज्ञान**  
में

**डॉक्टर ऑफ फिलॉसफी**

की उपाधि आज दिनांक 08 जुलाई, 2023 को प्रदान की जाती है।

The Board of Governors of  
the Indian Institute of Science Education and Research Bhopal  
on the recommendation of the Senate hereby confers on

**Ankit Singh**

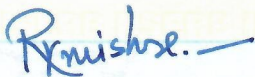
the degree of

**Doctor of Philosophy**

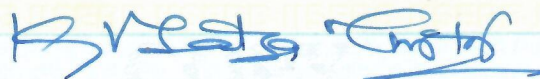
in

**Earth and Environmental Sciences**

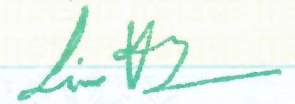
upon fulfillment of the requirements of the Ph.D. degree programme  
on this day, the 08<sup>th</sup> of July, 2023.



शैक्षणिक अधिष्ठाता  
Dean, Academic Affairs

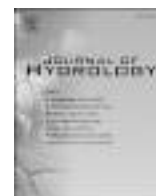


कुलसचिव  
Registrar



अध्यक्ष, विद्या परिषद् एवं निदेशक  
Chairperson, Senate & Director





## Research papers

# Identification of sensitive parameters in daily and monthly hydrological simulations in small to large catchments in Central India

Ankit Singh, Sanjeev Kumar Jha \*

Indian Institute of Science Education and Research Bhopal, Madhya Pradesh, India



## ARTICLE INFO

This manuscript was handled by Marco Borga, Editor-in-Chief, with the assistance of Eylon Shamir, Associate Editor

## Keywords:

Parameter Sensitivity analysis  
Hydrological Modelling  
SWAT  
SUFI-2 algorithm  
Catchment Size  
Narmada River Basin

## ABSTRACT

Hydrological models have many parameters representing various hydrological processes. These parameters are effective at different spatial and temporal resolution. Most of the parameters can be measured such as slope, elevation, area, vegetation type etc., but others cannot be estimated from the available data. Thus, they remain unknown in a hydrological simulation. Local and Global Sensitivity Analyses (LSA and GSA respectively) are therefore used to reduce the number of parameters that need to be equipped with input–output data. GSA also improves the efficiency of the model calibration and validation which in turn increases the reliability of the model. In this paper, we investigate into the effect of size of a catchment (small, medium, and large) time steps of simulation (Daily and Monthly), and the choice of GSA method in performing sensitivity analysis. A Soil and Water Assessment Tool (SWAT) hydrologic model is developed for 10 subbasins of Narmada River basin at daily and monthly temporal simulations from January 1991 to December 2000. The sensitivity of 29 input parameters have been analysed with two GSA methods: the multilinear regression SA used by sequential uncertainty fitting algorithm (SUFI-2) in SWAT – Calibration and Uncertainty procedure (SWAT-CUP), and the first order sensitivity indices driven by Fourier Amplitude Sensitivity Test (FAST). Our results show that a hydrological model set up with only sensitive parameters can also produce similar results as when all the parameters are considered. We concluded that the selection of catchment size and simulation time step strongly influence the parameter sensitivity. Our results show that the sensitivity of some of the parameters like Curve number for moisture condition (CN2.mgt), baseflow alpha factor for bank storage (ALPHA\_BNK.rte) and lateral flow travel time (LAT\_TTIME.hru) are independent of catchment size and simulation time step. Moreover, baseflow alpha factor for the recession constant (ALPHA\_BF.gw), manning's value for overland flow (OV\_N.hru) and soil erodibility factor (USLE\_K(..).sol) are not sensitive for large and medium range watersheds but those are sensitive for small watershed at a monthly time step. Ground water delay (GW\_DELAY.gw), average slope steepness (HRU\_SLP.hru) and support practice (p) factor of USLE soil equation (USLE\_P.mgt) are not sensitive for large watersheds but sensitive for small and medium range watersheds at a daily time step. Our results strongly recommends that a detailed parameter sensitivity analysis is an important step in setting up any hydrological model to reduce the number of parameters while addressing all relevant hydrological processes.

## 1. Introduction

The parameters of a hydrological model represent different hydrological processes in a basin. In developing a hydrological model for a basin, we need an optimum set of parameters to represent all relevant hydrological processes while avoiding over-parametrization which is one of the main sources of errors in the simulated results. Sensitivity analysis approaches are used to reduce the number of parameters that need to be equipped with input–output data (Guo and Su, 2019; Kumar

et al., 2017; Me et al., 2015; Sudheer et al., 2011; van Griensven et al., 2006). The research questions related to parameter sensitivity in a hydrological model have been explored by many researchers since last several decades. McCuen (1973) discussed the importance of parameter sensitivity analysis to reduce the number of parameters and avoid complexity in a hydrological model. Bahremand and Smedt (2008) used WetSpa hydrological model in the Torysa River basin, Eastern Slovakia to assess the sensitivity of the model parameter and concluded that only by using sensitive parameters one can produce accurate results. da Silva

\* Corresponding author.

E-mail address: [sanjeevj@iiserb.ac.in](mailto:sanjeevj@iiserb.ac.in) (S.K. Jha).<https://doi.org/10.1016/j.jhydrol.2021.126632>

Received 27 January 2021; Received in revised form 23 April 2021; Accepted 27 June 2021

Available online 14 July 2021

0022-1694/© 2021 Elsevier B.V. All rights reserved.

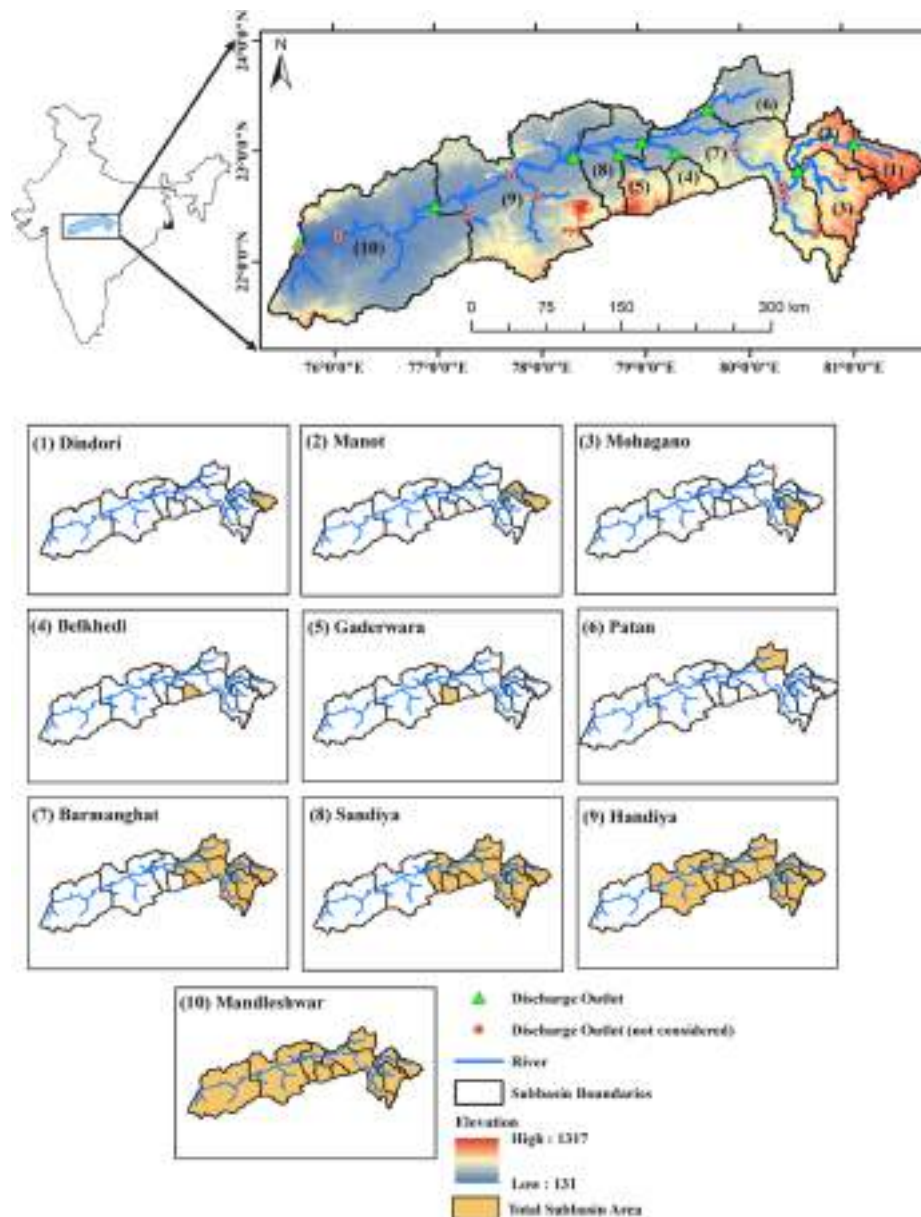


Fig. 1. Location of study area in Narmada river basin and different watersheds (1 to 10) used for the parameter sensitivity.

et al. (2015) also demonstrated the use of parameter sensitivity analysis in a SWAT model to select a set of parameters for Poxim River basin in northeastern Brazil.

To identify a set of sensitive parameters in a hydrological model for a basin, different sensitivity analysis techniques can be used. Broadly, the sensitivity analysis techniques can be divided into two categories: local sensitivity analysis (LSA) and global sensitivity analysis (GSA). Local sensitivity analysis such as one-variable-at-a-time (OAT) and differential analysis (DA) methods are less reliable because LSA considers one parameter at one time and keep the other parameters as constant (Douglas-Smith et al., 2020; Murphy et al., 2004; Nossent and Bauwens, 2012; Saltelli and Annoni, 2010). GSA is an advanced version of sensitivity analysis that overcomes the drawbacks of LSA. Regression analysis (RA), Morris screening, Sobol's methods, Fourier amplitude sensitivity test (FAST) and regional sensitivity analysis (RSA), are some of the examples of GSA (Bilotta et al., 2012; Gamerith et al., 2013; Guse et al., 2014; Himanshu et al., 2017; Norton, 2015; Van Griensven et al., 2008). Lenhart et al. (2002) compared two different sensitivity analysis methods to find out the sensitivity of different parameters of a SWAT

hydrological model. They concluded that both methods show the same result. Cibin et al. (2010) used variance based Sobol's sensitivity analysis with a SWAT hydrological model for parameters sensitivity analysis in St. Joseph River watershed and Illinois River watershed. They demonstrated that the sensitivity of parameters also depend upon the climate of the study area. Further, they found that the various flow regimes also affect the sensitivity of the model parameters. Yang (2011) examined five different sensitivity analysis methods on an environmental model and showed that the Sobol's method of sensitivity analysis method is the robust.

There is another aspect to the research on the topic of parameter sensitivity, which is related to time steps (Daily and Monthly) of simulation and size of the basin. Different parameters are effective at different time steps and for different sized basin. Most of the parameter like slope, elevation, area, vegetation type etc. can be estimated but some of the parameters are unknown. The appropriate selection of a combination of parameters for different time steps and for different size of basins increases the complexity of the modelling (Sharma et al., 1987; Troch et al., 2003; Ye et al., 2008; Zhang et al., 2012). Hydrological

features of a catchment such as imperviousness, soil water property, vegetation type; and topographical features such as slope, aspect, elevation of the area have a wide range of possible values in a large basin. On the other hand, small basin/subbasins are likely to have a similar type of hydrological and topographical features with less range of values (Baduna et al., 2017; Fang et al., 2016; Randhir and Tsvetkova, 2011; Shriver and Randhir, 2006; Zhang and Montgomery, 1994). It is a well-known fact that hydrological variables, such as rainfall, runoff, evaporation, baseflow and groundwater recharge fluctuate over time and are constantly associated with their temporal fluctuations (Amenu et al., 2005; Godsey et al., 2010; Kirchner and Neal, 2013; Pandey et al., 1998; Gond et al 2019; Das et al., 2016).

To study the role of catchment size on the parameter sensitivity analysis, the area of the basin can vary from a few square kilometers to the size of the continent (Gentine et al., 2012). Duan and Mei (2014) argued that the practical behaviour of basins would differ significantly with the catchment size and many processes of the hydrological cycle vary with time. Hence, it may not be recommended to use the same model parameters for simulation at different time steps and for different catchment size (Kumar and Merwade, 2009; Pushpalatha et al., 2011; Region et al., 2012; Reusser et al., 2011; Veith et al., 2010). Thampi et al. (2010) used catchments of two different sizes in Chaliyar river basin in Kerala, India with the same land use, soil type, topography and management practices to demonstrate the effect of basin size on the sensitivity of parameters. They found that the parameters related to curve number, soil evaporation compensation factor, available water holding capacity, average slope length and baseflow alpha factor are the critical parameters. Tobin and Bennett (2009) used three rainfall products over three different watersheds with a SWAT model to assess the sensitivity of parameters used in streamflow calculation. Muleta et al., (2007) developed six different models to simulate streamflow and sediment transport in the Big Creek Watershed with different numbers of subbasins and concluded that the streamflow simulation is comparatively less affected by the spatial distribution of subbasins than the sediment simulation.

Based on the above literature review, it is clear that there have been studies separately addressing three important aspects of the sensitivity analysis: the effect of catchment size, simulation time steps, and the choice of GSA method. However, to the best of our knowledge, an analysis explicitly looking at the effect of variation in watershed size, simulation time step, and GSA method is not available. Different hydrological processes may interact with each other by considering a combination of these three aspects in hydrological simulations. Therefore, it is necessary that sensitivity analysis should be performed considering different spatial extent and simulation time steps to identify sensitive parameters. In other words, such analysis can provide guidance to the modellers to avoid omitting important parameters while reducing the complexity of the calibration process. Our aim in this study is to identify a set of parameters covering all the important hydrological processes when a particular combination of catchment size, model time step and GSA method is used. The specific objectives of this study are: (1) to set up a SWAT hydrological model in small to large watersheds in order to analyse the effect of variation in catchment size on the sensitivity of model parameters; (2) to set up SWAT hydrological models at daily and monthly time steps in small to large watersheds in order to analyse the effect of daily and monthly time step simulation on the sensitivity of model parameters; (3) to apply two GSA techniques in objectives (1) and (2); and (4) to identify any notable variation where the sensitivity of model parameters is either independent or highly dependent on the catchment size and time step of simulation. To achieve these objectives, SWAT models are developed for 10 different sized watersheds of Narmada River Basin at daily and monthly time steps with two GSA techniques: Multiple regression method that is used by Sequential Uncertainty Fitting algorithm (SUFI-2) and Fourier Amplitude Sensitivity Testing (FAST).

## 2. Study area

Our study area is upper and middle basin of Narmada river in Central India as shown in Fig. 1. Narmada River is the largest west flowing non-perennial rivers of India. It originates from Amarkantak Plateau of Maikala range in the Shahdol district of Madhya Pradesh at an elevation of 1057 m above mean sea level, the latitude and longitude of the origin of Narmada River are 22° 40' North and 81° 45' East. The total length of the river from Amarkantak Plateau to the Arabian Sea is 1312 km. Some of the main tributaries of Narmada River are Shakkar River, Ganjal River, Chhota Tawa River, Hiran River, Jamtara River, Kolar River, Orsang River, Sher River and Tawa River. The Narmada River Basin covers the states of Madhya Pradesh, Maharashtra, and Gujarat with a total area of 98,796 km<sup>2</sup>. The whole basin is divided into three parts i.e., upper Narmada basin (from origin to the Sandiya), middle Narmada basin (from Sandiya to Sardar Sarovar dam), and lower Narmada basin (from Sardar Sarovar dam to Arabian Sea). For the current study, only the upper and middle Narmada basin is considered. The geographical extent of upper and middle basin of Narmada is from 75°33'E to 81°45'E and from 21°9'N to 23°50'N (as shown in Fig. 1). The basin is located on the Deccan plateau and is bounded by the Vindhyas from the north, Maikala range from the east, Satpura range from the south and Arabian Sea from the west. The high elevated regions of the basin are well forested, while the plains are large and fertile. The elevation of the basins varies from 131 m to 1317 m. The basin is largely plain and has the elevation less than 500 m from the mean sea level. Only some parts of upper Narmada River have elevation more than 1000 m from the mean sea level. The climate of the basin is humid tropical ranging from sub-humid in the east to semi-arid in the west. Most of the rainfall received in the basin is due to the southwest monsoon that usually starts in June and ends in September. Temperature varies from 8°C to 14°C in winter and 30°C to 40°C in summer. To study the effect of catchment size on the sensitivity of parameters, Narmada river basin has been divided into ten subbasins as shown in Fig. 1.

## 3. Model and methods

### 3.1. Soil and water assessment tool (SWAT)

SWAT is a semi-distributed ecohydrological model (Arnold et al., 1998; Gassman et al., 2007). SWAT divides the watershed into subbasins based on the topography. Further, each subbasin is partitioned into hydrologic response unit (HRU) which is a unique combination of land use, soil and slope (Guse et al., 2014). For this study, SWAT (version 2012 with its ArcSWAT interface) was used to simulate daily and monthly streamflow.

SWAT uses a typical setup with two phases, a rainfall-runoff phase based on a water balance for each subbasin [Equation (1) is taken from Niehoff et al. (2002)] and a routing phase connecting all subbasins to produce spatially explicit outputs at the subbasin outlet.

$$SW(t) = SW(t - \Delta t) + R_{day}(t) - Q_{surf}(t) - E_a(t) - W_{seep}(t) - Q_{gw}(t) \quad (1)$$

where SW(t) is the soil water content in mm on day t, SW(t - Δt) is the soil water content in mm on day t - Δt, R<sub>day</sub>, Q<sub>surf</sub>, E<sub>a</sub>, W<sub>seep</sub>, and Q<sub>gw</sub> represent precipitation (mm), surface runoff (mm), evapotranspiration (mm), percolation (mm) and groundwater flow (mm) respectively. Equation (1) determines the change in the soil water content for each day based on a daily calculation of the hydrological processes in the HRU. Each soil type is divided into different soil layers, and the soil water content is calculated for each soil layer separately and subsequently summed.

### 3.2. Sequential uncertainty fitting algorithm (SUFI-2)

SUFI-2 is a combined optimization approach that uses a global search

method and the Latin hypercube sampling technique to examine the behaviour of objective function (Abbaspour et al., 2004; Abbaspour et al., 2007). First it identifies the range of parameters and then Latin Hypercube sampling is performed to generate multiple sets of parameters according to their range. SWAT is run on each parameter set and objective function is calculated. The parameter range gets updated every iteration and tries to find the best range of parameters. Boundary conditions, parameters, model structures and measured data are the sources of uncertainty in the SUFI-2. After avoiding 5% of poor simulation, 95% prediction uncertainty (95PPU) is calculated, from the cumulative distribution of an output obtained through Latin hypercube sampling. The accuracy of model calibration and validation is determined by r-factor and p-factor. P-factor shows the observed data that is captured by 95PPU range and accounted for all the uncertainties associated with the SWAT model. The value of p-factor ranges from 1 to 0. A value 1 indicates that 100% of measured data comes under the 95 PPU. Low value of p-factor represents high uncertainty in the output and low percentage of measured data captured by 95 PPU. The r-factor is the average thickness of the 95PPU band divided by the standard deviation of the measured data. It describes the quality of the calibration. The value of r-factor also varies from 1 to 0 where a low value shows the less uncertainty in the output. To get an optimum result, p and r factors have to be balanced.

For using SUFI-2, we assume a wide range of values for the parameters so that large amount of data can come under the 95PPU. We then start reducing the range of parameters to decrease the 95PPU range. Two basic criteria have to be satisfied in SUFI-2: (i) most of the observed data should be bracted by the 95PPU band (p-factor) and (ii) the band width (r-factor) of the 95PPU must be smaller. These two criteria are problem dependent, for instance, when we have a high-quality data, we achieve high p-factor and vice-versa. For the second criterion, the width of the 95PPU should be smaller than the standard deviation of the measured data. A balance between p-factor and r-factor ensures bracketing most of the observed data within the 95PPU band (Abbaspour et al., 2015). The detailed description of SUFI-2 is given in the SWAT-CUP manual [https://swat.tamu.edu/media/114860/usermanual\\_swatcup.pdf](https://swat.tamu.edu/media/114860/usermanual_swatcup.pdf).

### 3.3. Global sensitivity analysis methods for selecting the sensitive parameters

To identify the most sensitive parameter and to select a set of sensitive parameters that cover most of the hydrological processes, we selected two different GSA methods:

(a) Multiple regression method that is used by SUFI-2 and (b) Fourier Amplitude Sensitivity Testing (FAST) method. FAST method was introduced by Cukier et al. (1978). It is widely used by the scientific community for sensitivity analysis in many research fields.

#### 3.3.1. Multiple regression method

The sensitivity of parameters in SUFI-2 is estimated by solving multiple regressions which regresses the parameters produced by the Latin Hypercube against the value of the objective function. Multiple regression method is considered as,

$$g = \alpha + \sum_{i=1}^m \beta_i b_i \quad (2)$$

where  $g$  is the objective function,  $b$  is a parameter,  $\alpha$  is a regression constant,  $\beta$  corresponds to the technical coefficient attached to the variable  $b$ , and  $m$  is equal to the number of parameters. The mean estimates the sensitivity of the changes in the objective function. It is determined one by one modifying each of the parameters while keeping all other parameters fixed. The higher value of absolute t-stat and a lower value of p-stat indicate that the parameter is more sensitive.

**Table 1**

Description of input data used in setting up a SWAT model.

Data	Description	Resolution	Source
Topography	Digital elevation model	90 m × 90 m	Shuttle Radar Topography Mission (SRTM)
Land use land cover	The Crop Data Layer	400 m × 400 m	Global Irrigated Area Mapping of International Water Management Institute (GWMI)
Soil	Soil Survey Geographic database		Harmonized World Soil Database (HWSD)
Meteorological data	Precipitation, maximum and minimum air temperature	1° × 1° and Daily/Monthly (mm)	Indian Meteorological Department (IMD)
Streamflow	Discharge	Daily/Monthly (m <sup>3</sup> /sec)	Central Water Commission of India (CWC)

#### 3.3.2. Fourier Amplitude Sensitivity Testing (FAST) method

FAST method (Cukier et al., 1978; Reusser et al., 2011) is a variance decomposition method that decomposes the total variance of the model's output into contributions of variance due to single factor (i.e., parameters and inputs). The method is described below

$$V = \sum_i^n V_i + \sum_i^n \sum_{j=i+1}^n V_{ij} + \sum_i^n \sum_{j=i+1}^n \sum_{k=j+1}^n V_{ijk} + \dots + V_{12\dots n} \quad (3)$$

where  $V$  is the total variance of the model outputs;  $i, j$ , and  $k$  are the parameters used; and  $n$  is the number of parameters.  $V_i$  and  $V_{ij}$  represent the variance described by the parameter  $i$  (first-order variance) and the variance that is described by parameters  $i$  (second-order variance) and  $j$ , respectively. The high-order variance represents the covariance due to multiple parameters. The ratio of the variance induced by a single parameter and total variance is the first-order sensitivity index ( $S_i$ ),

$$S_i = \frac{V_i}{V} \quad (4)$$

### 3.4. SWAT model input data

SWAT model requires many input data including topography, land use land cover, soil, meteorological data, and streamflow data. The details of data along with the source are listed in Table 1. Topography data was used to delineate subbasins within the watershed while the Crop data layer was used to represent the land use land cover in the basin. The Harmonized World Soil Database (HWSD) was used to provide physical and chemical properties of soil in the watershed. The meteorological data consisted of daily precipitation, and daily minimum and maximum temperature. Ten years (1991–2000) of daily precipitation and temperature data were used to simulate the climate in the watershed for this study. The remaining weather data including relative humidity, solar radiation, and wind speed were auto simulated by SWAT weather generator. The daily and monthly streamflow data were collected from Central Water Commission (CWC).

### 3.5. SWAT set-up

The SWAT watershed delineation resulted in 43 watersheds for Narmada River basin. There are 18 discharge locations (as shown in Fig. 1) but we selected only 10 discharge locations for watershed delineation due to proper data availability and size of the watersheds for this study. These 10 watersheds are classified into three groups based on the area: small watershed, middle-range watershed, and large watershed. (1) Dindori, (2) Manot, (3) Mohgaon, (4) Belkhedi, (5) Gaderwara



**Table 2**  
Soil and Landuse distribution in different watersheds.

		Percentage of area covered									
		Belkhedi	Gaderwara	Dindori	Patan	Mohagano	Manot	Barmanghat	Sandiya	Handiya	Mandleshwar
Area (sq. km.)		1477	2202	2309	4015	4256	4923	26,181	32,745	51,770	72,137
Soil class	Ao81-2b-3652 (Loam)	NA	NA	NA	NA	NA	0.68	NA	NA	NA	NA
	Bv12-3b-3696 (Clay- Loam)	NA	2.88	NA	NA	NA	28.17	NA	0.64	15.37	18.16
	I-bc-3735 (Loam)	NA	NA	88.67	NA	35.05	NA	21.45	17.12	10.84	7.78
	I-Bc-Lc-3714 (Clay- Loam)	NA	NA	NA	11.5	1.66	NA	1.33	1.06	3.64	2.61
	Lc75-1b-3780 (Sandy- Clay- Loam)	NA	NA	11.33	NA	1.05	NA	2.23	1.78	1.12	0.8
	Vc13-2-3b-3858 (Clay)	NA	NA	NA	NA	NA	14.65	NA	NA	NA	NA
	Vc21-3a-3859 (Clay)	NA	NA	NA	3.94	NA	1.27	0.63	0.5	0.34	0.24
	Vc43-3ab-3861 (Clay)	85.86	67.6	NA	70.62	62.23	55.22	61.25	57.44	44.23	48.67
	Vp20-3a-3866 (Clay)	14.14	29.52	NA	13.94	NA	NA	13.11	21.46	24.48	21.75
	Water (WATR)	0.04	NA	NA	0.08	14.41	36.04	0.71	0.57	0.68	0.51
landuse e class	Wetlands-Mixed (WETL)	NA	NA	NA	0.01	NA	0.18	NA	NA	NA	NA
	Arid Range	NA	NA	NA	NA	NA	6.55	NA	NA	0.03	0.08
	(SWRN)										
Range-Brush (RNGB)		56.65		24.61	17.5	25.16	NA	5.63	23.24	21.77	17.92
Agricultural Land-Generic (AGRL)		2.29		4.66	5.68	4.23	10.06	6.37	7.34	6.44	4.59
Irrigated, surface water, single crop (RI01)		0.61		0.14	0.06	1.38	0.18	0.71	1.25	1.05	0.87
Irrigated, surface water, double crop (RI02)		2.74		1.27	0.11	13.26	0.02	1.42	5.39	8.45	11.67
Irrigated, surface water, continuous crop (RI03)		NA	NA		NA	0.52	NA	11.67	0.09	0.09	0.61
Irrigated, ground water, single crop (RI04)		6.99		5.31	11.74	1.03	11.07	18.71	6.84	5.91	4.67
Irrigated, ground water, double crop (RI05)		16.61		15.81	13.41	5.12	7.28	9.99	8.24	9.1	8.96
Irrigated, conjunctive use, single crop (RI07)		0.98		2.66	6.45	1.84	0.26	2.26	3.21	2.87	2.82
Irrigated, conjunctive use, double crop (RI08)		1.82		4.43	0.81	28.8	0.24	0.43	10.88	11.84	11.6
Forest-Mixed (FRST)		11.26	41.11		44.24	18.58	56.47	0.04	32.81	31.92	35.57

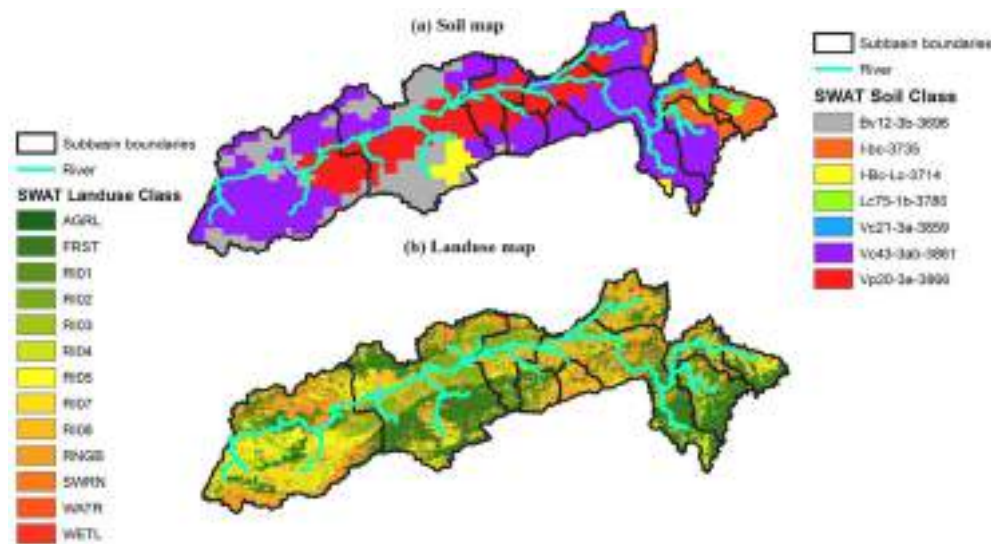


**Fig. 2.** Distribution of (a) soil and (b) landuse class for watersheds after reclassification in SWAT.

and (6) Patan watershed were classified as small watershed; (7) Barmanghat and (8) Sandiya as middle-range watershed and (9) Handiya and (10) Mandleshwar as large watershed. Watersheds used in this study have almost similar type of land use and soil type. As shown in Table 2, Range-Brush (RNGB), Forest-Mixed (FRST), and Irrigated groundwater double crop (RI05) are the major part of all watersheds that covers approximately 60 to 75 percent of the total landuse. Furthermore, the slope is classified in five classes (i.e. 0–5, 5–10, 10–15, 15–20 and >20) for all the watersheds. The soil and land use classification and percentage area covered by them are shown in Table 2. The distribution of Soil and land use type after reclassification is shown in Fig. 2.

The model was simulated from 1986 to 2000. First five years of warm up period (1986–1996) was assigned in the model to initialize model

parameters. Daily and monthly simulated streamflow output from the SWAT model were compared against the observation data. The calibration and validation periods were from 1991 to 1997 and 1998 to 2000 respectively.

### 3.6. Selection of SWAT parameters

SWAT model contains more than 210 hydrological parameters. All of them may not significantly contribute to the output. Therefore, it is important to identify the most sensitive input parameters and their ranges for streamflow simulation. Based on the available literature, 29 parameters were selected for this study (Garg et al., 2012; Narsimlu et al., 2015 Schmalz and Fohrer, 2009) to cover various relevant

**Table 3**

Descriptions and initial ranges of the parameters used for model calibration.  
<sup>b</sup>Type of change to be applied to the existing parameter value: '1' means a value from the range is added to the original value, '2' means the original value is to be replaced by a value from the range, '3' means the original value is multiplied by the adjustment factor (add 1 to the given value within the range).

Parameter Name	Definition	Process	Adjustment <sup>b</sup>	Initial Range
ALPHA_BF.gw	Baseflow alpha factor for recession constant (days)	Groundwater	2	0 to 1
ALPHA_BNK.rte	Baseflow alpha factor for bank storage (days)	Groundwater	2	0 to 1
CANMX.hru	Maximum canopy storage (mm H <sub>2</sub> O)	Evapotranspiration	3	−1 to 1
CH_K2.rte	Effective hydraulic conductivity in main channel alluvium (mm/hr)	Channel routing	2	−0.01 to 500
CH_N2.rte	Manning's "n" value for the main channel	Channel routing	2	−0.01 to 0.3
CH_S1.sub	Average slope of tributary channels (m)	Surface runoff	3	0.0001 to 1
CH_S2.rte	Average slope of main channel (m/m)	Channel routing	3	−0.001 to 1
CH_W2.rte	Average width of main channel at top of bank (m)	Channel routing	2	0 to 1000
CN2.mgt	Curve number for moisture condition II	Surface runoff	3	−0.1 to 0.1
DEEPST.gw	Initial depth of water in shallow aquifer (mm H <sub>2</sub> O)	Groundwater	2	0 to 50,000
EPCO.hru	Plant uptake compensation factor.	Evaporation	3	0 to 1
ESCO.hru	Soil evaporation compensation factor.	Evaporation	2	0 to 1
GW_DELAY.gw	Groundwater delay time (days)	Groundwater	1	0 to 500
GW_REVAP.gw	Groundwater re-evaporation coefficient	Groundwater	2	0.02 to 0.2
GWHT.gw	Initial groundwater height (m)	Groundwater	2	0 to 25
GWQMN.gw	Threshold depth of water in the shallow aquifer required for return flow to occur (mm)	Groundwater	1	0 to 5000
HRU_SLP.hru	Average slope steepness (m/m)	Topographic	3	0 to 1
LAT_TTIME.hru	Lateral flow travel time (days)	Soil water	2	0 to 180
OV_N.hru	Manning's "n" value for overland flow	Overland flow	3	0.01 to 1
		Groundwater	1	0 to 1

**Table 3 (continued)**

Parameter Name	Definition	Process	Adjustment <sup>b</sup>	Initial Range
RCHRG_DP.gw	Deep aquifer percolation fraction			
REVAPMN.gw	Threshold depth for exchange with deep aquifer	Groundwater	1	0 to 500
SLSOIL.hru	Slope length for lateral subsurface flow (m)	topographic	2	0 to 150
SLSUBBSN.hru	Average slope length (m)	topographic	3	−1 to 1
SOL_AWC(..).sol	Available water capacity of the soil layer (mm H <sub>2</sub> O/mm Soil)	Soil water	3	−1 to 1
SOL_BD(..).sol	Moist bulk density (Mg/m <sup>3</sup> )	Soil water	3	−1 to 1
SOL_K(..).sol	Saturated hydraulic conductivity (mm/hr)	Surface runoff	3	−1 to 1
SURLAG.bsn	Surface runoff lag time.	Runoff	2	0.05 to 24
USLE_K(..).sol	fraction change in USLE equation soil erodibility factor (%)	Erosion	2	0 to 0.65
USLE_P.mgt	USLE equation support practice (P) factor	Erosion	2	0 to 1

hydrological processes in the Narmada River Basin (see Table 3). A core description of these parameters is presented in Appendix-1 (see Neitsch et al. (2011) for more details). Since the average minimum temperature in the study area is always more than 4 °C, any snow-related parameter is not considered in this study.

### 3.7. Calibration-validation

The calibration and validation were conducted using SWAT Calibration and Uncertainty Procedure (SWAT-CUP) to handle a large number of simulations. For the global sensitivity process, 2000 simulations were conducted to identify the most sensitive input parameters. The Sequential Uncertainty Fitting (SUFI-2) optimization algorithm with Nash-Sutcliffe efficiency (NSE) as objective function was used to obtain the prediction accuracy in the model. NSE can be defined as,

$$NSE = 1 - \frac{\sum_i (Q_m - Q_i)^2}{\sum_i (Q_{m,i} - \bar{Q}_m)^2} \quad (5)$$

where,  $Q_s$  is simulated discharge,  $Q_m$  is measured discharge and  $\bar{Q}_m$  is average of measured discharge. NSE value more than 0.5 is acceptable for rainfall-runoff modelling. SWAT-CUP uses t-stat (high absolute values suggest more sensitivity) and p-value (values close to zero suggest a high level of significance) to identify the relative significance of the individual parameter (Khatun et al., 2018; Kumar et al., 2017; Visakh et al., 2019). A p-factor of 1 and r-factor of 0 indicate the simulated and observed data are equal. Fig. 3 represents the overall approach used for the model development and parameter sensitivity analysis. First, we setup a SWAT model for Narmada River basin. Then SWAT-CUP with SUFI-2 algorithm is used for calibrating the Arc-SWAT generated output for 10 subbasins with 29 parameters (hereafter we will refer as SA\_29). After reaching a desirable calibration result, we perform a global

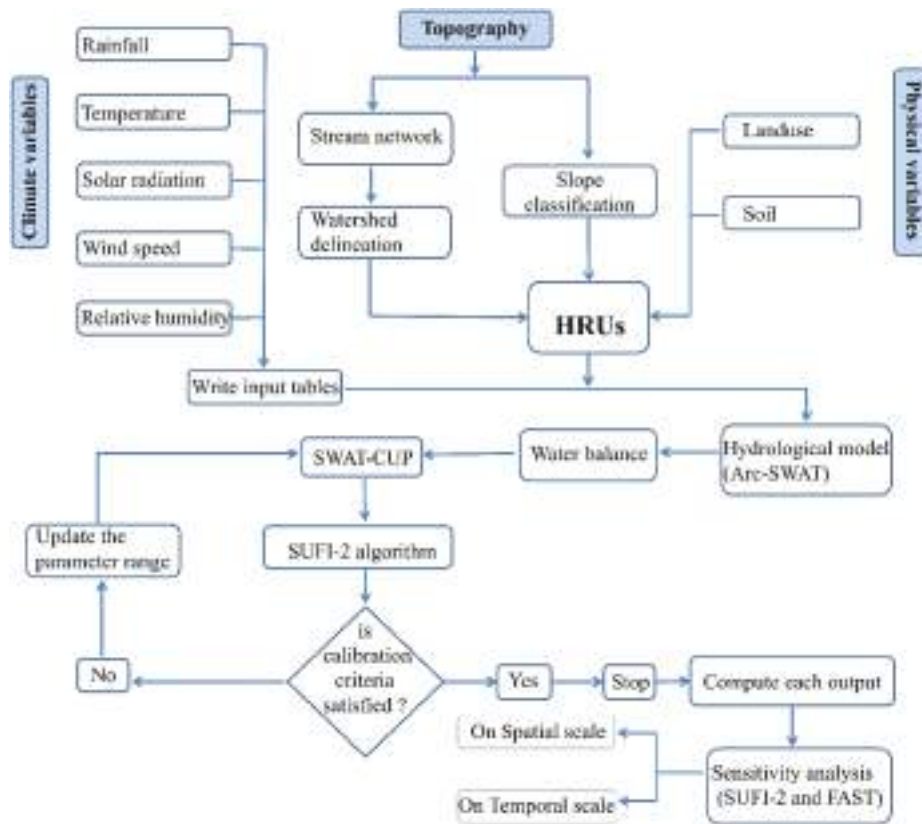


Fig. 3. Flow diagram showing the model set up and parameter sensitivity.

sensitivity analysis to estimate the sensitivity of SA<sub>29</sub> parameters by using multilinear regression sensitivity analysis. After ranking all parameters, we select first 16 sensitive parameters (will refer as SA<sub>16</sub>) for the Fourier Amplitude Sensitivity Testing (FAST) analysis.

It is worth pointing out that there are a number of assumptions made in this study. We have highlighted the main assumptions here. Due to restriction of the number of simulation in SUFI-2, we could include only 2000 simulation for SA<sub>29</sub>. We used only one landuse map for the entire calibration and validation time period. The climatic condition is assumed to be same for all the ten watersheds because they are part of a single river. The parameters are based on the literature and we did not consider exhaustive list of potential parameters to reduce the initial uncertainty. We did not consider the error propagation through the algorithm and structure used by SWAT and uncertainty in the input data (rainfall and temperature).

## 4. Results

### 4.1. Calibration and validation of SWAT model with 29 parameters

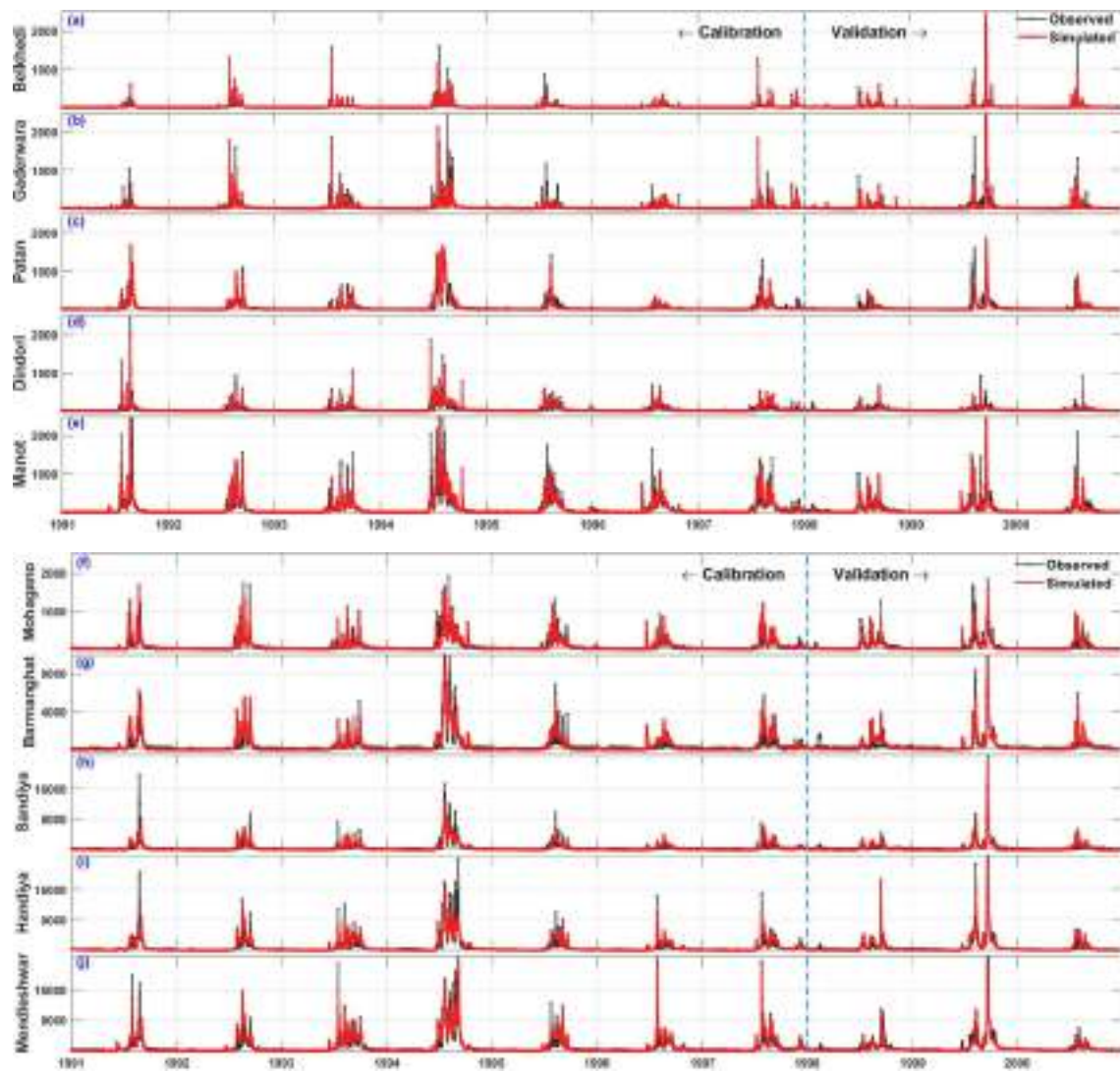
SWAT-CUP analysis tool with SUFI-2 algorithm is used for calibration and validation. Generally 60 to 70 % of data from the available data set is used for calibration and rest of the data is used for validation. For this study daily and monthly average discharge data from 1<sup>st</sup> January 1991 to 31<sup>st</sup> December 2000 is analysed.

Fig. 4(a-j) and 5 (a-j) show the simulated and observed discharge values associated with 10 distinct subbasins (i.e. Belkhedi(1), Gaderwara(2), Patan(3), Dindori(4), Manot(5), Mohagano(6), Barman ghat(7), Sandiya(8), Handiya(9) and Mandleshwar(10)) at daily and monthly time steps. Fig. 4 (a to j) show the hydrograph from January 1991 to December 2000 (calibration period: January 1991 to December 1997 and validation period: January 1998 to December 2000). All 10 watersheds were considered to study the effect of Catchment Size on the

simulation accuracy at a daily time step. Different watersheds are in the descending order (from Mandleshwar(10) watershed with entire study area) with total area of 72173 km<sup>2</sup> to Belkhedi(1) watershed with total area of 1477 km<sup>2</sup>) with NSE as the objective function. By visual analysis of Fig. 4(a to j), it is evident that the simulation with NSE as an objective function produces reasonably good results. Except some of the high peaks, simulated high and low flows are in good match with the observed flows. Since the patterns of simulated flow (rise and fall of flow values, duration of peak and low flows, and overall variation in the time series) are matching with the observed flows and all the statistical criteria (such as NSE) show acceptable values, we accepted the calibration results. If we try to match all the peak flows in the simulation by modifying some of the parameters, the baseflow will be altered. The reasons for deviation in simulated and observed flow values could be many, such as, errors in the input data, limitation of model structure, limitation in the governing equations solved by SWAT, error in neglecting the other parameters in the calibration etc.

To study the effect of daily and monthly time steps on the simulation accuracy, the simulated and observed hydrograph associated with all ten watersheds at monthly time steps with NSE objective functions are plotted in Fig. 5 (a to j). Visual inspection of Fig. 5(a to j) show that the simulation outputs are similar to the observed flows. Overall, the variation between simulated and observed values at a daily time step is found to be more, especially for the large catchments (i.e. Mandleshwar (10), Handiya(9) and Sandiya(8)) as shown in Fig. 4 (a to c). The variation is less for monthly time step (Fig. 5(a to j)).

Table 4 represents the model performance criteria i.e., p-factor, r-factor, and NSE for different watersheds (i.e. Belkhedi(1), Gaderwara (2), Patan(3), Dindori(4), Manot(5), Mohagano(6), Barman ghat(7), Sandiya(8), Handiya(9) and Mandleshwar(10)) with SA<sub>29</sub> and SA<sub>16</sub>. As shown in Table 4, p-factor varies from 0.72 to 0.95 and 0.55 to 0.95 for daily and monthly simulations respectively. For the calibration period, average p-value for daily and monthly simulations is 0.89 and



**Fig. 4.** Daily time series plot of observed and simulated hydrograph at (a) Belkhedi, (b) Gaderwara, (c) Patan, (d) Dindori, (e) Manot, (f) Mohagano, (g) Barman ghat, (h) Sandiya, (i) Handiya and (j) Mandleshwar watershed.

0.82 respectively. Table 4 shows that for daily simulation for SA\_29, NSE varies from 0.58 to 0.75 with an average value of 0.67. For monthly simulation, NSE varies from 0.89 to 0.97 and the average value is 0.93. When we use only SA\_16, NSE values of the model performance of the watersheds don't deviate from those obtained from model with SA\_29. Sometimes NSE value of the model with SA\_16 is better than that of SA\_29. For instance, Dindori(4), Manot(5) and Barman Ghat(7) at monthly time step show high NSE value with the set of SA\_16. Overall, from Table 4 we can say that the SA\_16 also produce the accurate result compared to simulations with SA\_29. The reduction of parameters is very helpful to reduce the complexity of the model.

## 4.2. Sensitivity analysis results

### 4.2.1. Effect of catchment size on the sensitivity of parameters on daily simulation

To study the variation in parameter sensitivity with catchment size, the calibration was performed using 10 different sized watersheds. Fig. 6 shows the parameter sensitivity results based on p-value with SA\_29 (Fig. 6(a)) and FAST indices with SA\_16 (Fig. 6(b)) for 10 different watersheds under three categories i.e. small watershed (Belkhedi(1), Gaderwara(2), Patan(3), Dindori(4), Manot(5) and Mohagano(6)), medium-range watershed (Barman ghat(7) and Sandiya(8)) and large

watershed (Handiya(9) and Mandleshwar(10)). In Fig. 6, parameters used for this study are shown on the y-axis and the watersheds are listed on the x-axis. The sequence of these watersheds is in the increasing order of their area. FAST sensitivity analysis is performed on 16 most sensitive parameters (SA\_16) which were obtained from SUFI-2 analysis. It is worth repeating here that SUFI-2 analysis was performed using 29 parameters selected from the literature (SA\_29). Parameters which are not included in SA\_16 for a watershed are represented by NaN value (shown in black colour in Fig. 6(b)). It is evident from the figures that the sensitivity of parameters for daily simulations depend upon the catchment size. Baseflow alpha factor for bank storage (ALPHA\_BNK.rte), hydraulic conductivity in main channel (CH\_K2.rte), manning's value for main channel (CH\_N2.rte), average width of main channel bank (CH\_W2.rte), curve number (CN2.hru), threshold depth of water in shallow aquifer to return (GWQMN.gw) and soil bulk density (SOL\_BD(..).sol) are the most sensitive parameters for all the watersheds. Our results indicate that the sensitivity of these parameters does not depend upon the catchment size at a daily simulation time step. On the other hand, following parameters are not sensitive in any watershed: Baseflow alpha factor for recession constant (ALPHA\_BF.gw), maximum canopy storage (CANMAX.hru), initial ground water height (GWHT.gw), lateral flow time (LAT\_TTIME.hru) and Threshold depth for exchange with deep aquifer (REVAPMN.gw). We can conclude that these parameters



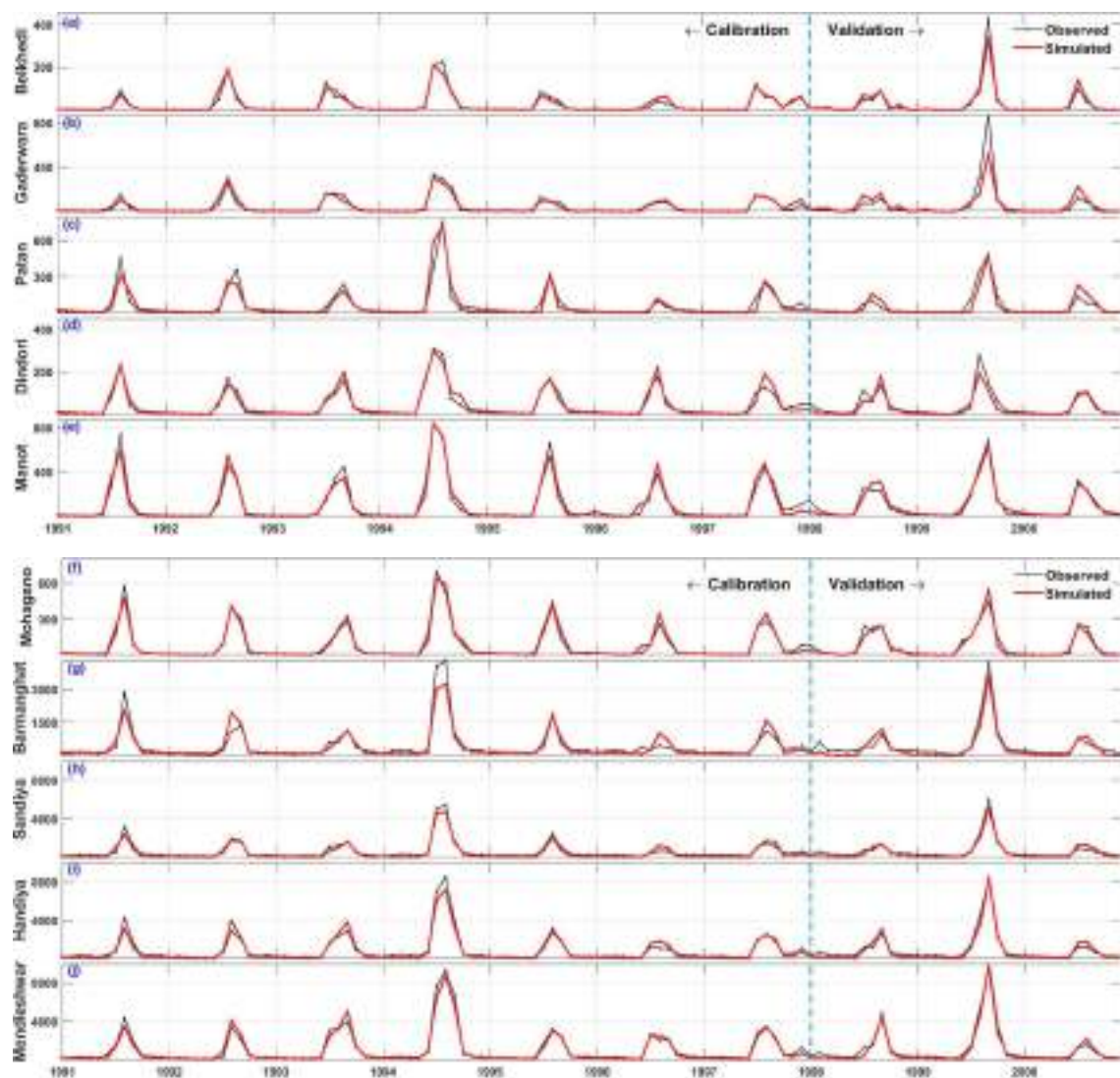


Fig. 5. Monthly time series plot of observed and simulated hydrograph at (a) Belkhedi, (b) Gaderwara, (c) Patan, (d) Dindori, (e) Manot, (f) Mohagano, (g) Barman ghat, (h) Sandiya, (i) Handiya and (j) Mandleshwar watershed.

Table 4

Statistics of model performance associated with calibration and validation for 10 different watershedes of Narmada River Basin at monthly and daily temporal resolutions.

		29 PARAMETERS (SA_29)			16 PARAMETERS (SA_16)					29 PARAMETERS (SA_29)			16 PARAMETERS (SA_16)		
		p factor	r factor	NSE	p factor	r factor	NSE			p factor	r factor	NSE	p factor	r factor	NSE
Belkhedi	Daily Calibration	0.94	0.34	0.58	0.86	0.32	0.57	Manot	0.92	0.49	0.64	0.77	0.26	0.61	
	Daily Validation	0.97	0.27	0.84					0.9	0.44	0.67				
	Monthly Calibration	0.93	0.44	0.94	0.95	0.41	0.83		0.96	0.67	0.96	0.86	0.47	0.97	
	Monthly Validation	0.97	0.28	0.94					0.92	0.74	0.95				
Gaderwara	Daily Calibration	0.89	0.35	0.62	0.54	0.29	0.6	Barmanghat	0.76	0.56	0.67	0.58	0.55	0.67	
	Daily Validation	0.92	0.26	0.69					0.66	0.51	0.85				
	Monthly Calibration	0.93	0.65	0.93	0.9	0.43	0.87		0.75	0.69	0.89	0.98	0.78	0.92	
	Monthly Validation	0.89	0.3	0.78					0.61	0.65	0.92				
Patan	Daily Calibration	0.92	0.51	0.72	0.34	0.49	0.72	Sandiya	0.72	0.59	0.73	0.64	0.52	0.71	
	Daily Validation	0.95	0.5	0.68					0.44	0.44	0.89				
	Monthly Calibration	0.94	0.56	0.89	0.68	0.28	0.73		0.62	0.8	0.93	0.98	0.69	0.92	
	Monthly Validation	0.97	0.86	0.85					0.44	0.56	0.93				
Dindori	Daily Calibration	0.94	0.45	0.71	0.94	0.51	0.7	Handiya	0.84	0.54	0.72	0.81	0.49	0.65	
	Daily Validation	0.93	0.76	0.49					0.88	0.67	0.79				
	Monthly Calibration	0.94	0.66	0.93	0.89	0.58	0.94		0.55	0.61	0.94	0.39	0.46	0.92	
	Monthly Validation	0.69	0.46	0.85					0.33	0.36	0.96				
Mohagano	Daily Calibration	0.95	0.64	0.68	0.92	0.58	0.63	Mandleshwar	0.91	0.59	0.76	0.94	0.68	0.74	
	Daily Validation	0.89	0.41	0.56					0.92	0.7	0.75				
	Monthly Calibration	0.88	0.6	0.97	0.95	0.6	0.93		0.68	0.66	0.97	0.32	0.22	0.94	
	Monthly Validation	0.94	0.76	0.93					0.67	0.69	0.97				

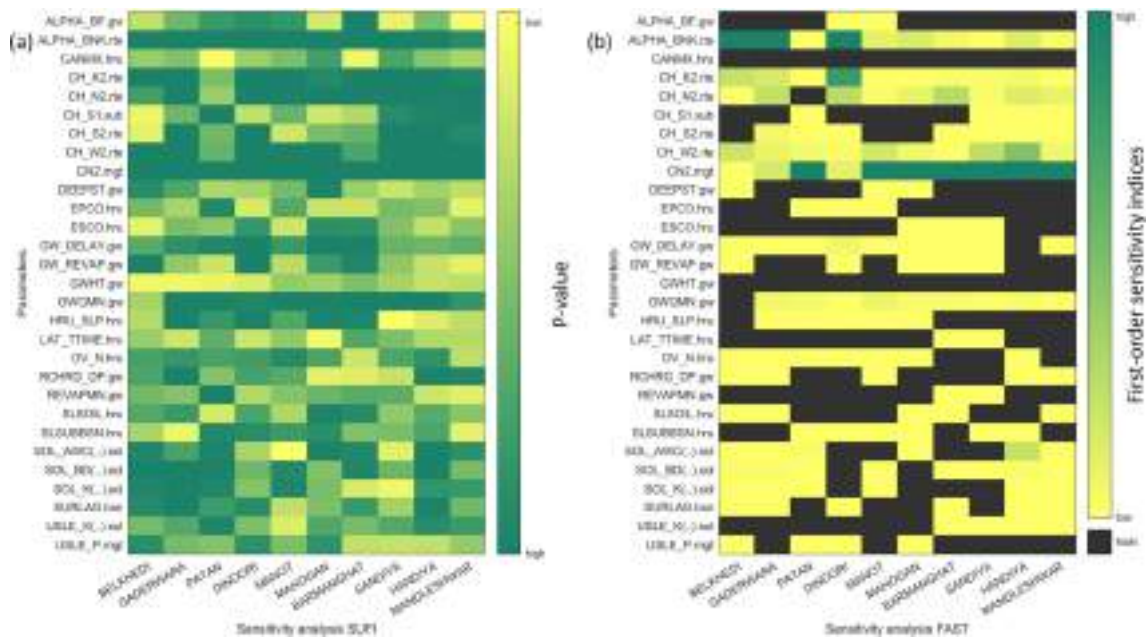


Fig. 6. The assessment of the parameter sensitivity for the Mandleshwar, Handiya, Sandiya, Barmanghat, Manot, Mahogan, Dindori, Patan, Gaderwara and Belkhedi watershed (as in increasing order of their area) at daily time steps for (a) SA\_29 (b) SA\_16.

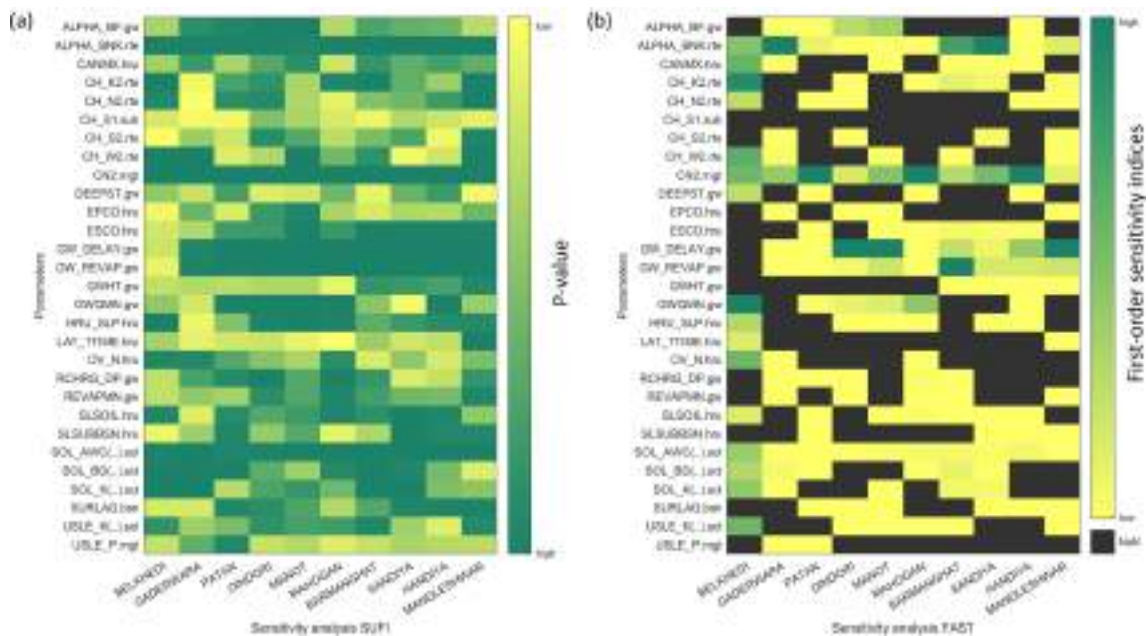
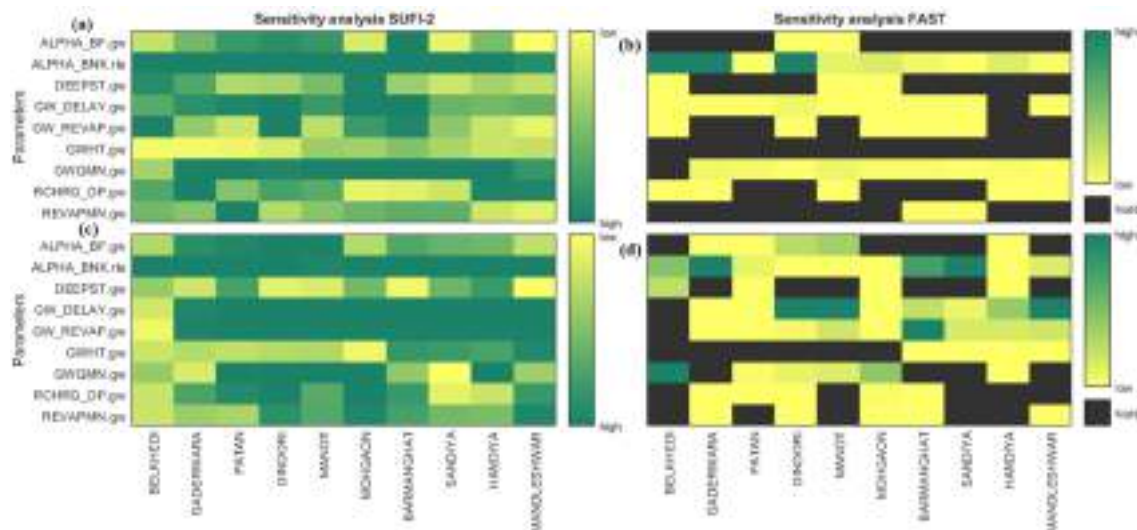


Fig. 7. The assessment of the parameter sensitivity for the Mandleshwar, Handiya, Sandiya, Barmanghat, Manot, Mahogan, Dindori, Patan, Gaderwara and Belkhedi watershed (as in increasing order of their area) at monthly time steps for (a) SA\_29 (b) SA\_16.

can be ignored and thus the number of parameters can be minimized in daily simulations. Some of the parameters are sensitive only for a range of watershed size. For instance, average slope of tributary channel (CH\_S1.sub), soil bulk density (SOL\_BD(.).sol) and soil erodibility factor (USLE\_K.sol) are sensitive for large watershed and middle-range watershed (Sandiya (8) watershed). Groundwater delay (GW\_DELAY.gw), Average slope steepness (HRU\_SLP.m) and support practice (p) factor of USLE soil equation (USLE\_P.mgt) are not sensitive for large watersheds but sensitive for small and middle-range watersheds.

#### 4.2.2. Effect of catchment size on the sensitivity of parameters on monthly simulation

Fig. 7(a) and (b) show the sensitivity of SA\_29 and SA\_16 of ten distinct watersheds when monthly simulations were performed. Fig. 7 shows that watershed size affects the parameter sensitivity. Overall, Baseflow alpha factor for bank storage (ALPHA\_BNK.rte), curve number (CN2.mgt), groundwater delay (GW\_DELAY.gw), ground water revap factor (GW\_REVAP.gw), and available soil water (SOL\_AWC(.).sol) are highly sensitive for almost all the watersheds at monthly time step, which implies that these parameters are significant irrespective of selected catchment size in the monthly simulation. Furthermore, average slope of tributary channels (CH\_S1.sub), lateral flow travel time



**Fig. 8.** The assessment of the groundwater related parameter sensitivity for watersheds (a) for SA\_29, (b) SA\_16 at daily time steps and for (c) SA\_29, (d) SA\_16 at monthly time steps.

(LAT\_TIME.hru) and support practice (p) factor of USLE soil equation (USLE\_P.mgt) are least sensitive for almost all the watersheds at monthly simulation time step, which implies that these parameters are not significant and can be ignored to avoid over parameterization in the monthly simulation. Some parameters are highly effective for some watersheds (based on size), for example, Baseflow alpha factor for recession constant (ALPHA\_BF.gw), Manning's value for overland flow (OV\_N.hru) and soil erodibility factor (USLE\_K(.).sol) are sensitive for small watershed but not at all sensitive for large and medium-range watersheds. Initial ground water height (GWHT.gw) and average slope length (SLSUBBSN.hru) are sensitive in large watersheds but not sensitive in small watersheds.

#### 4.2.3. Effect of daily and monthly simulations on the sensitivity of parameters

Figs. 6 and 7 also show that the sensitivity of parameters depends on the time step of the simulation (daily and monthly). Baseflow alpha factor for bank storage (ALPHA\_BNK.rte) and curve number (CN2.hru) are the sensitive parameters and Soil evaporation compensation factor (ESCO.hru), soil, erodibility factor (USLE\_K.sol), and surface runoff lag time (SURLAG.bsn) are the least sensitive parameters in both daily and monthly simulations. Ground water delay (GW\_DELAY.gw), ground water revap factor (GW\_REVAP.gw), and available soil water (SOL\_AWC(.).sol) are sensitive in monthly simulation. Manning's value for main channel (CH\_N2.rte), average width of main channel bank (CH\_W2.rte), threshold depth of water in shallow aquifer to return (GWQMN.gw) and soil bulk density (SOL\_BD(.).sol) are sensitive at daily simulation time step.

## 5. Discussion

In this section, we try to infer common points from the results presented in the previous section. We now categorize the parameters according to their association with a hydrological process, such as groundwater, surface runoff, evapotranspiration etc. Further, we attempt to explain the possible reasons behind a set of parameters being highly/least sensitive to variation in the watershed size and simulation time step.

### 5.1. Sensitivity of groundwater related parameters

The multilinear regression sensitivity analysis and the first order sensitivity indices derived from FAST analysis for groundwater related

parameters are shown in Fig. 8(a-d) at daily and monthly simulation time steps for SA\_29 and SA\_16 respectively. It is worth pointing here that Fig. 8 is the subplot of Figs. 6 and 7. ALPHA\_BNK.rte regulates the outflow of the ground/soil water from the bank to the river. It also directly contributes in the main channel flow as bank storage and groundwater. Thus the sensitivity of ALPHA\_BNK.rte is more than other groundwater parameters for all watersheds and for both monthly and daily simulations. Similar results were also reported by Nilawar and Waikar (2018) and Narsimlu et al. (2015) in their studies. For large watersheds at monthly time step, initial groundwater height (GWHT.gw) shows high sensitivity in case of analysis with SUFI-2 method (with all 29 parameters) but least sensitivity when we use only 16 parameters in the FAST method. This indicates that the sensitivity of GWHT.gw is affected by the presence of other ground water related parameters which we don't include in the FAST method.

ALPHA\_BF.gw regulates the outflow of the groundwater to the river. The baseflow alpha factor is a function of the watershed topography, drainage pattern and soil properties. SWAT has the limitations in rigorously simulating the groundwater flow. The interaction between groundwater flow and baseflow is high for smaller and mountainous region thus the small watersheds i.e. Patan (3), Dindori (4) and Manot (5) show high sensitivity at both daily and monthly simulation time steps. Our results show that the sensitivity of ALPHA\_BF.gw is more than the sensitivity of other groundwater parameters. Dhami et al. (2018) also reported in their study that ALPHA\_BF.gw is sensitive parameter in Karnali River basin in a mountainous region of Nepal. Our study area is also surrounded by different mountainous ranges (see Section 2 about the details of our study area).

Groundwater starts transporting from shallow aquifer to river channel when the depth of water in the aquifer is equal or greater than the GWQMN. Perhaps, this is one of the reasons why its sensitivity is independent of the size of the watershed in the daily simulations. In monthly simulations, change in the water level in the shallow aquifer is dependent on the area of the watershed. Therefore GWQMN.gw is more sensitive in small watersheds but less sensitive in large watersheds. Our result is supported by the findings of Guse et al. (2014), who reported that the parameter GWQMN.gw was highly sensitive in Treene lowland catchment in Northern Germany. Ground water delay (GW\_DELAY.gw) is the time required for water to reach the shallow aquifer from root zone. It mainly depends on the soil property and height of the water table. Therefore, its sensitivity is independent of the watershed size and simulation time steps, which is also confirmed by other studies such as Keery et al. (2007), Tolley et al. (2019), and Borgonovo et al. (2017).



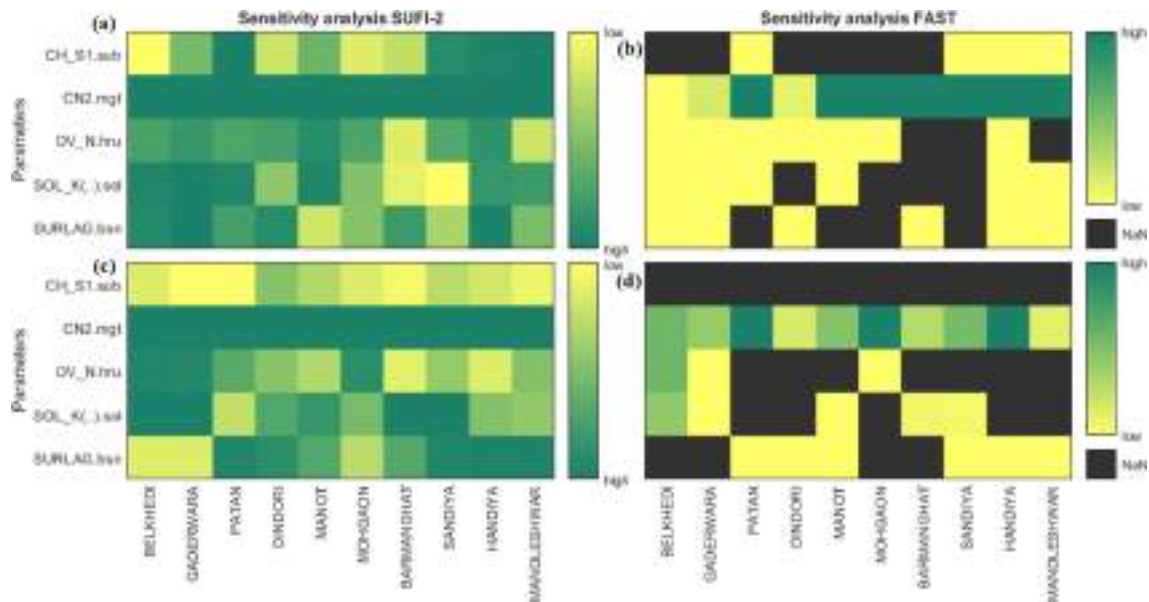


Fig. 9. The assessment of the runoff related parameter sensitivity for watersheds (a) for SA\_29, (b) SA\_16 at daily time steps and for (c) SA\_29, (d) SA\_16 at monthly time steps.

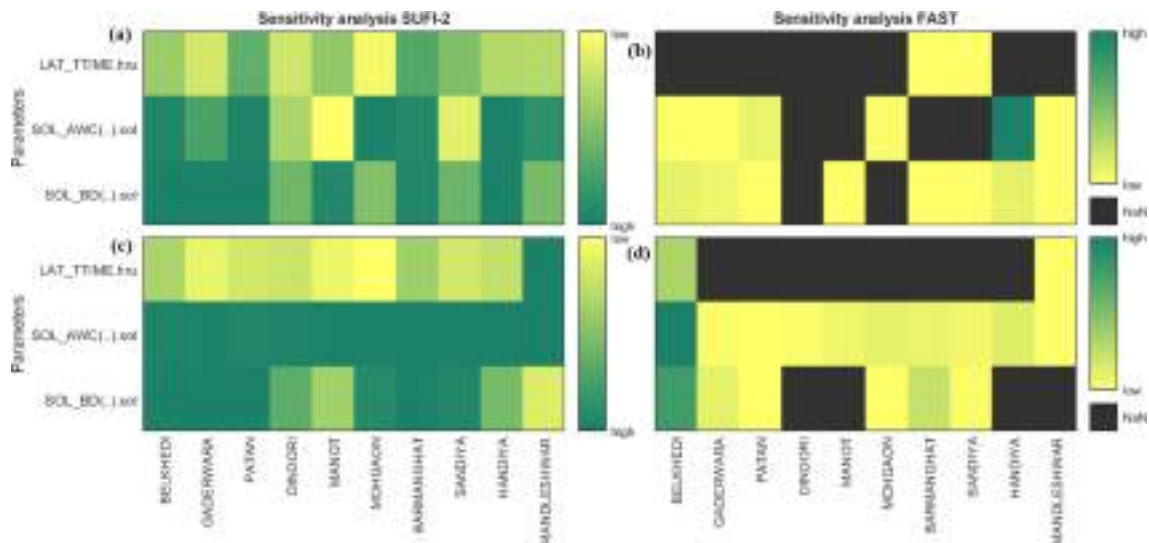


Fig. 10. The assessment of the soilwater related parameter sensitivity for watersheds at (a) for SA\_29, (b) SA\_16 at daily time steps and for (c) SA\_29, (d) SA\_16 at monthly time step.

## 5.2. Sensitivity of runoff related parameters

The sensitivity of runoff related parameters is shown in Fig. 9(a-d). The arrangement of the figure is similar to that of Fig. 8. The parameter CN2.mgt (curve number for moisture condition) has the primary influence on the amount of runoff generated from a hydrologic response unit. Hence, a relatively greater sensitivity index for CN2.mgt can be expected for most of the watersheds. The value of curve number depends on landuse and soil type. It is not affected by the size of the watershed and simulation time step (Sharma et al., 2019; McCuen 1973).

Large subbasins have more tributaries so the average slope of tributaries channel (CH\_S1.sub) is sensitive parameter for large subbasins at a daily time step (Emery et al., 2016; Pontes et al., 2016). The contribution of the small tributaries varies frequently especially in a rainy day, which could be the reason why the parameter is sensitive at a daily time step. Since the accumulated streamflow at monthly time step is more than that at a daily time step, the parameter is not sensitive in case of

monthly simulations. The surface runoff lag time (SURLAG.bsn) is sensitive when the time of concentration is high. This parameter does not show significant sensitivity in daily simulations. However, in monthly simulations, it is sensitive for almost all the watersheds. For runoff, the lag time is in days, so in monthly simulations it is more uncertain compare to daily simulations (Rahman et al., 2013; Uniyal et al., 2015). The value of saturated hydraulic conductivity (SOL\_K(..).sol) (Beven and Germann, 2013; Pue et al., 2019) depends on various factors like soil moisture, soil hydro group etc. Therefore, the sensitivity of these two parameters (SURLAG.bsn and SOL\_K(..).sol) in case of SA\_29 (with more parameters) is more as compared to SA\_16 simulation.

## 5.3. Sensitivity of soilwater related parameters

The sensitivity of soilwater related parameters is shown in Fig. 10 (a to d). Moist bulk density (SOL\_BD(..).sol) and lateral flow from the soil (LAT\_TTIME.hru) are directly affected by available water capacity of the



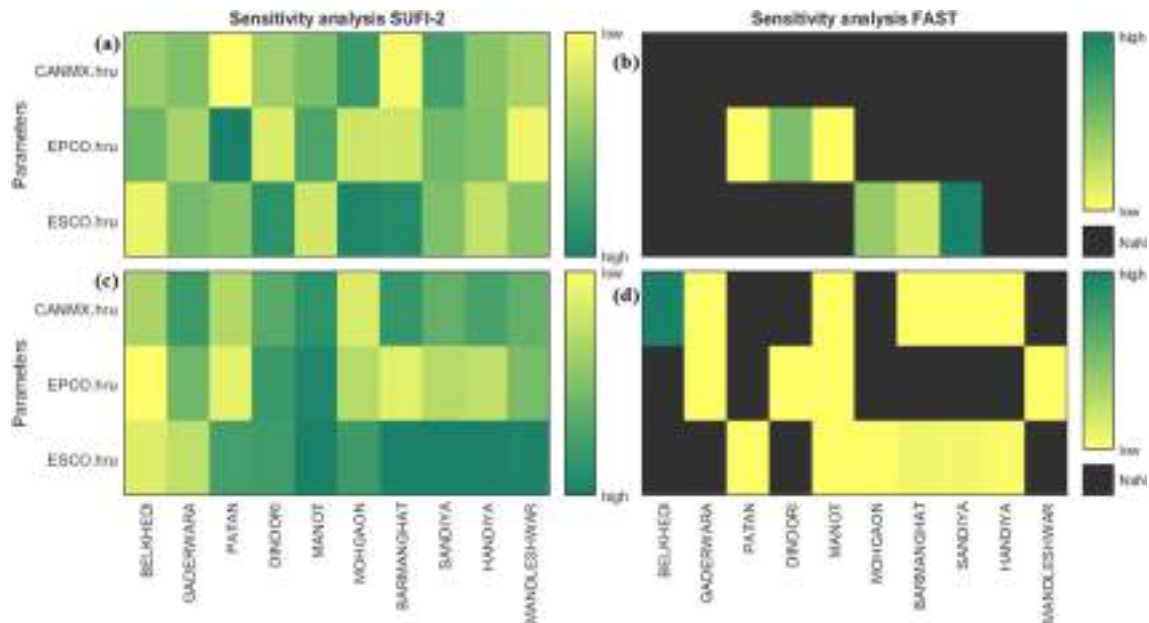


Fig. 11. The assessment of the evapotranspiration related parameter sensitivity for watersheds at (a) for SA\_29, (b) SA\_16 at daily time steps and for (c) SA\_29, (d) SA\_16 at monthly time steps.

soil (SOL\_AWC(..).sol). The available soil water capacity (SOL\_AWC) is the amount of water that is available for plant uptake when the soil is at field capacity. The available water capacity varies in three different soil layers. Since there is no role of the catchment size in transferring water from lower level of soil to the root zone, our results show that the sensitivity of SOL\_AWC(..).sol does not depend on the size of the watershed. This parameter depends on the soil property like permeability of soil, capillaries and macropores which are highly sensitive and changes frequently. When the available water capacity of soil decreases, the effect of evaporation decreases and the amount of subsurface flow increases within the soil profile. The value of SOL\_AWC(..).sol is more in dry months than in wet months. The sensitivity of SOL\_AWC(..).sol is more in daily simulations than in monthly simulations. The other related

studies also indicate that the available water capacity of soil is sensitive parameter in their study areas (Bosch et al., 2004; Ghasemizade et al., 2017; Zhang et al., 2013).

The amount of lateral flow discharged to the river on a particular day is controlled by LAT\_TTIME. In our study area, all the watersheds have such a shape that the lateral flow discharge to the river is small and almost constant in all the watersheds. Thus, LAT\_TTIME is not sensitive in any watershed in daily and monthly simulations.

#### 5.4. Sensitivity of evapotranspiration related parameters

Fig. 11 (a-d) summarizes the sensitivity of evapotranspiration related parameters. Soil water availability for evaporation is represented by

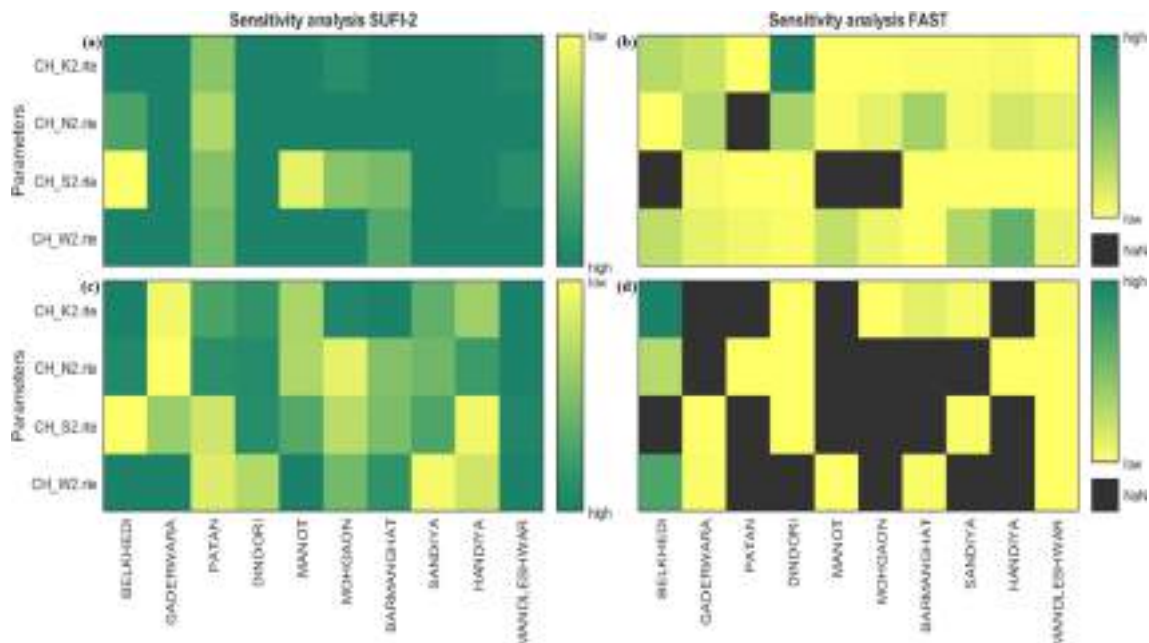
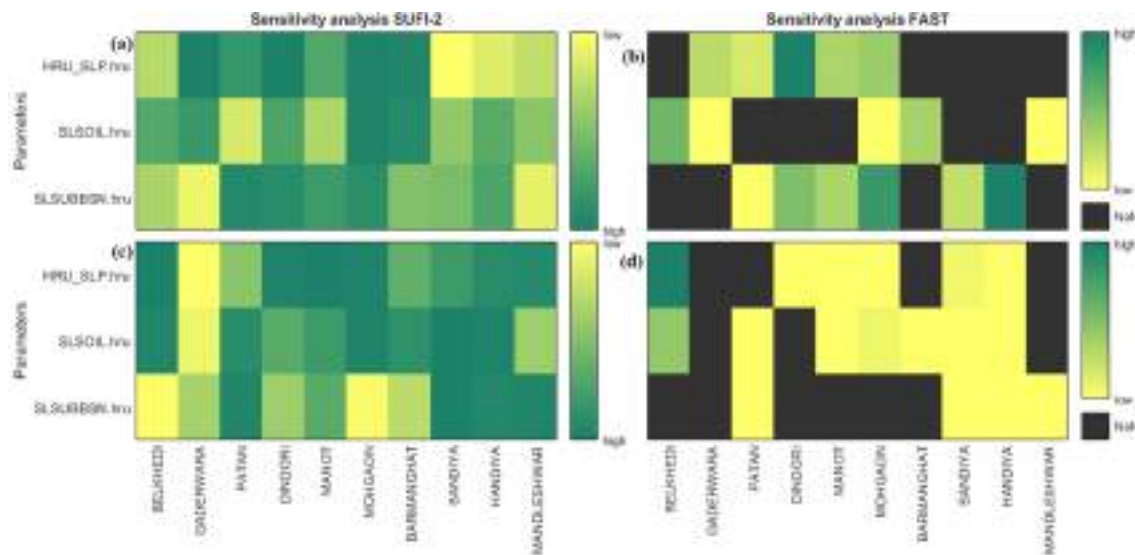


Fig. 12. The assessment of the routing related parameter sensitivity for watersheds at (a) for SA\_29, (b) SA\_16 at daily time steps and for (c) SA\_29, (d) SA\_16 at monthly time steps.



**Fig. 13.** The assessment of the topographic related parameter sensitivity for watersheds at (a) for SA\_29, (b) SA\_16 at daily time steps and for (c) SA\_29, (d) SA\_16 at monthly time steps.

ESCO.hru. The effect of soil capillary, crust and cracking on soil is reflected by this parameter. Since the depth distribution of the water content in the layers is modified by ESCO.hru, it is sensitive for the clay-loam soil. Clay-loam soil is known to have high response towards the transfer of water from the soil in the form of evaporation (Guse et al., 2014; Schaake et al., 1996). At a daily time step, there is less time for water to evapotranspire; therefore, it can be concluded that the evapotranspiration parameters are more sensitive at monthly time step but less sensitive at daily time step. Our results show that ESCO.hru is sensitive in medium-sized watersheds which is also reported by other researchers such as, Suryavanshi et al. (2017) and Spruill and Taraba (2000). Another parameter, EPKO.hru represent plant uptake compensation factor which is sensitive in small watersheds where there is less irrigation area (watershed Patan(3), Dindori(4) and Manot(5)). Maximum canopy storage (CANMX.hru) is not sensitive for any watershed in daily simulations.

### 5.5. Sensitivity of routing related parameters

The sensitivity of routing related parameters are shown in Fig. 12(a-d). Manning's coefficient of the main channel (CH\_N2.rte) is the key parameter that controls the flow in the river. Since this is the property of the channel itself, it does not depend on the size of the watershed. Our results don't show any change in the sensitivity of CH\_N2.rte with respect to catchment size. However, it is sensitive at both monthly and daily time steps. Addressing daily changes in the channel's property is more challenging than monthly changes. Therefore, all the parameters related to routing shows more sensitivity at daily time step compared to monthly time step (Shivhare et al., 2018; Himanshu et al., 2017).

Effective hydraulic conductivity in the main channel (CH\_K2.rte) shows the movement of water from streambed to subsurface for any watershed. Therefore, the sensitivity of CH\_K2.rte is independent of watershed size. The average slope (CH\_S2.rte) and average top width

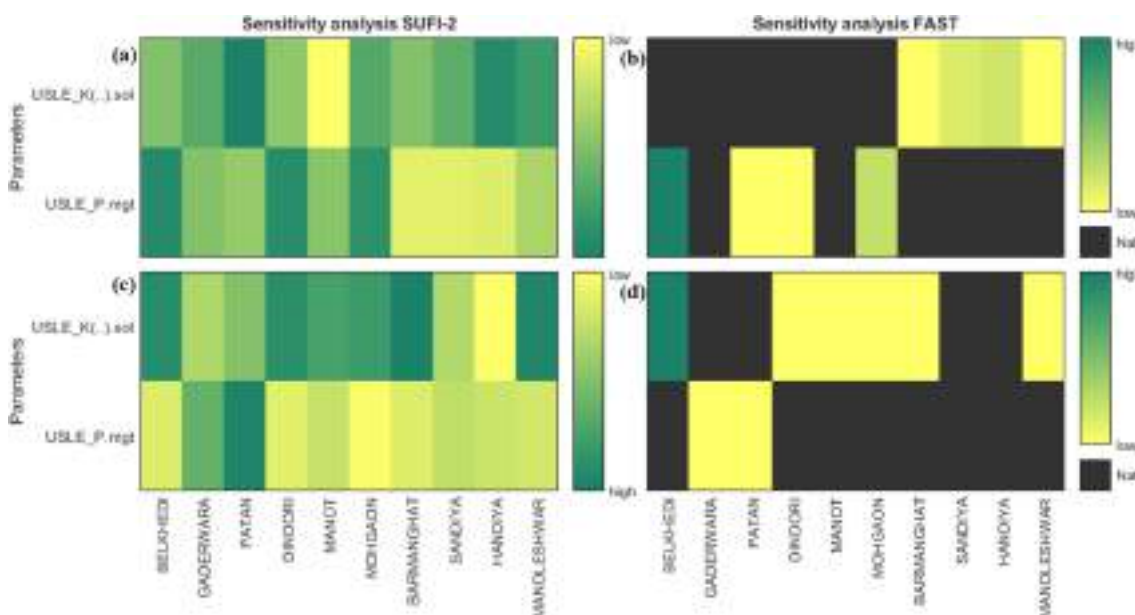


**Fig. 14.** The assessment of the erosion related parameter sensitivity for watersheds at (a) for SA\_29, (b) SA\_16 at daily time steps and for (c) SA\_29, (d) SA\_16 at monthly time steps.

**Table 5**

Sensitive parameters at daily and monthly time steps for different sized watersheds

Parameters	At daily time step		At monthly time step	
	Sensitive for small watersheds	Sensitive for large watersheds	Sensitive for small watersheds	Sensitive for large watersheds
ALPHA_BF.gw			Y	
ALPHA_BNK.rte	Y	Y	Y	Y
CANMX.hru				
CH_K2.rte	Y	Y		
CH_N2.rte	Y	Y		
CH_S1.sub				Y
CH_S2.rte	Y	Y		
CH_W2.rte	Y	Y		
CN2.mgt	Y	Y	Y	Y
DEEPT.gw				
EPCO.hru			Y	
ESCO.hru				Y
GW_DELAY.gw	Y	Y	Y	Y
GW_REVAP.gw		Y	Y	Y
GWHT.gw				Y
GWQMN.gw	Y	Y	Y	
HRU_SLP.hru	Y			
LAT_TTIME.hru				
OV_N.hru	Y			
RCHRG_DP.gw			Y	
REVAPMN.gw			Y	
SLSOIL.hru				Y
SLSUBBSN.hru				Y
SOL_AWC(..).sol	Y	Y	Y	Y
SOL_BD(..).sol	Y	Y	Y	
SOL_K(..).sol	Y			
SURLAG.bsn			Y	Y
USLE_K(..).sol		Y		Y
USLE_P.mgt	Y		Y	

(CH\_W2.rte) of the main channel are more sensitive when the sum of the length of main channel is more than the sum of the length of tributaries (Heuvelmans et al., 2006).

### 5.6. Sensitivity of topographic related parameters

The sensitivity of topographic related parameters is shown in Fig. 13 (a-d). From the figure, it is clear that the average slope steepness (HRU\_SLP.hru) decreases with the increase in watershed size. It could be attributed to fact that if the slope is steeper, naturally less time is required for runoff to percolate from surface to subsurface. Also, the steepness of the slope helps runoff water to reach the stream/river. Therefore, in small watersheds, HRU\_SLP.hru is showing high sensitivity.

Average slope length of the subbasin (SLSUBBSN.hru) directly affects the average streamflow amount and positively correlate with the streamflow. As the size of watershed increases, the slope length also increases. We noticed that this parameter is sensitive for large watershed but not sensitive for small watershed. A study on the Tons River basin in India by Kumar et al. (2017) reported that SLSUBBSN.hru is sensitive parameter for small sized watersheds. The slope of the watershed for lateral flow in subsurface is shown by the parameter SLSOIL.hru. Our results show that SLSOIL.hru is sensitive at monthly time step when the time of flow is more in large watersheds. Our results are supported by

the findings of Kim and Mohanty (2015) who reported that SLSOIL.hru is sensitive parameter for large watersheds.

### 5.7. Sensitivity of erosion related parameters

The sensitivity of erosion related parameters is shown in Fig. 14(a-d). The erodibility factor (USLE\_K(..).sol) depends on the property of the soil. Large watersheds have more variation in soil than the same in a small watershed. The small watershed may have only one or two soil type, which increases the sensitivity of USLE\_K(..).sol for large watershed. The sensitivity of USLE\_K(..).sol is more at a daily time step compared to simulations with monthly time step in both SA\_29 and SA\_16 (Arabi et al., 2006; Misra and Rose, 1996). Small watersheds have less varying slope than the large watersheds which need more support practice to control the soil loss. Therefore, Soil support practice factor (USLE\_P(..).sol) is more sensitive for small watersheds than for large watersheds. USLE\_P.mgt is less sensitive as compared to USLE\_K(..).sol when we use less number of parameters (SA\_16 simulations) than the simulations with more numbers of parameters (SA\_29).

## 6. Summary and conclusions

In this paper, we analysed the effect of catchment size, simulation time steps and the type of global sensitivity analysis on the parameter sensitivity. We developed SWAT hydrological model for ten watersheds in Narmada River basin. We conducted two types of global sensitivity analysis (SA\_29 and SA\_16) – (i) with 29 parameters using SUFI-2 and (ii) with 16 most sensitive parameters using FAST. The summary of our results is presented in Table 5. We have clearly indicated which parameters are sensitive in small and large watersheds at which simulation time step (daily or monthly). From the table we can easily identify the parameters which are not affected by the variation in both simulation time step and size of the watersheds. The conclusions of this study are as follows:

- SA\_16 is efficient and reduces the complexity of semi-distributed hydrological models for any watershed. Simulations with SA\_16 produced better results than SA\_29 in some watersheds. Dindori(4), Manot(5) and Barman Ghat(7) at monthly time steps with SA\_16 shows higher NSE than in case of SA\_29.
- Our results show that parameter sensitivity depends heavily upon the selection of catchment size and time step used in the simulation. However, there are several parameters with their sensitivity independent of above-mentioned selections. For instance, the curve number (CN2.mgt), and Baseflow alpha factor for bank storage (ALPHA\_BNK.rte) are highly sensitive for almost all the catchment size and time steps. While Lateral flow travel time (LAT\_TTIME.hru) is least sensitive for almost all the catchment size and time steps. These observations imply that many parameters may not be significant and can be ignored to avoid over-parameterization of the model.
- The sensitivity of several parameters significantly depends on catchment size. For instance, ALPHA\_BF.gw, OV\_N.hru and USLE\_K(..).sol are sensitive for small watershed but not at all sensitive for large and medium sized watersheds. GWHT.gw and SLSUBBSN.hru are sensitive for large watershed but not sensitive for small watersheds at monthly time step.
- Sensitive parameters at daily time step for large and medium range watershed are CH\_S1.sub, SOL\_BD(..).sol and USLE\_K.sol. On the other hand, GW\_DELAY.gw, HRU\_SLP and USLE\_P.mgt are not sensitive for large watershed but sensitive for other watersheds.
- The sensitivity of several parameters primarily depends on time step used in the simulation. For instance, GW\_DELAY.gw, GW\_REVAP.gw, and SOL\_AWC(..).sol are sensitive on monthly time step and CH\_K2.rte, CH\_N2.rte, CH\_W2.rte, GWQMN.gw and SOL\_BD(..).sol are sensitive at daily time step.

- Evapotranspiration parameters are less sensitive at monthly and daily time steps. Routing related parameters are also less sensitive when we reduce the number of parameters (SA<sub>16</sub>).
- To avoid complexity and uncertainty in any hydrological model, reducing the number of parameters is important. At the same time, it is also necessary to select a parameter set that accounts for all the hydrological process. Our results indicate that depending on the size of the catchment and simulation time step, suitable recommendations can be provided to the modeler. For instance, based on our results, we can pick GW\_DELAY.gw, ALPHA\_BNK.rte from ground water related parameters, CN2.mgt from runoff related parameter, SOL\_AWC(.).sol from soil water related parameter, EPCO.hru from evapotranspiration related parameter, CH\_N2.rte from routing related parameters and HRU\_SLP.hru from topographic related parameters, and that would hopefully be sufficient for the simulation of a small sized watershed. Erosion related parameters need not be considered.
- Based on our results, we recommend that it is necessary to perform such analysis before selecting a set of parameters in a semi-distributed hydrological model.

The encouraging results for the parameter sensitivity in SWAT hydrological model in this study seem to indicate that the approach has the potential to address the problems related to over parameterization, hydrological modelling accuracy and spatio-temporal variation of hydrological processes.

#### CRediT authorship contribution statement

**Ankit Singh:** Data curation, Formal analysis, Methodology, Validation, Visualization, Writing – original draft. **Sanjeev Kumar Jha:** Conceptualization, Funding acquisition, Investigation, Supervision, Writing – review & editing.

#### Declaration of Competing Interest

The authors declare that they have no known competing financial interests or personal relationships that could have appeared to influence the work reported in this paper.

#### Acknowledgements

This research has been completed thanks to the support of the Science and Engineering Research Board (SERB), project number CRG/2018/000649 awarded to Sanjeev Kumar Jha. Data used in this study is available on public domain for all the researchers. We thank two Reviewers for their valuable comments which improved the quality of the manuscript significantly.

#### Appendix 1

##### *Descriptions of the parameters used in the sensitivity analysis (Neitsch et al. (2011))*

The surface runoff is characterized by the curve number (CN2.mgt), time of concentration (SURLAG.bsn, LAT\_TTIME.hru), and slope (HRU\_SLP.hru, SLSUBBSN.hru). The curve number (CN2.mgt) for distinct slopes is obtained from the average slope steepness parameter (HRU\_SLP.hru). A reduction of the curve number results in a lower surface runoff, which implies lower streamflow peak in the river. The time of concentration relies on the timing parameters i.e., SURLAG.bsn and LAT\_TTIME.hru. A time of concentration of more than 1 day implies that the cumulative amount of surface runoff does not reach the river on a given day. Average slope length (SLSUBBSN.hru) and manning's roughness coefficient for the subbasin (OV\_N.hru) contribute in the

computation of the time of concentration of channel flow and average velocity.

The available soil water capacity (SOL\_AWC.sol), moist bulk density (SOL\_BD.sol), and saturated hydraulic conductivity (SOL\_K.sol) are selected as the soil parameters. SOL\_AWC.sol is the estimation of the field capacity for each soil layer. SOL\_BD.sol defines the relative amount of pore space and soil matrix. Travel time of water for percolation is calculated by SOL\_K.sol. These soil water parameters regulate the percolation into the groundwater and the frequency of surface and lateral flows along with evaporation. The evapotranspiration is represented by maximum canopy storage (CANMX.hru), soil evaporation compensation factor (ESCO.hru) and plant uptake compensation factor (EPCO.hru). CANMX.hru depicts the water capacity of the canopy storage and depends on the leaf area index of the specific crop. Precipitation only enters the soil once the canopy storage is completely filled. Once the canopy storage is empty, soil water is utilized for the evaporation, characterized by the depth of soil evaporation (ESCO.hru). ESCO.hru determines the contribution of each soil layer to the evaporation. Furthermore, EPCO.hru is the compensation factor for the water uptake by the plants. As EPCO.hru increases, the water uptake from the lower zone of the soil also increases. Processes involving groundwater are represented by groundwater time delay (GW\_DELAY.gw), baseflow recession constant (ALPHA\_BF.gw), aquifer fraction coefficient (RCHRG\_DP.gw), groundwater "revap" coefficient (GW\_REVAP.gw), threshold depth of water in the shallow aquifer for "revap" to occur (REVAPMN.gw), initial groundwater height (GWHT.gw), threshold depth of water in the shallow aquifer required for return flow to occur (GWQMN.gw), and initial depth of water in shallow aquifer (DEEPST.gw). The groundwater time delay (GW\_DELAY.gw) and baseflow recession constant (ALPHA\_BF.gw) are related to the timing of the process. The GW\_DELAY.gw (measured in days) regulates the time delay for recharging the shallow aquifer and increase in this delay factor leads to a slower recharging process. The ALPHA\_BF.gw delays the outflow of groundwater and estimates the time required by water to flow from groundwater to the river reach. The aquifer fraction coefficient (RCHRG\_DP.gw) determines the splitting between deep and shallow aquifers. The "revap" is defined as the movement of water from the lower soil surface to the overlying unsaturated layer for evapotranspiration, which is done by deep-root of plant. The revap-parameters majorly depend upon landuse and landcover. The movement of water from shallow aquifer to evapotranspiration depends upon GW\_REVAP.gw and REVAPMN.gw parameters. GWQMN.gw is the threshold water level of shallow aquifer required for moving the water from the aquifer to the upper soil layer. Decreasing the value of GW\_REVAP.gw and GWQMN.gw reduces evapotranspiration and increases the base flow.

Routing related parameter are represented by average width of main channel (CH\_W2.rte), channel slope (CH\_S2.rte), manning's value for the main channel (CH\_N2.rte), Effective hydraulic conductivity in main channel (CH\_K2.rte), and base flow recession constant for bank storage (ALPHA\_BNK.rte). Discharge in the channel is calculated by cross-sectional area of the channel, channel slope (CH\_S2.rte), average width of the channel (CH\_W2.rte) and the flow velocity (which is dependent upon CH\_N2.rte). Furthermore, the transmission loss from channel is directly related to the hydraulic conductivity of the channel alluvium (CH\_K2.rte). ALPHA\_BNK.rte measures the volume of water added to the channel from the bank storage. USLE\_K(.).sol and USLE\_P.mgt are related to erosion. USLE\_P.mgt is defined as the ratio of soil loss associated with a specific support practice to the corresponding losses with the varying slope culture, whereas, USLE\_K(.).sol is defined as the soil erodibility factor.

#### References

- Abbaspour, K.C., Johnson, C.A., van Genuchten, M.T., 2004. Estimating uncertain flow and transport parameters using a sequential uncertainty fitting procedure. *Vadose Zo. J.* 3, 1340–1352. <https://doi.org/10.2136/vzj2004.1340>.



- Abbaspour, K.C., Yang, J., Maximov, I., Siber, R., Bogner, K., Mieleitner, J., Zobrist, J., Srinivasan, R., 2007. Modelling hydrology and water quality in the pre-alpine/alpine Thur watershed using SWAT. *J. Hydrol.* 333, 413–430. <https://doi.org/10.1016/j.jhydrol.2006.09.014>.
- Abbaspour, K.C., Rouholahnejad, E., Vaghefi, S., Srinivasan, R., Yang, H., Kløve, B., 2015. A continental-scale hydrology and water quality model for Europe: calibration and uncertainty of a high-resolution large-scale SWAT model. *J. Hydrol.* 524, 733–752. <https://doi.org/10.1016/j.jhydrol.2015.03.027>.
- Amenu, G.G., Kumar, P., Liang, X.-Z., 2005. Interannual variability of deep-layer hydrologic memory and mechanisms of its influence on surface energy fluxes. *J. Climate. American Meteorological Society* 18 (23), 5024–5045. <https://doi.org/10.1175/JCLI3590.1>.
- Arabi, M., Govindaraju, R.S., Hantush, M.M., Engel, B.A., 2006. Role of watershed subdivision on modeling the effectiveness of best management. *Water Resour.* 42(6), 513–528. <https://doi.org/10.5465/AMR.1990.4308277>.
- Arnold, J.G., Srinivasan, R., Muttiah, R.S., Williams, J.R., 1998. Large area hydrologic modeling and assessment part I: Model development. *J. Am. Water Resour. Assoc.* 34, 73–89. <https://doi.org/10.1111/j.1752-1688.1998.tb05961.x>.
- Baduna Kocuyigit, M., Akay, H., Yanmaz, A.M., 2017. Effect of watershed partitioning on hydrologic parameters and estimation of hydrograph of an ungauged basin: a case study in Gokirmak and Kocanaz, Turkey. *Arabian J. Geosci. Springer Verlag* 10 (15). <https://doi.org/10.1007/s12517-017-3132-8>.
- Bahreman, A., De Smedt, F., 2008. Distributed hydrological modeling and sensitivity analysis in Torysa Watershed. *Slovakia. Water Resour. Manag.* 22, 393–408. <https://doi.org/10.1007/s11269-007-9168-x>.
- Beven, K., Germann, P., 2013. Macropores and water flow in soils revisited. *Water Resour. Res.* 49, 3071–3092. <https://doi.org/10.1002/wrcr.20156>.
- Bilotta, G., Cappello, A., Hérault, A., Vicari, A., Russo, G., Del Negro, C., 2012. Sensitivity analysis of the MAGFLOW Cellular Automaton model for lava flow simulation. *Environ. Model. Softw.* 35, 122–131. <https://doi.org/10.1016/j.envsoft.2012.02.015>.
- Borgonovo, E., Lu, X., Plischke, E., Rakovec, O., Hill, M.C., 2017. Making the most out of a hydrological model data set: sensitivity analyses to open the model black-box. *Water Resour. Res.* 53, 7933–7950. <https://doi.org/10.1002/2017WR020767>.
- Bosch, D.D., Sheridan, J.M., Batten, H.L., Arnold, J.G., 2004. E Valuation of the Swat M Odel on a C Oastal. *Trans. ASAE* 47, 1493–1506.
- Cibin, R., Sudheer, K.P., Chaubey, I., 2010. Sensitivity and identifiability of stream flow generation parameters of the SWAT model. *Hydrol. Process. John Wiley & Sons Ltd* 24 (9), 1133–1148. <https://doi.org/10.1002/HYP.7568>.
- Cukier, R.I., Levine, H.B., Shuler, K.E., 1978. Nonlinear sensitivity analysis of multiparameter model systems. *J. Comput. Phys.* 26, 1–42. [https://doi.org/10.1016/0021-9991\(78\)90097-9](https://doi.org/10.1016/0021-9991(78)90097-9).
- da Silva, M.G., de Aguiar Netto, A., de Jesus Neves, R.J., do Vasco, A.N., Almeida, C., Faccioli, G.G., 2015. Sensitivity analysis and calibration of hydrological modeling of the watershed Northeast Brazil. *J. Environ. Prot. (Irvine, Calif)* 06, 837–850. <https://doi.org/10.4236/jep.2015.68076>.
- Das, P., Mukherjee, A., Jamal, S., Gond, S., Layek, M., Sengupta, P., Basu, A., 2016. Groundwater evolution and its impact on potability of water in a central Gangetic aquifer system: Varanasi, India.
- Dhami, B., Himanshu, S.K., Pandey, A., Gautam, A.K., 2018. Evaluation of the SWAT model for water balance study of a mountainous snowfed river basin of Nepal. *Environ. Earth Sci.* 77, 1–20. <https://doi.org/10.1007/s12665-017-7210-8>.
- Douglas-Smith, D., Iwanaga, T., Croke, B.F.W., Jakeman, A.J., 2020. Certain trends in uncertainty and sensitivity analysis: an overview of software tools and techniques. *Environ. Model. Softw.* <https://doi.org/10.1016/j.envsoft.2019.104588>.
- Duan, K., Mei, Y., 2014. Comparison of meteorological, hydrological and agricultural drought responses to climate change and uncertainty assessment. *Water Resour. Manage. Springer* 28 (14), 5039–5054. <https://doi.org/10.1007/S11269-014-0789-6>.
- Emery, C.M., Biancamaria, S., Boone, A., Garambois, P.A., Ricci, S., Rochoux, M.C., Decharme, B., 2016. Temporal variance-based sensitivity analysis of the river-routing component of the large-scale hydrological model ISBA-TRIP: application on the Amazon Basin. *J. Hydrometeorol.* 17, 3007–3027. <https://doi.org/10.1175/JHM-D-16-0050.1>.
- Fang, Z., et al., 2016. Scale dependent parameterization of soil hydraulic conductivity in 3D simulation of hydrological processes in a forested headwater catchment. *J. Hydrol. Elsevier* 536, 365–375. <https://doi.org/10.1016/J.JHYDROL.2016.03.020>.
- Gamerith, V., Neumann, M.B., Muschalla, D., 2013. Applying global sensitivity analysis to the modelling of flow and water quality in sewers. *Water Res.* 47, 4600–4611. <https://doi.org/10.1016/j.watres.2013.04.054>.
- Garg, K.K., Bharati, L., Gaur, A., George, B., Acharya, S., Jella, K., Narasimhan, B., 2012. Spatial mapping of agricultural water productivity using the swat model in upper Bhima catchment, India. *Irrig. Drain.* 61, 60–79. <https://doi.org/10.1002/ird.618>.
- Gassman, P.W., Reyes M.R., Green C.H., Arnold J.G., 2007. The soil and water assessment tool: historical development, applications, and future research directions. *Trans. ASABE* 50, 1211–1250. <https://doi.org/10.13031/2013.23637>.
- Gentine, P., et al., 2012. Scaling in surface hydrology: progress and challenges. *J. Contemp. Water Res. Educ. John Wiley & Sons Ltd* 147 (1), 28–40. <https://doi.org/10.1111/J.1936-704X.2012.03105.X>.
- Ghasemzade, M., Baroni, G., Abbaspour, K., Schirmer, M., 2017. Combined analysis of time-varying sensitivity and identifiability indices to diagnose the response of a complex environmental model. *Environ. Model. Softw.* 88, 22–34. <https://doi.org/10.1016/j.envsoft.2016.10.011>.
- Godsey, S.E., et al., 2010. Generality of fractal 1/f scaling in catchment tracer time series, and its implications for catchment travel time distributions. *Hydrol. Process. John Wiley & Sons Ltd* 24 (12), 1660–1671. <https://doi.org/10.1002/HYP.7677>.
- Gond, S., Gupta, N., Gupta, S., 2019. Evaluation of Drought Severity Indices and their Trend for Mirzapur (Uttar Pradesh).
- Guo, J., Su, X., 2019. Parameter sensitivity analysis of SWAT model for streamflow simulation with multisource precipitation datasets. *Hydrol. Res.* 50, 861–877. <https://doi.org/10.2166/nh.2019.083>.
- Guse, B., Reusser, D.E., Fohrer, N., 2014. How to improve the representation of hydrological processes in SWAT for a lowland catchment - temporal analysis of parameter sensitivity and model performance. *Hydrol. Process.* 28, 2651–2670. <https://doi.org/10.1002/hyp.9777>.
- Heuvelmans, G., Muys, B., Feyen, J., 2006. Regionalisation of the parameters of a hydrological model: comparison of linear regression models with artificial neural nets. *J. Hydrol.* 319, 245–265. <https://doi.org/10.1016/j.jhydrol.2005.07.030>.
- Himanshu, S.K., Pandey, A., Shrestha, P., 2017. Application of SWAT in an Indian river basin for modeling runoff, sediment and water balance. *Environ. Earth Sci.* 76. <https://doi.org/10.1007/s12665-016-6316-8>.
- Keery, J., Binley, A., Crook, N., Smith, J.W.N., 2007. Temporal and spatial variability of groundwater-surface water fluxes: development and application of an analytical method using temperature time series. *J. Hydrol.* 336, 1–16. <https://doi.org/10.1016/j.jhydrol.2006.12.003>.
- Khatun, S., Sahana, M., Jain, S.K., Jain, N., 2018. Simulation of surface runoff using semi distributed hydrological model for a part of Satluj Basin: parameterization and global sensitivity analysis using SWAT CUP. *Model. Earth Syst. Environ.* 4, 1111–1124. <https://doi.org/10.1007/s40808-018-0474-5>.
- Kim, J., Mohanty, B.P., 2015. J. Geophys. Res.: Atmospheres 704–721. <https://doi.org/10.1002/2015JD024067>. Received.
- Kumar, S., Merwade, V., 2009. Impact of watershed subdivision and soil data resolution on swat model calibration and parameter uncertainty. *J. Am. Water Resour. Assoc.* 45, 1179–1196. <https://doi.org/10.1111/j.1752-1688.2009.00353.x>.
- Kumar, N., Singh, S.K., Srivastava, P.K., Narsimlu, B., 2017. SWAT Model calibration and uncertainty analysis for streamflow prediction of the Tons River Basin, India, using Sequential Uncertainty Fitting (SUFI-2) algorithm. *Model. Earth Syst. Environ.* 3, 30. <https://doi.org/10.1007/s40808-017-0306-z>.
- Lenhart, T., Eckhardt, K., Fohrer, N., Frede, H.-G., 2002. Comparison of two different approaches of sensitivity analysis. *Phys. Chem. Earth* 27, 645–654. [https://doi.org/10.1016/S1474-7065\(02\)00049-9](https://doi.org/10.1016/S1474-7065(02)00049-9).
- McCuen, R.H., 1973. The role of sensitivity analysis in hydrologic modeling. *J. Hydrol.* 18, 37–53. [https://doi.org/10.1016/0022-1694\(73\)90024-3](https://doi.org/10.1016/0022-1694(73)90024-3).
- Me, W., Abell, J.M., Hamilton, D.P., 2015. Effects of hydrologic conditions on SWAT model performance and parameter sensitivity for a small, mixed land use catchment in New Zealand. *Hydrol. Earth Syst. Sci.* 19, 4127–4147. <https://doi.org/10.5194/hess-19-4127-2015>.
- Misra, R.K., Rose, C.W., 1996. Application and sensitivity analysis of process-based erosion model GUEST 593–604.
- Muleta, M.K., Nicklow, J.W., Bekele, E.G., 2007. Sensitivity of a Distributed Watershed Simulation Model to Spatial Scale 163–172.
- Murphy, J.M., Sexton, D.M.H., Barnett, D.N., Jones, G.S., Webb, M.J., Collins, M., Stainforth, D.A., 2004. Quantification of modelling uncertainties in a large ensemble of climate change simulations. *Nature* 430, 768–772. <https://doi.org/10.1038/nature02771>.
- Narsimlu, B., Gosain, A.K., Chahar, B.R., Singh, S.K., Srivastava, P.K., 2015. SWAT model calibration and uncertainty analysis for streamflow prediction in the Kunwar River Basin, India, using sequential uncertainty fitting. *Environ. Process.* 2, 79–95. <https://doi.org/10.1007/s40710-015-0064-8>.
- Neitsch, S.L., Arnold, J.G., Kiniry, J.R., Williams, J.R., 2011. College of Agriculture and life sciences Soil and Water Assessment Tool Theoretical Documentation Version 2009.
- Niehoff, D., Fritsch, U., Bronstert, A., 2002. Land-use impacts on storm-runoff generation: Scenarios of land-use change and simulation of hydrological response in a meso-scale catchment in SW-Germany. *J. Hydrol.* 267, 80–93. [https://doi.org/10.1016/S0022-1694\(02\)00142-7](https://doi.org/10.1016/S0022-1694(02)00142-7).
- Nilawar, A.P., Waikar, M.L., 2018. Use of SWAT to determine the effects of climate and land use changes on streamflow and sediment concentration in the Purna River basin. *India. Environ. Earth Sci.* 77, 1–13. <https://doi.org/10.1007/s12665-018-7975-4>.
- Norton, J., 2015. An introduction to sensitivity assessment of simulation models. *Environ. Model. Softw.* 69, 166–174. <https://doi.org/10.1016/j.envsoft.2015.03.020>.
- Nossent, J., Bauwens, W., 2012. Multi-variable sensitivity and identifiability analysis for a complex environmental model in view of integrated water quantity and water quality modeling. *Water Sci. Technol.* 65, 539–549. <https://doi.org/10.2166/wst.2012.884>.
- Pandey, G., Lovejoy, S., Schertzer, D., 1998. Multifractal analysis of daily river flows including extremes for basins of five to two million square kilometres, one day to 75 years. *J. Hydrol. Elsevier* 208 (1–2), 62–81. [https://doi.org/10.1016/S0022-1694\(98\)00148-6](https://doi.org/10.1016/S0022-1694(98)00148-6).
- Pontes, L.M., Viola, M.R., Silva, M.L.N., Bispo, D.F.A., Curi, N., 2016. Hydrological modeling of tributaries of cantareira system, southeast brazil, with the swat model. *Eng. Agric.* 36, 1037–1049. <https://doi.org/10.1590/1809-4430-eng.agric.v36n6p1037-1049/2016>.
- Pue, J.D., Rezaei, M., Meirvenne, M.V., Cornelis, W.M., 2019. The relevance of measuring saturated hydraulic conductivity: sensitivity analysis and functional evaluation. *J. Hydrol.* 576, 628–638. <https://doi.org/10.1016/j.jhydrol.2019.06.079>.

- Pushpalatha, R., Perrin, C., Le Moine, N., Mathevet, T., Andréassian, V., 2011. A downward structural sensitivity analysis of hydrological models to improve low-flow simulation. *J. Hydrol.* 411, 66–76. <https://doi.org/10.1016/j.jhydrol.2011.09.034>.
- Rahman, K., Maringanti, C., Beniston, M., Widmer, F., Abbaspour, K., Lehmann, A., 2013. Streamflow modeling in a highly managed mountainous glacier watershed using SWAT: the Upper Rhone River Watershed case in Switzerland. *Water Resour. Manag.* 27, 323–339. <https://doi.org/10.1007/s11269-012-0188-9>.
- Randhir, T.O., Tsvetkova, O., 2011. Spatiotemporal dynamics of landscape pattern and hydrologic process in watershed systems. *J. Hydrol. Elsevier* 404 (1–2), 1–12. <https://doi.org/10.1016/J.JHYDROL.2011.03.019>.
- Region, R., Shen, Z.Y., Chen, L., Chen, T., 2012. Analysis of parameter uncertainty in hydrological and sediment modeling using GLUE method : a case study of SWAT model applied to Three Gorges Reservoir Region , China. <https://doi.org/10.5194/hess-16-121-2012>.
- Reusser, D.E., Buytaert, W., Zehe, E., 2011. Temporal dynamics of model parameter sensitivity for computationally expensive models with the Fourier amplitude sensitivity test. *Water Resour. Res.* 47 <https://doi.org/10.1029/2010WR009947>.
- Saltelli, A., Annoni, P., 2010. How to avoid a perfunctory sensitivity analysis. <https://doi.org/10.1016/j.envsoft.2010.04.012>.
- Schaake, J.C., Koren, V.I., Duan, Q.-Y., Mitchell, K., Chen, F., 1996. Simple water balance model for estimating runoff at different spatial and temporal scales. *J. Geophys. Res. Atmos.* 101, 7461–7475. <https://doi.org/10.1029/95JD02892>.
- Schmalz, B., Fohrer, N., 2009. Comparing model sensitivities of different landscapes using the ecohydrological SWAT model. *Adv. Geosci.* 21, 91–98. <https://doi.org/10.5194/adgeo-21-91-2009>.
- Sharma, M.L., Luxmoore, R.J., DeAngelis, R., Ward, R.C., Yeh, G.T., 1987. Subsurface water flow simulated for hillslopes with spatially dependent soil hydraulic characteristics. *Water Resour. Res.* 23, 1523–1530. <https://doi.org/10.1029/WR023i008p01523>.
- Sharma, S., Siddique, R., Reed, S., Ahnert, P., Mejia, A., 2019. Hydrological model diversity enhances streamflow forecast skill at short- to medium-range timescales. *Water Resour. Res.* 55, 1510–1530. <https://doi.org/10.1029/2018WR023197>.
- Shivhare, N., Dikshit, P.K.S., Dwivedi, S.B., 2018. A Comparison of SWAT model calibration techniques for hydrological modeling in the ganga river watershed. *Engineering* 4, 643–652. <https://doi.org/10.1016/j.eng.2018.08.012>.
- Shriver, D.M., Randhir, T.O., 2006. Integrating stakeholder values with multiple attributes to quantify watershed performance. *Water Resour. Res. John Wiley & Sons Ltd* 42 (8). <https://doi.org/10.1029/2005WR004413>.
- Spruill, C.A., Taraba, J.L., 2000. Simulation of daily and monthly stream discharge from small watersheds using the SWAT model. *Am. Soc. Agric. Eng.* 1, 1431–1439.
- Sudheer, K.P., Lakshmi, G., Chaube, I., 2011. Application of a pseudo simulator to evaluate the sensitivity of parameters in complex watershed models. *Environ. Model. Softw.* 26, 135–143. <https://doi.org/10.1016/j.envsoft.2010.07.007>.
- Suryavanshi, S., Pandey, A., Chaube, U.C., 2017. Hydrological simulation of the Betwa River basin (India) using the SWAT model. *Hydrol. Sci. J.* 62, 960–978. <https://doi.org/10.1080/02626667.2016.1271420>.
- Thampi, S.G., Raneesh, K.Y., Surya, T.V., 2010. Influence of scale on SWAT model calibration for streamflow in a River Basin in the Humid Tropics. *Water Resour. Manag.* 24, 4567–4578. <https://doi.org/10.1007/s11269-010-9676-y>.
- Tobin, K.J., Bennett, M.E., 2009. Using SWAT to model streamflow in two river basins with ground and satellite precipitation data. *J. Am. Water Resour. Assoc.* 45, 253–271. <https://doi.org/10.1111/j.1752-1688.2008.00276.x>.
- Tolley, D., Foglia, L., Harter, T., 2019. Sensitivity analysis and calibration of an integrated hydrologic model in an irrigated agricultural basin with a groundwater-dependent ecosystem. *Water Resour. Res.* 55, 7876–7901. <https://doi.org/10.1029/2018WR024209>.
- Troch, P.A., Paniconi, C., McLaughlin, D., 2003. Catchment-scale hydrological modeling and data assimilation. *Adv. Water Resour.* 26, 131–135. [https://doi.org/10.1016/S0309-1708\(02\)00087-8](https://doi.org/10.1016/S0309-1708(02)00087-8).
- Uniyal, B., Jha, M.K., Verma, A.K., 2015. Parameter identification and uncertainty analysis for simulating streamflow in a river basin of Eastern India. *Hydrol. Process.* 29, 3744–3766. <https://doi.org/10.1002/hyp.v29.1710.1002/hyp.10446>.
- van Griensven, A., Meixner, T., Grunwald, S., Bishop, T., Diluzio, M., Srinivasan, R., 2006. A global sensitivity analysis tool for the parameters of multi-variable catchment models. *J. Hydrol.* 324, 10–23. <https://doi.org/10.1016/j.jhydrol.2005.09.008>.
- Van Griensven, A., Meixner, T., Srinivasan, R., Grunwald, S., 2008. Fit-for-purpose analysis of uncertainty using split-sampling evaluations. *Hydrol. Sci. J.* 53, 1090–1103. <https://doi.org/10.1623/hysj.53.5.1090>.
- Veith, T.L., Liew, M.W.V., Bosch, D.D., Arnold, J.G., 2010. Parameter sensitivity and uncertainty in SWAT: a comparison across five USDA-ARS watersheds. *Am. Soc. Agric. Biol. Eng.* 1477–1486. ISSN 2151-0032 53.
- Visakh, S., Raju, P.V., Kulkarni, S.S., Diwakar, P.G., 2019. Inter-comparison of water balance components of river basins draining into selected delta districts of Eastern India. *Sci. Total Environ.* 654, 1258–1269. <https://doi.org/10.1016/j.scitotenv.2018.11.162>.
- Yang, J., 2011. Convergence and uncertainty analyses in Monte-Carlo based sensitivity analysis. *Environ. Model. Softw.* 26, 444–457. <https://doi.org/10.1016/j.envsoft.2010.10.007>.
- Ye, M., Meyer, P.D., Neuman, S.P., 2008. On model selection criteria in multimodel analysis. *Water Resour. Res.* 44 <https://doi.org/10.1029/2008WR006803>.
- Zhang, C., Chu, J., Fu, G., 2013. Sobol 0 ' s sensitivity analysis for a distributed hydrological model of Yichun River Basin. *China. J. Hydrol.* 480, 58–68. <https://doi.org/10.1016/j.jhydrol.2012.12.005>.
- Zhang, W., Montgomery, D.R., 1994. Digital elevation model grid size, landscape representation, and hydrologic simulations. *Water Resour. Res. John Wiley & Sons Ltd* 30 (4), 1019–1028. <https://doi.org/10.1029/93WR03553>.
- Zhang, D., Zhang, L., Guan, Y., Chen, X.i., Chen, X., 2012. Sensitivity analysis of Xinanjiang rainfall-runoff model parameters: a case study in Lianghui, Zhejiang province. *China. Hydrol. Res.* 43, 123–134. <https://doi.org/10.2166/nh.2011.131>.